Laser induced forward transfer of biomaterials to create a skin substitute for burn patients

Von der Naturwissenschaftlichen Fakultät

der Gottfried Wilhelm Leibniz Universität Hannover
zur Erlangung des Grades einer

Doktorin der Naturwissenschaften
Dr. rer. nat.

genehmigte Dissertation
von

Diplom-Biologin Stefanie Michael, geb. Kuhn

geboren am 02.06.1980 in Bielefeld

2013

Referent:
Prof. Dr. Peter M. Vogt

Koreferent:
Prof. Dr. Anaclet Ngezahayo

Tag der Promotion:
05.07.2013

Skin is a truly amazing organ, rarely properly appreciated until it is missing.

[69, chapter 15]

Zusammenfassung

Verbrennungen entstehen in vielen verschiedenen Situationen im Leben und umfassen z.B. Verbrühungen, Gasexplosionen, Unfälle durch Chemikalien oder Grillunfälle. Während oberflächliche Verbrennungen spontan und ohne Probleme heilen, führen großflächige und tiefe Verbrennungen häufig zu massiven Komplikationen wie Infektionen oder der Verbrennungskrankheit. Um dieses zu verhindern und um die Regeneration der Haut zu ermöglichen, werden die Wunden nach Entfernung der verbrannten Haut mit autologer Haut gedeckt. Letztere reicht jedoch häufig nicht aus. Ebenfalls kommt es zu Narbenbildung und damit zu Einschränkungen auf ästhetischer und funktionaler Ebene. Bisher stehen noch keine vollständig zufriedenstellenden Hautäquivalente für eine Therapie zur Verfügung, da die vorhandenen weder Haarfollikel noch Talg- oder Schweißdrüsen beinhalten. Ferner wachsen große Transplantate aufgrund einer ungenügenden Vaskularisierung oft nicht ein.

Daher besteht das Langzeitziel unserer Forschung in der Entwicklung eines Hautersatzes, welcher die Eigenschaften einer normalen Haut so gut wie möglich nachbilden kann. Außerdem soll er der schnellen und permanenten Wundbedeckung dienen. Mein Kurzzeitziel war die Etablierung und die Nutzung des laserbasierten Bioprintings - speziell des Laserinduzierten Vorwärtstransfers (laser induced forward transfer, LIFT) - für die Herstellung eines einfachen Hautäquivalentes mit seinem spezifischen dreidimensionalen (3D) Aufbau. Das Alleinstellungsmerkmal des Bioprintings besteht in dessen Möglichkeit, die gewünschten Zellen in einem präzisen räumlichen Muster mit einer hohen Auflösung zu positionieren.

Verschiedene Zelltypen - einschließlich Zelllinien und primäre Zellen - wurden schadenfrei transferiert. Sie überlebten den LIFT Prozess zu einem hohen Anteil und ohne Veränderungen des Phänotyps im Vergleich zu nicht-transferierten Kontrollzellen. Auch transferierte mesenchymale Stammzellen exprimierten das gleiche Muster an Oberflächenantigenen wie nicht-transferierte Zellen. Des Weiteren wurden hoch aufgelöste zwei-dimensionale (2D) Muster mit verschiedenen Zelltypen und in unterschiedlichen Größen gedruckt, z.B. ein Schachbrettmuster bestehend aus zwei Hautzelltypen.

Im weiteren Verlauf wurden auch erfolgreich 3D Gewebe hergestellt. Dafür wurden verschiedene Hydrogele gestestet, von denen sich jedoch nur Kollagen als geeignet für den erfolgreichen Transfer und die anschließende Gewebebildung von Hautzellen erwies. Die Gewebe bestanden aus Fibroblasten und Keratinozyten und wurden zum einen *in vitro*, sowie zum anderen *in vivo* in der Rückenhautkammer in Mäusen kultiviert. Im Vorfeld konnte ich zeigen, dass diese Kammern eine adäquate Methode darstellen, um *in vivo* durch Tissue Engineering hergestellte Hautkonstrukte zu evaluieren. In den gedruckten Konstrukten entstanden Zell-Zell-Kontakte, insbesondere zwischen den Keratinozyten, welche eine epidermis-ähnliche Struktur erzeugten. Zellproliferation konnte über den gesamten Kultivierungszeitraum detektiert werden. Eine beginnende Differenzierung der gedruckten Keratinozyten konnte *in vivo* nachgewiesen werden.

Um in Zukunft eine klinische Anwendbarkeit des LIFTs zu erreichen, muss der von uns verwendete Aufbau vergrößert und an sterile Transferbedingungen angepasst werden. Ferner muss die Kultivierung der resultierenden großen Hautäquivalente etabliert und deren Testung im Großtiermodell durchgeführt werden. Weitere Zelltypen sollen integriert werden, insbesondere vorgeformte Muster von Endothelzellen, um eine schnelle Vaskularisierung und damit ein besseres Einwachsen des Hautersatzes zu erreichen.

Zusammenfassend kann gesagt werden, dass Bioprinting ein großes Potential im Bereich des Tissue Engineerings und seiner verschiedenen Anwendungen bietet, wobei die verwendete Matrix - wie am Beispiel der Hautherstellung zu sehen ist - an die verwendeten Zellen angepasst werden muss.

Stichpunkte: Hautersatz, Verbrennungen, Laserinduzierter Vorwärtstransfer (LIFT)

Abstract

Burn injuries occur in many different situations in life, comprising e.g. sunburns, scalding, explosions of gas, and chemical or barbecue accidents. While superficial burns heal spontaneously without problems, large and deep burn injuries frequently cause major complications like infections and burn disease. To avoid this and to enable the regeneration of the skin, the wounds are covered with autologous skin subsequent to the removal of the burned skin. However, this often does not suffice. Also, scarring often occurs, leading to impairments on the aesthetical as well as on the functional level. Up to now, no totally satisfactory skin equivalents for the treatment of burns have been produced as the existing ones lack hair follicles and sebaceous and sweat glands. Also, large grafts often do not grow in due to insufficient vascularisation.

Therefore, the long term aim of our research is the development of a skin equivalent that is able to mimic the properties of a normal skin as well as possible and allows for the fast and permanent wound coverage of burn injuries. My short term goal was the establishment and use of a laser based bioprinting technique, namely the laser induced forward transfer (LIFT), for the production of a simple skin equivalent with its specific three-dimensional (3D) composition. As its unique feature, LIFT allows for the precise spatial positioning of cells in a high resolution.

Several cell types - including cell lines as well as primary cells - were transferred without harm and survived the LIFT process to a high degree, without changes in their phenotype compared to non-transferred control cells. Transferred mesenchymal stem cells expressed the same surface antigenes as non-transferred cells. Furthermore, high resolution two-dimensional (2D) patterns of different cell types and different sizes were printed, e.g. a chess board pattern composed of different skin cells.

Continuative, also 3D tissues consisting of keratinocytes transferred on top of fibroblasts were printed. For the 3D printing process, different hydrogels were tested, but only collagen was suitable for the successful transfer and subsequent tissue formation of skin cells. The tissue was successfully cultured *in vitro* as well as *in vivo* employing the dorsal skin fold chamber in mice. The chamber was previously shown by me to be a suitable means for the *in vivo* assessment of tissue engineered skin constructs. Cell-cell-contacts were established in our printed skin constructs, especially between the keratinocytes, which formed an epidermis-like structure. Cell-proliferation could be detected during the whole culturing period, while starting differentiation of the printed keratinocytes could be perceived *in vivo*.

In future, to reach clinical applicability, our LIFT setup has to be expanded and adapted to sterile transfer conditions. Furthermore, the cultivation of the resulting large skin equivalents needs to be established and these large equivalents should be tested in a large animal model. Further cells types should be included, especially preformed patterns of endothelial cells to achieve a fast vascularisation and better ingrowth of the skin substitutes.

In conclusion, it can be said that bioprinting offers a great potential in tissue engineering und its various applications, but - as demonstrated by the skin tissue generation - the used matrix needs to be adapted to the employed cell types.

Keywords: skin substitute, burn injuries, laser induced forward transfer (LIFT)

Contents

List of abbreviations

2D	Two-dimensional
2PP	Two-photon polymerization
3D	Three-dimensional
AMG	Arzneimittelgesetz
AMM	Amniotic mesenchymal stem cells
ASC	Adipose-derived mesenchymal stem cells
ATMP	Advanced therapies medicinal products
bFGF	Basic fibroblast growth factor
BM-MNCs	Bone marrow derived mononuclear cells
bmMSC	Bone marrow derived mesenchymal stem cells
BMP-2	Bone morphogenetic protein 2
BSA	Bovine serum albumin
CAF	Carcinoma-associated fibroblasts
cDNA	Complementary DNA
CE	Cornified envelope
CFDA	Carboxy-fluorescein-diacetate
CSC	Cancer stem cells
CTA	Committee for Advanced Therapies
Cx	Connexins
DMEM	Dulbecco's modified Eagle's medium
DNA	Desoxyribonucleic acid
EC	Endothelial cells
ECFCs	Endothelial colony forming cells
ECM	Extracellular matrix
EDTA	Ethylenediaminetetraacetic acid
EGF	Epidermal growth factor
EMA	European Medicines Agency
EPCs	Endothelial progenitor cells
EU	European Union
FACS	Fluorescence activated cell sorting
FBS	Foetal bovine serum
FDA	Food and Drug Administration
FDA	Fluorescein-diacetate
FP	Fluorescent proteins
GewebeG	Gewebegesetz
GFP	Green fluorescent protein
GMP	Good manufacturing practice
H&E	Haematoxylin and eosin
HBSS	Hank's balanced salt solution
HPV	Human papilloma virus
HUVEC	Human umbilical vein endothelial cells
IGF-1	Insulin-like growth factor
IL-8	Interleukin 8
KGF	Keratinocyte growth factor
LaBP	Laser assisted bioprinting
LIFT	Laser induced forward transfer
LLNA	Local lymph node assay
LY	Lucifer yellow

MIC	Minimum inhibitory concentration
MSC	Mesenchymal stem cells
$NaHCO_3$	Sodium hydrogencarbonate
PBS	Phosphate buffered saline
PEG	Poly(ethylene glycol)
PEGDMA	Poly(ethylene glycol) dimethacrylate
PEG-tube	Percutaneous endoscopic gastrostomy tube
PI	Propidium iodide
RNA	Ribonucleic acid
SDF-1	Stromal cell-derived factor-1
SDS-PAGE	Sodium dodecyl-sulfate-polyacrylamide gel electrophoresis
SEM	Standard error of the mean
SVF	Stromal vascular fraction
TA	Transit amplifying cell
TFG	Transfusionsgesetz
TGase	Transglutaminase
TPG	Transplantationsgesetz
VEGF	Vascular endothelial growth factor
WST-1	Water-soluble tetrazolium salt

1 Introduction

Burn injuries occur in many different situations in life, reaching from sunburn or accidental scalding with hot coffee in everyday life to special injuries due to electricity or chemicals. Burns can be caused by many means like heat, electricity, chemicals, light, irradiation or friction in the form of liquid, gas, vapour, flames, explosions, electric current, lightning or intense solar irradiation (sunburn). They appear not only in form of domestic (e.g. scalding, barbecue accident) or work accidents (e.g. chemicals) but also in traffic (e.g. cars, trains, planes) or military actions (e.g. gunshot residues) [128], [69, chapter 2].

Light burn injuries occur with an incidence of 6 ‰, severe ones with 0.02 to 0.05 ‰, respectively [1]. The most frequent form of deep and large burn injuries is the scalding with hot water, soups or sauces, especially when young children or elderly persons are involved [69, chapter 2]. It accounts for up to 70 % of the burns in toddlers [1]. The ranking order proceeds with flame burns, house fires, and flash burns, the latter including explosions of natural gas, propane or gasoline [69, chapter 2]. While adolescents are mainly hurt due to improper handling of fire and flammable liquids (e.g. gasoline), with adults, flame burn is the most common type of burn wounds, a third of them being work accidents [1]. The next common type of injuries are contact burns, caused by hot metals, plastic, glass, coals or stoves [69, chapter 9]. Electrical or chemical burn injuries are more seldom. In any case, the extent of tissue destruction is always dependent on the present temperature as well as the duration of contact and the thickness of the involved skin [69, chapter 9].

Unfortunately, in case of large and deep burns, appropriate treatment only has limited success (see section 1.2.2.4). After removal of the burned skin, autologous split-thickness skin grafts are used to cover the burn wounds and to enable skin regeneration and protection against infections as well as fluid and temperature loss. Nevertheless, scarring often occurs. This is especially disturbing on the aesthetic but also on the functional level as e. g. the fingers cannot be completely stretched out any more. Skin substitutes do not provide hair follicles, sebaceous or sweat glands and large grafts may fail to take due to insufficient vascularisation.

Therefore, a skin substitute as similar to physiological skin as possible is needed. This, however, is the long term goal of our research. As a preparation, this thesis focuses on the establishment of the laser induced forward transfer (LIFT) for the production of a suitable skin equivalent. Transferred cells were assessed for potential damage, hydrogels were tested for their suitability during the transfer process and printed 3D skin constructs were examined for viability, tissue formation, and keratinocyte differentiation *in vitro* as well as *in vivo*.

In the following, the introduction first describes the composition and organisation of skin, subsequently turning to burn injuries, which includes the occurring problems and possible treatments. The field of tissue engineering and its challenges are specified. This is followed by an overview of skin equivalents used in research. The existing methods of bioprinting as an important means for the creation of engineered tissue are described. Subsequently, the bioprinting setup used for the experiments of this thesis is depicted in detail.

1.1 Skin - function and structure

1.1.1 Function

The skin is the largest organ in the human body, having a surface area of 1.5 to 2 m^2 and a weight of 3 to 10 kg [155], [107], [156]. Covering the whole body, it represents an effective barrier between the organism (inside) and the environment (outside). As such, it functions as a powerful protection against harmful environmental influences. These comprise chemical, mechanical, and thermal factors as well as pathogens and irradiation [155], [107], [156]. Regarding these harmful factors, a very important function is the maintenance of temperature and water balance homeostasis [107]. If this is impaired, liquid, electrolyte, and protein losses can strongly damage the body, as in case of severe burns (see section 1.2.1.3). Moreover, the skin plays a role in metabolism and is part of the immune system. In this context, Langerhans cells are the antigen presenting cells which can be found in the skin. They are, however, supported by macrophages, leucocytes, plasma cells, mast cells and antimicrobial peptides (defensins) of the innate immune system [155], [107], [156]. Also, the acid mantle of the skin, with a pH of 5.5 to 5.7, plays an important role in the protection against pathogens [107], [156]. Furthermore, the apical surface of the skin is inhabited by various bacteria and fungi, which are the normal skin flora and contribute to its protecting function. As commensals they protect their habitat - and thereby us - against pathogenic microorganisms [155]. Finally, the skin acts as a sensory organ, being able to detect pain, contact, pressure, vibration, itching, and temperature [107], [156].

On the social level, the skin serves as a means for representation, communication, and displaying the current mood. Communication and expression of mood are tightly connected, being shown by e.g. blushing or blanching. Representation also affects our communication and serves as a statement about ourselves. Depending on age, situation and culture, e.g. a non-covered part of the body may be understood as appropriate (e.g. on the beach) or unfitting (e.g. during business meetings). Furthermore, the skin is also used to express oneself by tattoos. Moreover, the skin colour may state a person's likings and habits, e.g. having tanned skin due to staying outside often in contrast to regularly visiting a solarium. Even hair can send optical signals with social, cultural, psychological or political content. In this context, the form, colour, and presence/absence of the scalp hair as well as the beard are of central significance [156].

1.1.2 Structure

The skin is composed of four layers, namely the epidermis, the basement membrane, the dermis, and the hypodermis (see picture 1.1). All of these structures, except the basement membrane, contain various specialised cell types and serve different purposes.

1.1.2.1 Epidermis

The epidermis is the uppermost skin layer, consisting of a multi-layered stratified squamous epithelium [155], [107], [156]. Depending on where on the body it is

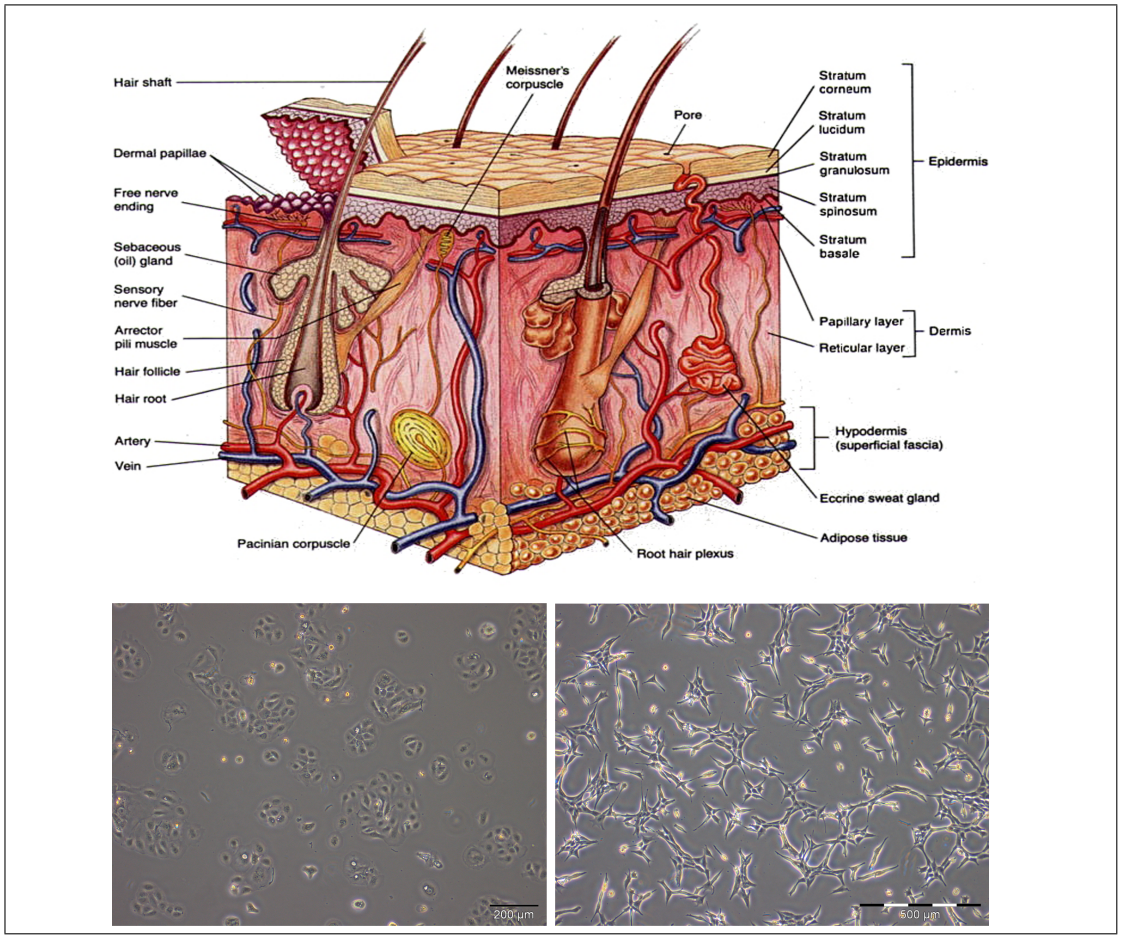

Figure 1.1: Structure of skin and pictures of skin cells The figure depicts the structure of human skin, including the epidermis with its different layers (stratae), the dermis, and the hypodermis (A). In the upper left corner, the dermal papillae can be seen. The blood vessels form two connected networks, one at the connective zone between the dermis and the hypodermis, while the other penetrates the dermal papillae and as such supplies the epidermis with oxygen and nutrients. Nerves, sebaceous glands, hair follicles/hairs, and sweat glands reside in the dermis and partially penetrate through the epidermis. In (B) and (C), the cultured human cell lines I used in the underlying experiments can be seen in phase contrast microscopy. (B = HaCaT, human keratinocytes, C = NIH3T3, murine fibroblasts) (origin of (A) [2])

located, it is usually around 0.05 mm thick, but can reach a thickness of up to several millimetres at the palms and the sole of the feet [156]. The epidermis regenerates continuously throughout life with a turnover rate of about 30 to 56 days in healthy persons [84], [155] and comprises four layers (from bottom to top):

- Basal layer (*stratum basale*)
- Spinous layer (*stratum spinosum*)
- Granular layer (*stratum granulosum*)
- Cornified layer (*stratum corneum*)

The main constituent of the epidermis - with up to 90 % - are keratinocytes. Among those, epidermal stem cells, residing at the basal layer, are responsible

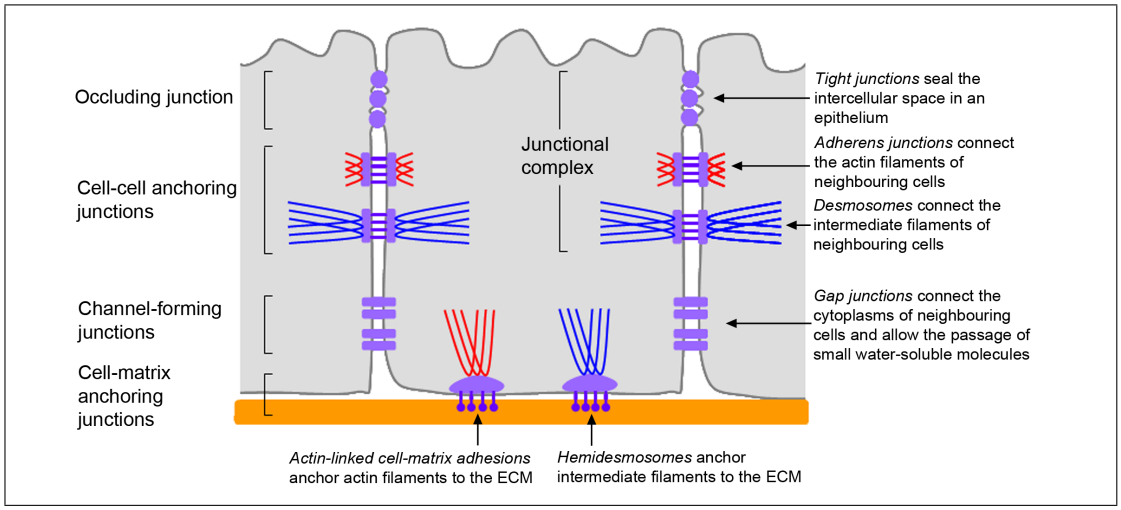

Figure 1.2: Scheme of the different cell-cell and cell-matrix junctions in epithelia Tight junctions at the apical part of the cells form a tight barrier between the upper and the lower part of the epithelium. Adherens junctions are coupled to actin filaments in the cells, and play a role in the mechanical stability of the epithelium by providing a stable cell-cell contact. Desmosomes are responsible for the mechanical stability as well, coupling neighbouring cells by connecting their intermediate filaments. Together, these three types of junctions are called the junctional complex, and can often be found close to each other. Gap junctions form channels between the cytoplasms of neighbouring cells, contributing to cell-cell communication. Cell-matrix adhesion is either imparted by hemidesmosomes, which couple the ECM to intermediate filaments, or by actin-linked cell-matrix adhesions. (Scheme according to [4, chapter 19])

for the regenerative capacity of the epidermis, leading to a continuous turnover. They are characterized by a slow cell cycle, a long life span, and a high proliferative potential. β1-Integrin imparts adhesion to the basal membrane and is thought to inhibit differentiation of the stem cells [72]. The epidermal stem cells express cytokeratins 5 and 14 and can be divided into interfollicular stem cells, hair follicle stem cells, and sebaceous gland stem cells [84], [107].

Different cell-cell and cell-matrix junctions are needed to form a stable epithelium. Adherens junctions and desmosomes provide a mechanical connection and thereby mechanical strength between neighbouring cells, while hemidesmosomes and actin-linked cell-matrix adhesions are responsible for the coupling of cells to the underlying basement membrane (see picture 1.3 and table 1.1). Adherens junctions contain classical cadherins as transmembrane adhesion proteins. Especially e-cadherin is abundantly found in the epidermis. While in case of adherens junctions the adhesion proteins are coupled to the actin filaments of the cytoskeletton, in desmosomes they are connected to intermediate filaments. A similar situation can be found in cell-matrix interactions. In hemidesmosomes extracellular matrix (ECM) molecules are connected to the intermediate filaments of the cells, whereas in actin-linked cell-matrix adhesions actin is linked to the ECM. The cell-matrix adhesion is realised by integrins, which are situated between the cell-originating filaments and the ECM molecules [4, chapter 19].

Tight junctions (see picture 1.3) close the intercellular space and thereby constitute a tight barrier between the apical and the basal part of the epithelium, contributing to its structural polarisation. The barrier, however, has a selective permeability, which can be altered depending on the circumstances [4, chapter 19].

Table 1.1: Anchoring junctions. (According to [4, chapter 19])

Junction	Transmembrane adhesion protein	extracellular ligand	intracellular cytoskeletal attachment	intracellular anchor proteins
Cell-cell				
adherens junction	cadherin (classical cadherin)	cadherin in neighbouring cell	actin filaments	e.g. α-catenin, β-catenin, plakoglobin (γ-catenin)
desmosome	cadherin (desmoglein, desmocollin)	desmoglein and desmocollin in neighbouring cell	intermediate filaments	e.g. plakoglobin (γ-catenin), desmoplakin
Cell-matrix				
actin-linked cell-matrix adhesion	integrins	extracellular matrix proteins	actin filaments	e.g. talin, vinculin, α-actinin, filamin
hemidesmosome	integrin α6β4, type XVII collagen	extracellular matrix proteins	intermediate filaments	e.g. plectin, dystonin

Moreover, gap junctions can be found to form channels between the cytoplasms of neighbouring cells via transmembrane proteins (connexins). They serve the exchange of low molecular substances (e.g. hormones, glucose, or vitamins) as well as ions (e.g. electrical coupling in the heart muscle) and furthermore are essential for cell-cell communication [4, chapter 19].

During their differentiation, keratinocytes undergo many biochemical and morphological changes [84], [72], [138]. After the division of a stem cell, one daughter cell may become a transit amplifying cell (TA) while the other remains a stem cell. The TA completes a few more proliferation cycles before being submitted to terminal differentiation. During this process, the TA looses its replicative capability and starts to produce different proteins, among which cytokeratins 1 and 10 can be found [107]. Profilaggrin is the major protein component of the now occurring keratohyalin granules. When processed, the mature filaggrin helps the cytokeratins to form tight bundles of intermediate filaments, which are important for the structural integrity of the cell and finally promote the collapse of the cell into a flattened shape [72].

The so-called cornified envelope (CE) develops just below the cytoplasmic membrane, and consists of proteins like e.g. involucrin, loricrin (main protein component), filaggrin, and trichohyalin as well as different lipids. The development of the lipid part of the CE is connected to the degradation of the organelles and is formed via fusion of their surrounding membranes with the plasma membrane [72]. Thereby, also cell-cell junction proteins like the components of desmosomes are incorporated into the CE. Both, proteins and lipids, are covalently linked, with the linking being catalysed by three different transglutaminases (TGase). The activity of the present TGases is induced by a rising calcium concentration [44].

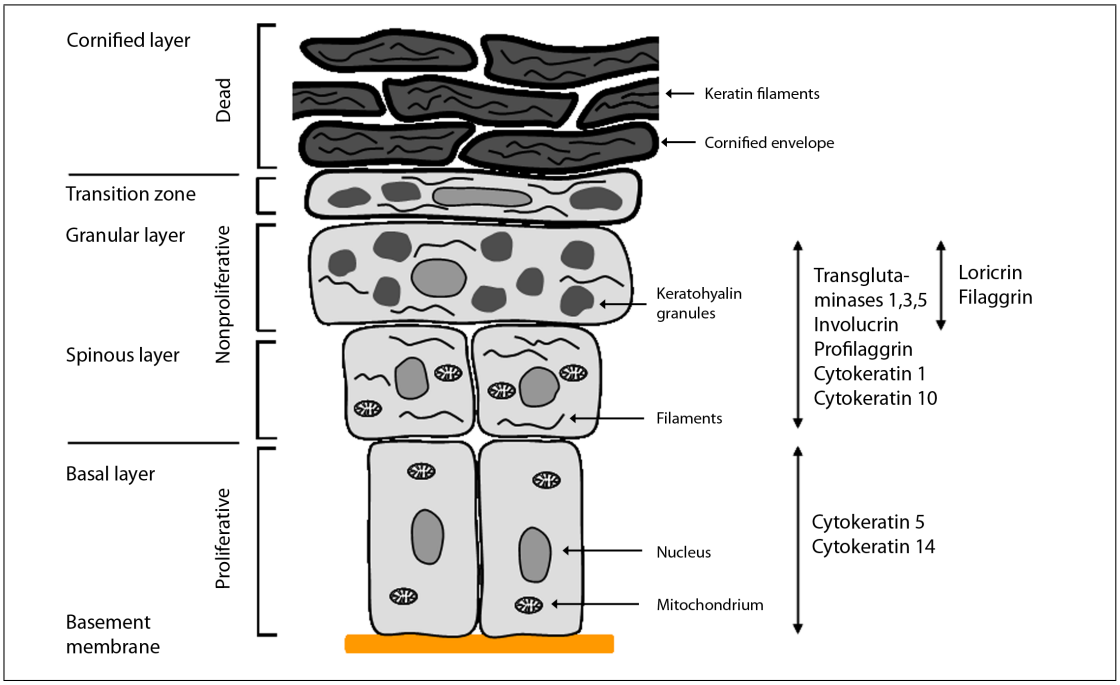

Figure 1.3: Scheme of keratinocyte differentiation The keratinocytes in the basal layer proliferate, being responsible for the turn-over of the skin. The differentiating keratinocytes produce different proteins, which form tight bundles of intermediate filaments. Among these, cytokeratin 1, cytokeratin 10, profilaggrin, filaggrin, involucrin and loricrin can be found. The proteins are connected covalently by transglutaminases. Keratohyalin granules develop, being filled with e.g. profilaggrin. The cornified envelope (CE) starts to develop directly beneath the cytoplasmic membrane, being composed of the mentioned proteins as well as lipids. The cell organelles are destroyed and their membranes are incorporated into the CE. In the last step, the cells die and form horny, flat flakes, which are embedded into a self-produced intercellular lipid matrix.

In the transition phase the cells commit programmed cell death. They are now called corneocytes, and are embedded into a self-produced intercellular lipid matrix, comprising cholesterol, free fatty acids and other lipids. They form lateral lipid lamellae with a repeating pattern, using ceramides (special lipids) as a template. The low permeability of skin to water is due to these tightly packed lipids. As such, the epidermis serves as a tight permeability barrier, starting with the *stratum corneum* as the uppermost layer. Nevertheless, also the lower layers contribute to the barrier function via the formation of tight junction. The cells are now largely filled with intermediate filaments, while the plasma membrane is replaced by the CE, the organelles are destroyed and the desoxyribonucleic acid (DNA) is degraded. Several cells together form horny flakes, the uppermost layer of the skin. The final shedding off of the corneocytes is called desquamation and is imparted by the degradation of desmosomes [72].

The balance between proliferation and differentiation needs to be controlled tightly. It is accompanied, and partly induced, by a rising intracellular Ca^{2+} concentration in direction to the apical surface, and among other regulative factors p63 plays a central role in this situation [84]. If the differentiation is impaired, a disturbance of the skin barrier may occur, resulting in the formation of inflammation, dermatitis, ichthyosis, psoriasis, and the entry of pathogens [138].

Apart from keratinocytes, melanocytes are resident in the epidermis. They are located in the basal layer, having contact to the basement membrane and the keratinocytes. Melanocytes exhibit a star shaped appearance and are responsible for the skin colour. By synthesis of melanin and its distribution to the surrounding keratinocytes, melanocytes protect the skin cells against UV irradiation and corresponding mutagenesis [155], [156].

Langerhans cells are the immune cells present in the epidermis, being responsible for antigen presentation as well as activation of T-cells [155].

The epidermis is free of blood vessels, being supplied with nutrition and oxygen by the dermis via diffusion [155], [107]. At the dermal-epidermal-junction both layers interdigitate, forming the rete ridges (epidermal part) and the papillae (dermal part) [107], [4, chapter 19]. This results in a high increase of the available surface for diffusion (see also section 1.1.2.3). The rete ridges/papillae are also very important for the mechanical stability of the skin, as they greatly increase the resistance of skin against shear forces.

1.1.2.2 Basement membrane

The basement membrane consists of extracellular matrix and connects the epidermis to the dermis. It is essential for the attachment of the epidermal epithelium to the connective tissue of the dermis. Furthermore, it stabilises the connection between the epithelial cells of the basal layer and prevents them from sliding apart. The basement membrane also promotes cell survival, proliferation and differentiation of the cells [4, chapter 19]. It is partly secreted by the epidermal cells and partly by the dermal cells, containing e.g. collagen type IV and VII, glycoproteins like laminin and fibronectin, nidogen, proteoglycans, and integrins [156]. Collagen type IV forms a felt-like network and gives the basement membrane its tensile strength, while most of the other components are integrated in this network. Collagen type VII forms anchoring fibrils, which help to attach the basement membrane to the underlying connective tissue [4, chapter 19], [107].

The basement membrane keeps the keratinocytes and fibroblasts in their respective spatial compartments, but can be passed by macrophages, lymphocytes or nerve cells. These cells possess distinct enzymes, which can degrade the components of the membrane [4, chapter 19]. Also, nutrients, oxygen, and metabolites can pass the membrane [4, chapter 19].

1.1.2.3 Dermis

The dermis is located beneath the epidermis and the basement membrane and varies between 0.6 mm thickness at the eyelids and more than 3 mm at the back and the sole of the feet. Its uppermost part, the papillary region (*stratum papillare*), contains most of the cells present in the dermis, while its lower part, the reticular region (*stratum reticulare*), includes hair follicles and glands [155].

The dermis is composed of abundantly present ECM, which is secreted by fibroblasts, the main cell type in the dermis [19]. The ECM contains proteoglycanes and glycoproteins, which bind liquid in form of hydrated water [19]. The resulting gel-like substance of the ECM can resist compressive forces very well, while simultaneously permitting diffusion of nutrients, metabolites and hormones [4, chapter 19]. Some free liquid resembles blood plasma and is collected by lym-

phatic vessels. Interweaving collagen type I enhances the mechanical stability of the dermis. The large elasticity of skin is manily due to elastic fibres formed by elastin [4, chapter 19], [107]. The interaction between the ECM, the water, and the cells is responsible for the pliability of the connective tissue. As such, the dermis also serves as a layer between skin and muscles.

In contrast to the epidermis, the dermis is strongly perfused by two plexuses of vessels. One is located directly above the hypodermis and comprises larger vessels, while the second plexus consists of a tight network of capillaries reaching into the papillae, the border zone to the epidermis [107], [156]. Apart from serving the nutrition of the dermis and epidermis, the blood vessels also supply the present sebaceous and perspiratory glands as well as the hair follicles. Furthermore, the blood vessels play an important role in the temperature regulation of the body [156]. Additionally, the dermis contains specialised nerves, which help us to perceive sensations like pain, touch, itch, and temperature [155]. Finally, cells of the innate as well as the adapted immune system are also located in the dermis: mast cells, macrophages, leucocytes and plasma cells [19], [107], [156].

1.1.2.4 Hypodermis

The hypodermis consists of connective tissue and fat. It serves as energy store, heat insulation, and protection against mechanical influences. Also, hormones are synthesised there [156]. Furthermore, the hypodermis connects the upper skin layers to the lower tissues, e.g. muscles, fascia, and bone. Apart from nerves, sensory organs, and glands it also contains a plexus of vessels, which are larger than those in the dermis, supplying the glands and hair bulges with nutrients and oxygen. In the hypodermis, adipocytes [156] as well as stem cells [179] can be found.

1.1.2.5 Cutaneous appendages

The skin not only forms different layers like the epidermis, dermis, and hypodermis, but also contains several cutaneous appendages formed by their specific cells. Those appendages comprise hair bulges/hair, nails, sebaceous glands, perspiratory glands, scent glands, and mammary glands [107], [156]. Mammary glands are responsible for feeding the offspring. While perspiratory glands are involved in temperature homoeostasis, the sebum produced by sebaceous glands keeps the skin and the hair pliable. Hair growth is sex specific and hormone dependent. Various specialized hair forms can be found as eyelashes, eyebrows, beard hairs, pubic and axillary hair, and hair in the nose or the outer ear canal. Generally, hairs protect the body from heat loss but are also involved in the tactile sensation [156]. An even more specialised version is represented by nails, which offer protection against mechanical injuries as well as support for the tactile ability of skin.

1.2 Burn injuries - problems and treatment

Large and severe burn injuries often change the patient's and his/her relatives' life profoundly. Questions concerning the injuries, as such, as well as their consequences occur and reach from the actual treatment, pain, and the possible

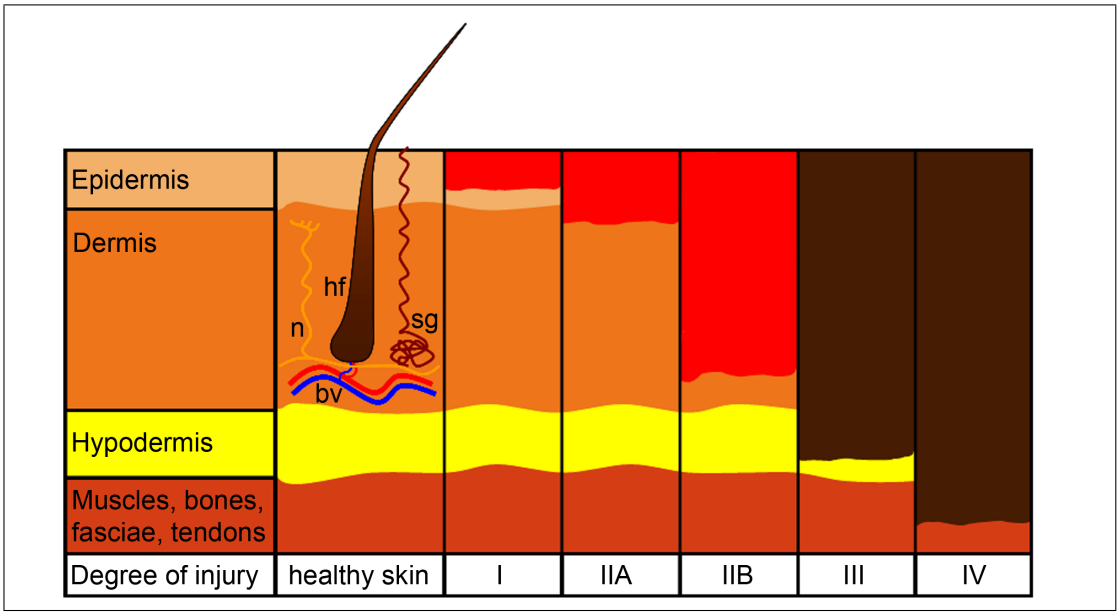

Figure 1.4: Scheme of the four degrees of burn injuries The figure shows the different degrees of possible burn injuries. As can be seen by the red and brown colour, respectively, different parts of the epidermis, dermis, hypodermis or underlying tissue structures are destroyed in the different degrees. This may include hair follicles (hf), nerves (n), sweat glands (sg) and blood vessels (bv).

aesthetic outcome, to doubts concerning self-esteem, future job possibilities, and financial security of oneself and the family. Often, several plastic operations may be required during the next years after the burn injury. Hence, stress with respect to the actual trauma, but also to the healing process and the possible disfiguration, frequently appears in the patients and their relatives. Therefore, psychological support from the first days after the trauma to several years afterwards is provided.

1.2.1 Frequent problems

1.2.1.1 Classification into four degrees

Burn injuries result in a local inflammatory response accompanied by reddening and swelling. They are classified into four degrees, depending on which skin structures are destroyed (see figure 1.4). If only the epidermis is concerned - like in case of sunburn - the burn injury is classified as degree I and is accompanied by weak to moderate pain and reddening. It normally heals without any problems. Burns leading to blistering between the epidermis and the dermis are classified as degree II and are characterized by strong pain and reddening. Here, a difference is defined between II A and II B burn injuries. The first is relatively superficial, only concerning the upper parts of the dermis. Thereby, the nerves, blood vessels and the elasticity of the skin are only destroyed scarcely and the skin often heals spontaneously without scarring. In contrast, in case of II B burns, the deeper parts of the dermis are also affected and scarring occurs due to impaired regeneration capacities, leading to irreversible damage. If all skin layers including the hypodermis are affected, burns of degree III are existent. As also the nerves are affected, no pain can be felt in the burned area. In case of even deeper burns

including muscles and bones, degree IV burns are present. Degree III and IV burn injuries include necrosis of the tissue and eschar formation and therefore need surgical and intensive care treatment (see section 1.2.2). Both represent irreversible damages to the included tissues.

Beside the depth and extent of the burn injuries, other factors, including the patient's age, are of central importance for the outcome. For example, victims of traffic accidents often have other injuries as well (co-morbidities). The larger the burned body surface and the deeper the burn, the worse the consequences and the worse the prognosis [69, chapter 4]. The prognosis is even worse for patients who suffer from co-morbidities as well as inhalation trauma.

1.2.1.2 Loss of barrier function

The main problem in case of burn injuries consists in the loss of the barrier function of the skin. As the cells of the immune system, especially the Langerhans cells, are mainly present in the epidermis, the loss of this barrier function already plays a role if only the epidermis is affected. In case of extensive and deep burns, massive infections including sepsis, pneumonia, urinary tract infections or endocarditis may occur due to the penetration of the body with pathogens, especially bacteria and fungi [69, chapter 11]. Temperature and water balance homeostasis are impaired if the dermis is destroyed because many of the blood vessels regulating, e.g. the temperature, are lacking. Therefore, patients are endangered by hypothermia, especially if the hypodermis is also affected by the injuries.

1.2.1.3 Burn disease and other complications

In case of large burn injuries, also the great water loss via vapour from the burned skin area poses a great threat to the patients. Additionally, due to inflammatory mediators, the blood vessels become more permeable, leading to so called capillary leakage. Liquid from the blood penetrates the surrounding tissues, resulting in massive oedemas and a dangerous decrease of blood volume (hypovolemia) as well as electrolyte imbalance [69, chapter 7]. This, in turn, entails a state of circulatory shock in the patient, which adds to the life threatening burn disease. This is further characterised by the leakage of blood plasma (including solved proteins) into the tissue. Since the blood cells remain in the vessels, the viscosity of the blood increases drastically. At the same time, the protein loss from the blood leads to a further liquid deprivation in the vessels. The destroyed tissue and denatured proteins have toxic effects, which in combination with the aforementioned situation lead to organ failure (e.g. of the kidneys, the lungs or the liver).

Another complication is represented by circumferential burns of digits, extremities or the thorax, which may lead to the compartment syndrome. As described above, burn injuries cause local swelling, which in case of a circumferential burn may result in a strong compression of nerves, muscles, and blood vessels, the latter leading to constricted circulation. This, in turn, leads to necrosis of the tissue due to lack of oxygenation. The compartment syndrome is a life and limb threatening condition. If the thorax is affected, ventilation may be impaired.

1.2.2 Possibilities of treatment including clinically used skin substitutes

1.2.2.1 Small and superficial burn injuries

Depending on the severity of the burn injuries, different treatment measures are needed. In case of small and superficial burns, quick cooling with lukewarm low-germ tap water reduces pain and the expansion of the burned area. The application of ice should be avoided because this may result in frostbite. Subsequent, a sterile wound coverage should be applied and a physician should be consulted. The wounds will normally heal spontaneously without scarring, helped by special ointments [128].

1.2.2.2 Large and deep burn injuries - burn centres

In case of a large burned area, cooling may result in drastic temperature loss of the whole body, which should be avoided. In any case, an emergency call is necessary. If the patient is unconscious, the recovery position needs to be applied.

For large and deep burns, which may lead to the burn disease, the treatment in specific burn intensive care units present in burn centres is necessary to provide an adequate therapy and monitoring of the patients. The monitoring includes parameters such as blood pressure, pulse rate, temperature, weight, and urine output. Burn centres provide specifically trained surgeons and nurses as well as anaesthesiologists, respiratory therapists, rehabilitation therapists, nutritionists, and psychologists. Also, the availability of an own operation theatre which can be heated to reach body temperature and other measures like pre-heating the infusions are important to counteract cooling [69, chapter 12]. To contribute to infection prevention, each patient is isolated in an own room. These rooms can also be heated to prevent hypothermia. The daily routine tasks need to be done in an aseptic manner.

1.2.2.3 Stabilisation of the patients and debridement

During the therapy, the first priority is the stabilisation of the patient's vital functions. This already begins directly when the emergency doctor arrives at the accident location [69, chapter 6]. To counteract the burn disease and hypovolemia, infusions with e.g. Ringer's lactate solution as volume replacement are one of the first and main elements of the therapy [69, chapters 7 and 8]. However, the choice and amount of infusion solutions depends on age as well as injury severity, physiological status, associated injuries, and the (non-)existence of inhalation trauma. Additionally, after reaching the burn centre, the necrotic and avital tissue needs to be removed quickly and completely by surgical excision (debridement) during anaesthesia [128], [164]. On one hand, damaged tissue still contributes to the burn disease by producing toxins and inflammation and therefore has to be removed. On the other hand, the debridement serves to avoid infections with bacteria and fungi. If, in spite of this, infections occur, they are consequently treated with systemically applied antibiotics or antifungals and topical antiseptic dressings [69, chapter 11]. Additionally, adequate infection prevention is needed.

Special care is indicated in case of circumferential burns. Here, the elevation of the limb may help but in severe cases an escharotomy (a cut through the eschar and underlying tissue down to the fasciae) is required to release the threatening pressure and to avoid the compartment syndrome or problems with ventilation. Special attention is required in case of burned hands, as nerves can easily be destroyed [128].

Of course, an appropriate analgesic treatment is required in any case, which reaches from simple analgesics like ibuprofen to narcotics, depending on the patient's state. Often, opioids are required. Another major issue is the suitable nourishment of the patient. This is very important as malnutrition leads to impaired healing. The nourishment can first be done by infusions (parenteral nourishment), but this may cause severe compliations. It is advised to switch to enteral modes of nutrition as soon as possible (nasogastric feeding tube, PEG-tube). Altogether, burn patients have an elevated basal metabolic rate.

1.2.2.4 Wound coverage - skin equivalents - skin grafts

After the patients are stabilized and the debridement is completed, wound healing and treatment come to the fore. In case of degree II burns, fresh wounds may be covered with e.g. hydrocolloid dressings, Suprathel® or Biobrane®. The wound coverages form a semi permeable protection until wound healing is completed [128], [165], [69, chapter 4]. Hydrocolloid dressings comprise a gently adherent inner layer, a methyl cellulose absorbent middle layer, and a semipermeable outer layer. Thereby, a moist wound environment is created, while wound exudate is absorbed [69, chapter 15]. Biobrane® consists of knitted nylon threads coated with porcine collagen with a silicone layer on top. It works especially well in case of superficial and moderate depth partial thickness burns and can also be applied subsequent to dermabrasion and skin-graft harvesting. In burn care, it reduces pain, healing time, and inpatient stay compared to traditional dressings [20], [169], especially in infants and children [86]. Although Suprathel®, which is a co-polymer consisting of polylactide, trimethylene carbonate and ε-caprolactone, is completely synthetic, it behaves like a biological dressing and exhibits properties of natural epithelium. Since no animal derived components are used, no risk of infection occurs, and the dressing is acceptable to all religious and ethnic groups [70]. Suprathel® is often used for partial thickness burns, and can be applied especially well for children, which often exhibit mixed depth wounds [70]. It offers a high elasticity, high water permeability, and transparency after application [106]. Furthermore, pain is greatly reduced and Suprathel® is well accepted by patients due to easy and painless dressing changes [70], [149].

In contrast, large and deep wounds (degree III and IV) normally require surgical closure with skin derivatives. In this situation, plastic surgery takes effect. The gold standard of burn injury therapy is the coverage of the wounds with autologous split-thickness skin grafts, but special types of injuries may require other kinds of treatment. For example, in case of large electro traumata with destroyed soft tissue, skin flaps are used to reconstruct and cover the wounds [164]. The problem with electro traumata is the necrosis of deep mucle layers, whereas the superficial skin is sometimes less affected. Full-thickness skin grafts are also possible for small defects and are employed on hands and in the face, e.g. if eye lids are harmed [164].

Since in large and deep burns the protection normally given by native skin is missing during the healing process, a temporary coverage of the wounds is indicated to prevent infection and water as well as temperature loss. Also, the temporary coverage protects the wound against mechanical influences [69, chapter 15]. For this, collagen sheets or cadaver allograft like Alloderm® (allogeneic, decellularised human cryo preserved cadaveric skin, see also table 1.2) is employed [128]. In the course of wound healing, the Alloderm® is either integrated or rejected by the body [164]. To minimise the danger of viral disease transmission, Alloderm® is tested extensively for the potential presence of viruses [69, chapter 15].

Table 1.2: Skin substitutes used in burn treatment.

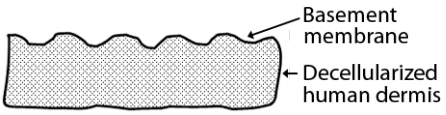	Alloderm®: Dermal equivalent consisting of allogeneic decellularised human cryo preserved cadaveric skin	[128], [164]
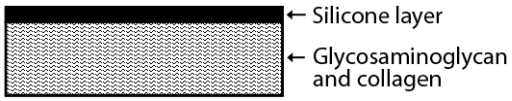	Integra®: Dermal equivalent consisting of glucosaminoglycan mixed with interwoven bovine collagen with a silicone layer on top	[27], [128], [69], [67]
	Matriderm®: Dermal equivalent consisting of a freeze dried collagen-elastin matrix	[65], [164], [144], [165]

For a successfull grafting and take of the graft, a good vascularisation of the existing wound bed is very important [128], either consisting of capillarised dermal layers (degree II) or muscle fasciae (degree III). If in case of very deep burns no sufficient dermal parts remain after the debridement, dermal substitutes are utilised to improve vascularisation of the wound bed. The wound is covered with Integra®, consisting of glycosaminoglycan (chondroitin-6-sulfate) mixed with interwoven bovine collagen and a silicone layer on top [27] (see also table 1.2). It is neovascularised from the wound bed prior to wound coverage with autologous split-thickness skin grafts or cultivated keratinocyte sheets in a second operation several weeks later (two step approach) [128], [69, chapter 12], [67]. Similarly, Matriderm® can be used as a dermal substitute, mainly being applied as coverage over joints [65] due to less scarring and more flexibility than Integra®. It consists of a collagen-elastin matrix [164] and is mostly used in a single-step operation in combination with split-thickness skin grafts [144], [165]. However, Matriderm® and Integra® do not differ with respect to quality of vascularisation, take rate, and thickness of resulting neodermis in a rat model [147]. Also, Alloderm® can be used as a dermal substitute [165]. In this case, the dermal substitute still possesses intact basement membrane proteins (laminin, collagen type IV and VII),

which might enhance keratinocyte adherence [69, chapter 15]. All of these dermal substitutes are gradually degraded and replaced by the patients' own tissue. Nevertheless, the time for a successful vascularisation is quite long. Besides, the high costs represent another drawback.

As just described, split-thickness skin grafts are used to cover the burn wounds. These grafts are taken from non burned areas, mainly the thighs. The nearer the donor region and the burned area lie together, the more similar are the skin colour and texture and the better is the outcome. If the available donor skin areas are too small, the skin grafts can be expanded by meshing (cutting the skin to reach a mesh structure after expansion). A further expansion is possible with the Meek-technique. Here, the donor skin is cut into small squares and attached to a carrier (e.g. silk) with space inbetween. Since burn injuries treated with meshing or Meek-technique never heal evenly and have a poor cosmetic appearance, both techniques are avoided in case of a burned face or hands. Broadly expanded skin is covered with allogeneic skin to improve healing [69, chapter 12], [165]. In any case, these techniques require an appropriate wound management at the donor site to minimise damage there.

To provide an epidermal replacement, autologous keratinocytes are applied. In this context, two different possibilities exist. In case of e.g. Epicell®, a biopsy of healthy skin is taken from the patient and keratinocytes are isolated and expanded in special laboratories. Subsequently, the cells are transferred to a special carrier, with which the wounds are covered. This technique requires the previous coverage of the wounds with Integra®. The advantage of this method is the use of autologous cells. The drawbacks are the long time period between the biopsy and the coverage (up to three weeks) as well as the fragility of the transplanted skin. Also, this method is quite expensive. Therefore, only patients with very large burned areas are treated this way [165], [128], [69, chapter 15]. Alternatively, as in case of e.g. ReCell®, epidermal cells (including melanocytes) can directly be isolated without a cultivation period and subsequently be applied to the burn wound. The major advantage of this approach is the fact that the cells can directly be applied to the patient without the need of culturing. Furthermore, the presence of melanocytes leads to an important improvement of the aesthetic aspect [165]. Even without melanocytes, keratinocytes applied by spray to face and neck burn injuries result in good cosmetic outcomes [64].

Regardless which treatment and which skin substitutes are used - either temporary or permanently - they are still highly imperfect [69, chapter 15]. As long as the deep dermis and possibly the hypodermis are destroyed, no sebaceous/perspiratory glands or hair follicles can regrow. This results in a poor cosmetic and functional outcome, which includes the lack of sweating in the burned areas. Therefore, a skin substitute containing all of these layers and components is highly desirable. This, however, is the long term goal of our research.

1.3 Tissue engineering

In surgery - especially in plastic and reconstructive surgery - one of the most important principles is to replace a special tissue with the same tissue, or if not available, at least with something as similar as possible. Here, tissue engineering is employed to artificially create tissues *in vitro* for their usage in patients, aim-

ing at the re-establishment, or the replacement, of the damaged tissue. Thereby, tissue engineering comprises a comprehensive field of disciplines and combinations of many different techniques and principles originating from engineering and materials sciences as well as life sciences.

As mentioned above in section 1.2.2.4, skin substitutes and autologous keratinocytes play an important role in burn treatment. Autologous cells are always the best way to replace missing tissue as they are not rejected by the immune system and do not carry the risk of infectious diseases. Many cell types may be used for the creation of skin equivalents, including fibroblasts, keratinocytes, and adipose derived stem cells.

Nevertheless, tissue engineering is not that simple as all cells highly depend on their immediate surroundings, the so-called microenvironment [75], [174]. The definition of a biological microenvironment includes the amount and density of certain cells and their defined 3D position in the tissue. Moreover, soluble factors, mechanical stimuli, and cell-cell contacts are very important. But also interactions between the cells and the ECM play an important role in the formation of tissue [4, chapter 19]. Especially stem cells are highly dependent on their microenvironment [47].

Therefore, specific cell culture methods have to be developed to ensure the best adapted way of tissue production and culturing. This is often realized by the use of special bioreactor systems. These provide physical, chemical, and mechanical stimuli, which are thought to influence the cells in the desired way, supplying a special biomimetic environment. This, in turn, stimulates the cells to produce their own needed ECM and cytokines to develop the desired tissue. In this context, self-assembly and self-organisation of cells are two of the main components for histogenesis and organogenesis [75].

In tissue engineering, cells are often seeded onto/into special pre-existing scaffolds, which vary concerning their substance, porosity, elasticity, stiffness, and shape, according to their specific uses. Typically, the scaffolds are needed to give the tissue its desired form and represent spatial templates. This aspect is especially important in case of bone engineering, as a certain mechanical strength is needed [142], [52], [96], [167]. However, it is very important that the cells are distributed evenly in the engineered tissue, provided that this is also the case in the original organ [75]. Apart from the aforementioned considerations, a very important factor of an engineered tissue is its integration - including the scaffold - into the host and the firm connection to the surrounding tissue. However, complications may arise after transplantation, often due to the scaffold material. These include a possible inflammatory response in the host, or a mechanical mismatch of the transplant with the surrounding tissues.

Alternatively, tissue engineering without a rigid scaffold exists, as in case of flexible tissues like skin. For the production of skin equivalents, often fibroblasts are seeded into a collagen type I gel, which is then kept under submerged culture conditions until the fibroblasts have contracted the gel. Subsequently, keratinocytes are seeded on top, which will then develop into a multi-keratinised epidermis when risen to the air-liquid-interface. This means, that the skin construct is supplied with nutrients and liquid from below, while the air from above serves as a differentiation stimulus to the keratinocytes. This mimics the natural physical conditions of skin growth. Furthermore, the culture medium contains

further supplements to induce differentiation, like hydrocortisone, ascorbic acid or cholera toxin [79], [168]. Under these conditions, the differentiation of the skin equivalents normally takes up to three weeks [148]. Additionally, other cell types than fibroblasts and keratinocytes may be added to the skin equivalents, to enhance their similarity to physiological skin (see also next section 1.4).

Especially in large tissues immediate and functional vascularisation is needed after transplantation to supply the tissue with nutrients and oxygen. In this regard, several approaches are possible, which are delineated in the discussion (section 4.3.2.1).

1.4 Existing skin equivalents in research

Tissue engineering, as described above, offers the possibility to provide skin equivalents for research, where they are urgently needed [85]. This includes the pharmacological as well as the cosmetic industry since *in vivo* animal experiments should be replaced by *in vitro* experiments whenever possible. The commonly used rabbit Draize test to assess the potentially harmful effects of new cosmetic ingredients does not always prove to be correct [97]. This test, as well as the also frequently used local lymph node assay (LLNA) in mice (OECD TG 429) [50], may show false positive or false negative results due to species differences between the respective animals and humans. Therefore, *in vitro* test systems using 3D skin equivalents need to be established and validated against existing and approved animal tests. The validation process is very extensive and lasts several years. However, based on the physiological similarity of 3D skin equivalents to natural skin, some equivalents are already accepted as a valid alternative to animal testing [56].

Many different skin equivalents are being developed continuously, including in-house skin equivalents of different research groups as well as already commercially available ones (also see tables 1.3, 1.4 and 1.5). In any case, an organotypic - meaning 3D - culture of skin cells is important, mimicking the structure of natural skin and therefore presenting better interactions of the different skin cells than 2D cultures. The equivalents may comprise different kinds of cells, materials, and structures, some including only the epidermis while others also contain a dermal part. The skin substitutes comprising a dermal part will resemble natural skin more, of course. Some equivalents are based on de-epidermised dermis while others are made of fibroblasts seeded into a collagen gel with keratinocytes placed on top. Other cell types, like melanocytes or Langerhans cells may be added. In contrast to simple 2D cell cultures, the skin equivalents possess a keratinized epidermis and a functional basement membrane. This enables the assessment of many parameters, e.g. the penetration of different agents through the skin.

In medical research, these manifold skin equivalents serve to answer many different questions. In the following, different examples of their potential applications are given.

Table 1.3: Skin equivalents used in research, based on collagen gel seeded with fibroblasts and keratinocytes.

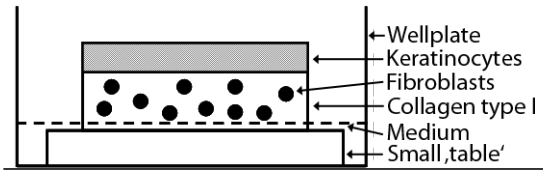	Basic model	
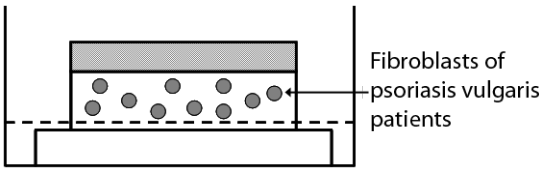	Psoriasis model	[83]
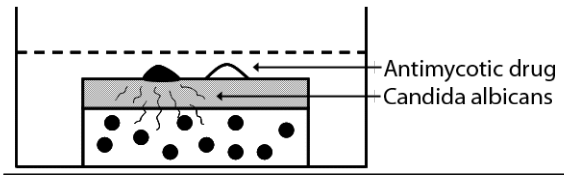	Screening of antimycotic treatment	[123], [101]
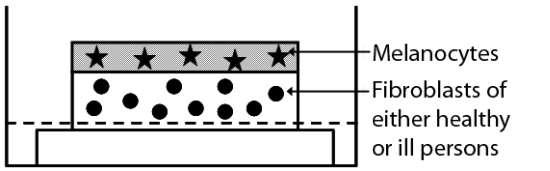	Pigmentation disorders	[122]
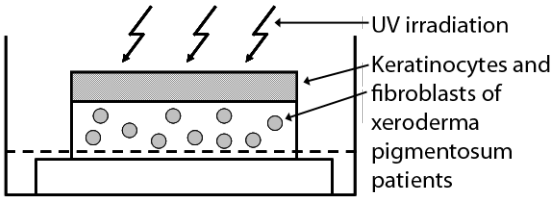	DNA repair deficiency model	[15]
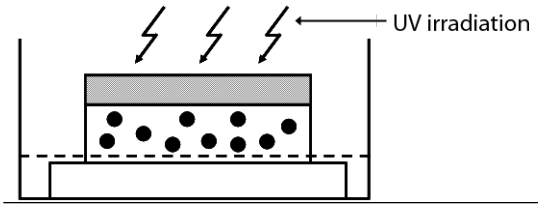	Effect of UV irradiation on keratinocytes	[68]
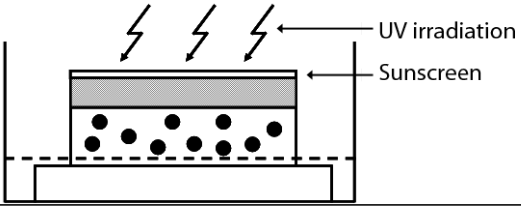	Testing of sunscreens	[116]
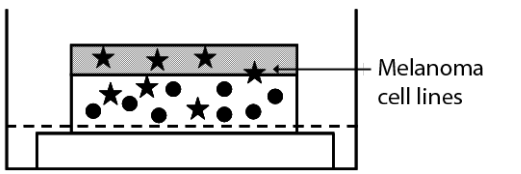	Cancer invasion	[101]

Continued on the next page

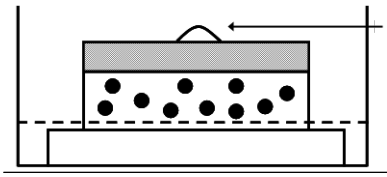	Irritancy and toxicity testing	[101], [56]
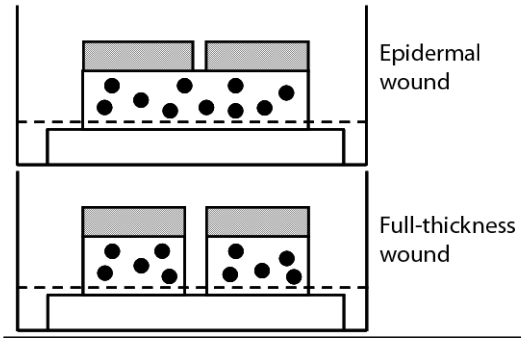	Wound healing model	[45], [101]
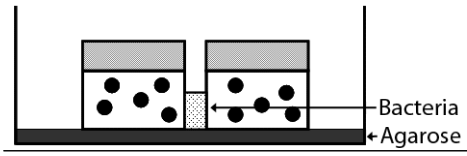	Biofilms in wound healing	[32]

As already mentioned before, skin substitutes are used to test the effect of topically applied drugs or cosmetic products, concentrating on their mode of penetration into the skin as a measure to assess their potential harm. Note, that this is only possible due to the presence of a keratinised epidermis. Other potential impairments of drugs, cosmetic products or nanoparticles with respect to the skin are the development of inflammations, irritancies or toxic effects, which can be examined likewise [56], [153], [36], [139], [124], [101].

An important issue for all human beings is the harmful effect of UV irradiation, causing mutations and resulting in cancer, especially if DNA repair systems are not functional (as in case of patients suffering from *xeroderma pigmentosum*). In order to reduce cancer incidences due to UV irradiation, skin equivalents are used to test the effect of sunscreens [116] and help to achieve a deeper understanding of photo aging, photo carcinogenesis, and tissue therapy [15].

In the field of cancer research, skin equivalents are applied to assess the genotoxicity of carcinogenic agents [177] as well as the invasion and metastatic potential of cancer cells [38], [78], [101]. Invasion can only be assessed in a 3D skin equivalent, which represents the normal structure of skin, including the basement membrane. Even the molecular mechanisms of cancer caused by human papilloma viruses (HPV) can be studied [3].

A further usage of artificial skin is the application of wound repair models, giving the opportunity to test new wound healing therapies as well as to optimise dosages [172]. Wounds in 3D skin equivalents are much more similar to real injuries than 'wounds' in 2D cell culture (scratch assays). Among others, the effect of different growth factors on the re-epithelialisation of wounds can be studied [45]. Infections are feared in the therapy of wounds, leading to complications in the healing process, chronicity of wounds or the rejection of skin substitutes in case of burn patients. In this context, skin equivalents may be used to study the formation, growth, prevention, and eradication of bacterial biofilms [32]. Also, they prove capable of assessing the therapeutic efficacies of antifungal drugs in

the treatment of candidiasis [123], [101] and allow for the measurement of the according cytokine expression profile [145].

Model skin equivalents are also applied to study pigmentation disorders [122] and to conduct mechanistic studies concerning melanocytes [159], [16], [66]. In this context, the construction of a skin equivalent with normal pigmentation is the aim [91]. Furthermore, skin equivalents are constructed as an *in vitro* model of psoriasis [83], [51]. Also in this case, the use of skin equivalents with their special 3D structure is necessary, since the interaction of the melanocytes and the other cells is dependent on their location.

Table 1.4: Skin equivalents used in research, based on de-epidermised dermis (DED).

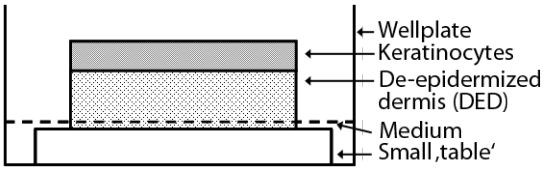	Basic model	
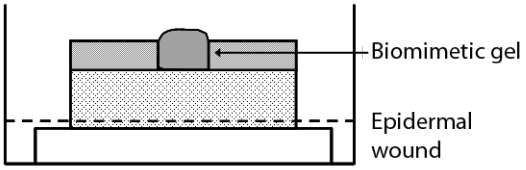 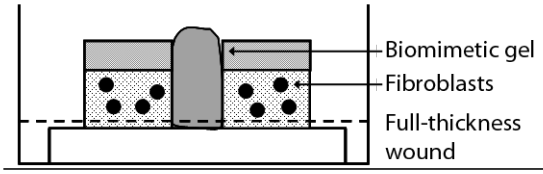	Wound healing	[172]
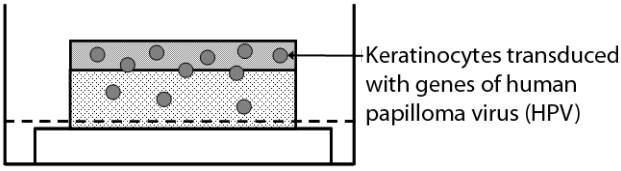	Model of cancer caused by human papilloma viruses (HPV)	[3]
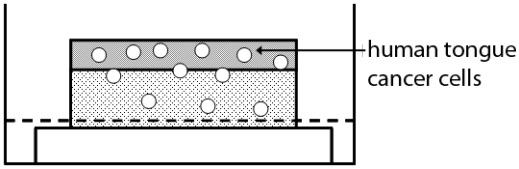	Cancer invasion	[78]
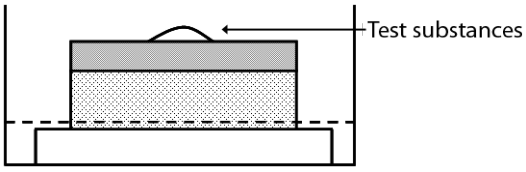	Irritancy testing, penetration of test substances	[137]
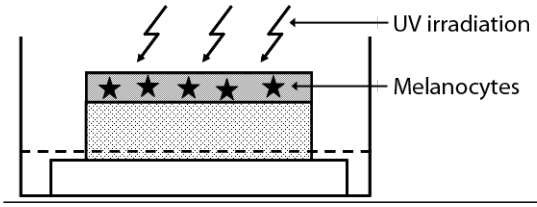	Effect of UV irradiation on melanocytes	[159], [16]

Table 1.5: Skin equivalents used in research, based on Matriderm® and excised skin. Epidermal equivalents used in research.

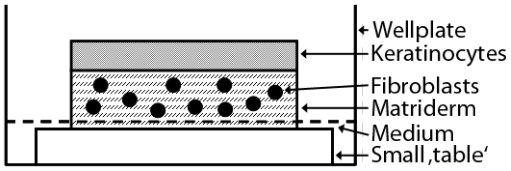	Burn injury treatment	[57]
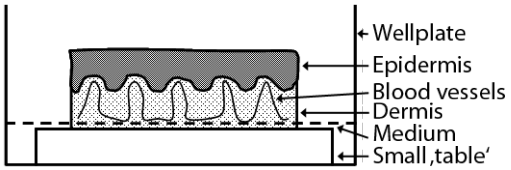	Basic model	
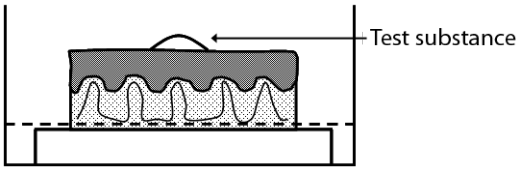	Irritancy testing	[56]
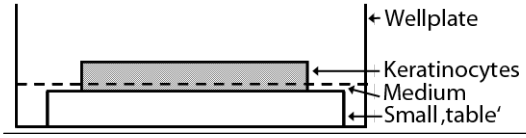	Basic model	
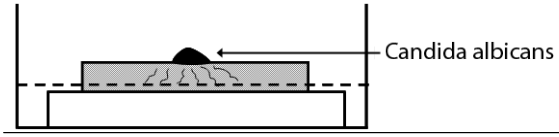	Model of cutaneous candidosis	[145]
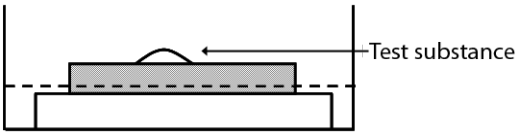	Irritancy and toxicity testing	[56]

1.5 Bioprinting - techniques and possibilities

As mentioned in sections 1.3 and 1.4, the specific 3D spatial positioning of cells is of utmost importance to create functional engineered tissues. Here, the techniques of bioprinting bear great promise, being able to print small amounts of biomaterials - containing different cell types - with high accuracy and high resolution in a specific 3D pattern to mimic their position in an organ. The tissue is printed in a layer by layer approach, transferring the biomaterial on top of each preceding printed layer. Very important for the successful and economical use of bioprinting is its computer aided control. This not only comprises the technical aspect of the transfer process as such, but also includes the possibility to use images of tissue constructs as a blueprint for the automatic creation of a specific tissue [7].

In contrast to normal tissue engineering, where cells are seeded onto/into a pre-existing scaffold, in case of bioprinting no such stiff scaffolds exists. However, as a certain rigidity is needed to create a 3D structure, hydrogels assume the role of a

scaffold and are printed together and simultaneously with the cells. As the tissue is formed layer by layer, different cell types can be printed and included with high spatial resolution; e.g. endothelial cells to facilitate vascularisation in large tissue constructs. This is unique to the technique of bioprinting and represents its major potential.

Bioprinting can be divided into two main approaches: inkjet printing and laser based printing. For the inkjet printing, most normal deskjet printers can be modified to print cell solutions instead of normal ink, resulting into low investment costs [127], [113], [112], [34], [170], [18], [7], [178], [173]. The cells are mixed with cell culture medium or biocompatible hydrogels, forming the so-called bioink. This can then be filled into the cartridges of the printer and be used to print different cell types, even in parallel. Inkjet printing is rapid, versatile, and cheap [75]. Its major disadvantage, however, is the high shear force at the inkjet nozzle, leading to cell damage [21], [31]. Also, printer head clogging may appear at high cell densities [62] and the consistency of the cell concentration may alter during the printing process [135]. Therefore, only bioink with low viscosity and low cell density can be printed.

In contrast, laser based bioprinting works nozzle-free, resulting in the possibility to use bioink with much higher viscosity and cell density [62]. This is especially important for the creation of tissues containing a very high cell density like skin. Also in case of laser based bioprinting, hydrogels are of major importance for the creation of tissue constructs. Different hydrogels used for bioprinting are discussed in section 4.2. For both approaches, one major requisite is the availability of pure, non-contaminated cell cultures of the desired cell types.

Applying both bioprinting approaches, different kinds of cells have successfully been transferred in diverse 2D and 3D patterns [30]. In case of inkjet printing, alginate is commonly used as hydrogel [7], [112], resulting in the creation of e.g. a cell containing pyramide, reaching 5 mm in height. Also, a cartilage-like tissue was formed using human chondrocytes together with a photopolymerized matrix [34]. Laser based bioprinting has been used to print stem cells with subsequent differentiation to bone, cartilage [58], or fat [59]. Human osteoprogenitor cells have also been used to print bone, together with nano-hydroxyapatite as a stabilizing matrix [28]. Additionally - as shown in this PhD thesis - skin tissue could successfully be printed [81], [103].

1.6 Laser induced forward transfer (LIFT)

LIFT is one form of laser based bioprinting and has originally been used in the production of construction material. The setup which has been used for this PhD thesis is described in detail in [82] and [163]. It consists of two coplanar glass slides (26 x 16 x 1 mm) with a gap in between ranging from 350 to 500 µm. The upper glass (donor slide) is coated underneath with a 60 nm thick light absorbing gold layer and the cell-matrix solution (bioink) which is intended to be transferred (see picture 1.5). In order to avoid dripping of the bioink, it has to possess a certain viscosity. The laser beam is then focused through the donor glass slide into the gold layer, which absorbs the whole energy and as a result evaporates locally and expands in all directions. As resistance against expansion is lowest at the front, a protrusion of the bioink layer develops, which elongates, thereby forming

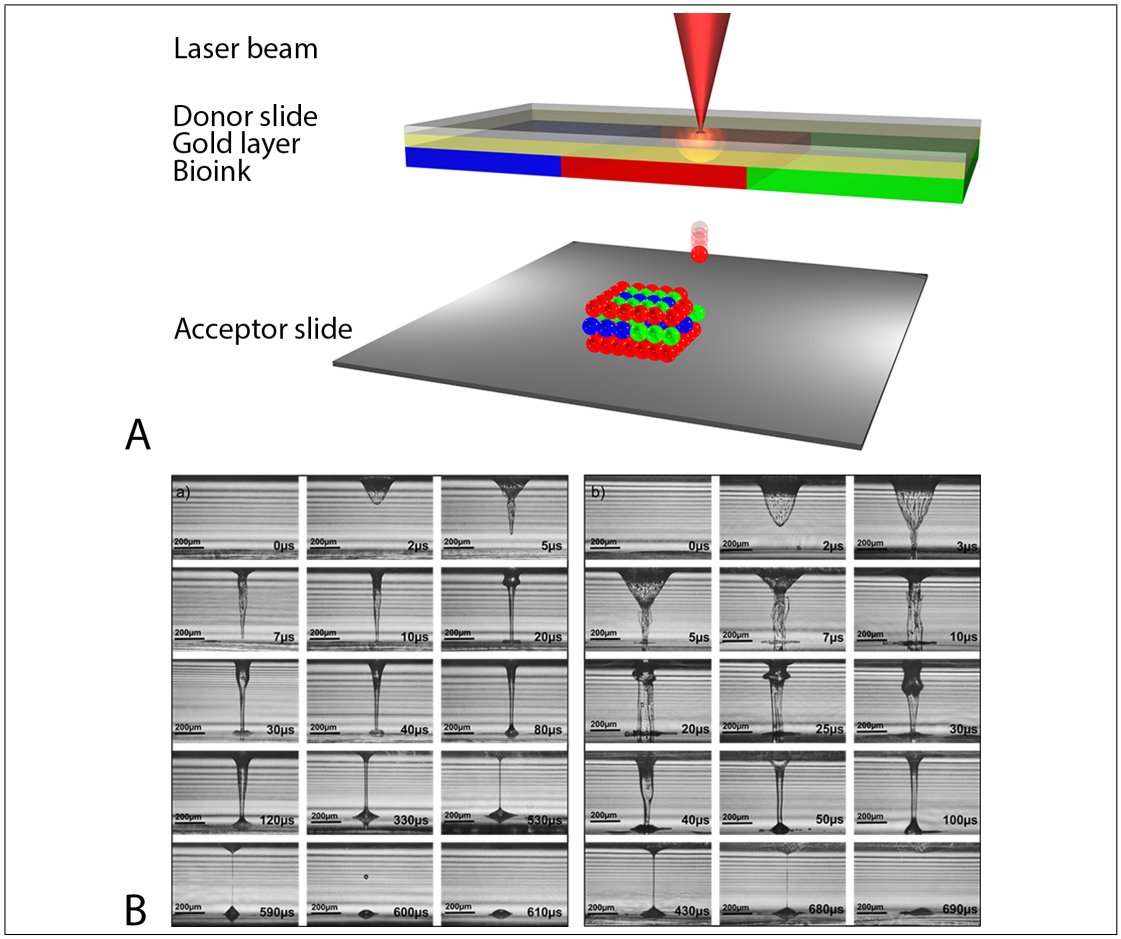

Figure 1.5: Process of the laser induced forward transfer (LIFT) In (A) a schematic overview over the LIFT process is presented (modified after [82]). By focusing the laser beam through the donor slide into the absorbing gold layer underneath, the gold absorbs all energy and evaporates. This results in the transfer of the underlying bioink to the acceptor slide. By moving the glass plates or the laser beam, 2D patterns can be printed. 3D constructs are formed by a layer-on-layer approach. The different colours represent different cell types. Part (B) depicts the actual transfer process as visualised by stroboscopic imaging [163]. After laser application, the hydrogel forms a jet from the donor slide towards the acceptor slide, onto which the bioink containing the cells is transferred. Under appropriate laser fluence conditions, the jet possesses laminar flow characteristics all the time (a), whereas with higher laser fluence turbulent flow appears in the initial transfer phase (b).

a jet. Via this jet, which - at appropriate laser fluence - exhibits laminar flow characteristics, the cells are transferred towards the lower glass slide (collector slide) [163]. During impingement the jet causes droplets with clean boundaries, spreading in a disk shape. To prevent the cells from dehydration, the collector slide may be covered with cell medium or some kind of matrix/hydrogel. However, this is not necessary as long as the bioink contains enough moisture for the cells to survive.

The applied laser is a Nd:YAG-laser with 1064 nm wavelength, 8 to 9 ns pulse duration and 20 Hz repetition rate. The laser pulse energy varies between 100 and 190 µJ, enabling us to print about 1200 droplets per minute. In our setup, gold is used as a light absorbing layer, but also titanium [28] or special polymers

may be used. Gold has the advantage of being relatively cheap and also harmless towards the cells.

By moving the laser beam, a variety of 2D patterns can be printed easily. If different cell types need to be used in the same layer, for each cell type one donor glass slide has to be employed. First, one cell type is printed at its desired positions, then the donor glass slide is changed and the second cell type is transferred. Different matrices might need to be used for each cell type (see section 4.2).

During the printing process, the droplet size depends on the laser pulse energy, the gap distance between the two glass slides, the focused laser spot size, as well as the thickness of the energy absorbing layer and the matrix (bioink) [82]. The resolution is correlated to the thickness of the bioink layer, its surface tension and viscosity, the laser fluence, and also the gap between donor and collector slide [62]. The higher the viscosity and the thicker the bioink layer, the more energy needs to be used for the transfer [61].

Different types of cells - including fragile primary cells - have successfully been transferred by laser based bioprinting. They survive the transfer well, without showing any difference in morphology or proliferation rate compared to non-printed control cells [141], [14], [13], [125], [71], [140], [58], [59], [28]. Further, LIFT does not induce apoptosis, and no signs of DNA-damage can be detected after the printing process [82]. Moreover, human mesenchymal stem cells (MSC) maintain their stem cell characteristics [82] and their ability to differentiate [58], [59]. Likewise, the differentiability of pluripotent murine embryonal carcinoma cells is preserved after transfer [140]. This shows the suitability of laser based bioprinting for its application in tissue engineering.

2 Aims and workflow

Major burn injuries pose difficulties with regard to their therapy. As autologous skin often does not suffice, skin equivalents are used as temporary or permanent wound coverage. Nevertheless, skin substitutes do not possess hair follicles, sebaceous or sweat glands, melanocytes or blood vessels. While the lack of hair, glands, and melanocytes decrease the functional and aesthetic capacity of skin substitutes, the lack of blood vessels is especially important for a sufficient vascularisation and therefore a good take. The precise positioning of different cell types in a complex 3D tissue, however, cannot be realized with the hitherto available methods. Thus, in this thesis laser based bioprinting is used for the creation of a skin equivalent because it offers the possibility to precisely position different cell types in a complex 3D mode. The overall aim is the creation of a skin substitute, which is as similar to native skin as possible. As a prerequisite, this thesis focuses on the establishment of the bioprinting technique for it's successful application in the field of skin tissue engineering. Both, the technical as well as the biological aspects, need to be considered in this context.

Long-term aim

Creation of a skin substitute as similar to physiological skin as possible.

Short-term aim

Establishment of the LIFT procedure for the production of a skin equivalent.

Workflow

- Establishment of the LIFT technology for the transfer of living cells in co-operation with the Laser Zentrum Hannover.
- Assessment of transferred living cells for potential damage by LIFT (immediate survival, proliferation behaviour, possible induction of apoptosis, possible DNA-damage, influence on stem cells).
- Isolation and culturing of primary cells, optimisation of their cell culture procedures, cultivation of cell lines.
- Printing of 2D patterns with several cell types. Adaptation and optimisation of the required evaluation methods.
- Assessment of different hydrogels for their suitability in the transfer process and their compatibility with regard to the cells.
- Printing of 3D cell constructs with several cell types. Adaptation and optimisation of the required evaluation methods.

- Analysis of the 3D skin constructs *in vitro* (viability, tissue formation, proliferation).
- Establishment of the dorsal skin fold chamber in mice for the assessment of tissue engineered skin constructs *in vivo*.
- Evaluation of the printed 3D skin constructs *in vivo* (viability, tissue formation, keratinocyte differentiation, vascularisation).

3 Publications

Contributions to publications

Our co-operation comprised three research groups with different foci: the technical aspects of the LIFT, the skin cell research and the stem cell research. In the Laser Zentrum Hannover the technical aspects of the laser transfer were of main interest, whereas the biological facets of the printing process and the influences on the cells were the focus of my work and our co-operation partners in Rostock. My thesis concentrated on the creation of a skin substitute for burn patients. For this, I used skin cells, i.e. mainly keratinocytes and fibroblasts. In Rostock the aim was the generation of cardiac patches for the treatment of myocardial infarction. This work group mainly used stem cells for their experiments.

The three work groups remained closely connected throughout the project, often discussing the experimental setups and results inter-disciplinary.

Regarding the experiments, I mainly planned, conducted, and analysed the experiments concerning the skin constructs and skin cells. This excluded, however, the counting of the skin cells for the assessment of the proliferation after LIFT (publication [82], page 36), the comet assay for detection of potential DNA-damage (publication [82], page 36) and the detection of tissue formation via immunofluorescence and the scrape loading assay in the *in vitro* experiments (publication [81], page 55).

On the other hand, I was involved in some of the experiments regarding the stem cells, i.e. the preparation and culturing of the stem cells (i.e. adipose-derived mesenchymal stem cells - ASC) for the fluorescence activated cell sorting (FACS) analysis to detect stem cell markers after LIFT (publication [82], page 36). Also, I contributed to the planning of these experiments. Furthermore, I conducted the ApoOne assay for the detection of possible apoptosis of not only the skin cells but also the stem cells (i.e. bone marrow derived mesenchymal stem cells - bmMSC) (publication [82], page 36).

Publication 1

Laser printing of skin cells and human stem cells

Koch L[1*], Kuhn S[2*], Sorg H[2,3*], Gruene M[1*], Schlie S[1], Gaebel R[3], Polchow B[3], Reimers K[2], Stoelting S[3], Ma N[3], Vogt PM[2], Steinhoff G[3], Chichkov B[1]

[*]These four authors equally contributed to the work.
[1]Department of Nanotechnology, Laser Zentrum Hannover e.V., Hannover, Germany
[2]Department or Plastic, Hand and Reconstructive Surgery, Hannover Medical School, Hannover, Germany
[3]Department of Cardiac Surgery, Research Center for Cardiac Tissue and Organ Regeneration, University of Rostock, Rostock, Germany

Published in

Tissue Eng Part C Methods, 2010, Oct, Vol 16 (5), p. 847 - 854
doi:10.1089/ten.tec.2009.0397.

TISSUE ENGINEERING: Part C
Volume 16, Number 5, 2010

DOI: 10.1089/ten.tec.2009.0397

Laser Printing of Skin Cells and Human Stem Cells

Lothar Koch, Ph.D.,[1,*] Stefanie Kuhn, Dipl.-Biol.,[2,*] Heiko Sorg, M.D.,[2,3,*] Martin Gruene, Dipl.-Ing.,[1,*] Sabrina Schlie, Dipl.-Biol., Ph.D.,[1] Ralf Gaebel, Dipl.-Biol.,[3] Bianca Polchow, Dipl.-Biol.,[3] Kerstin Reimers, Ph.D.,[2] Stephanie Stoelting, Ph.D.,[3] Nan Ma, Ph.D.,[3] Peter M. Vogt, M.D.,[2] Gustav Steinhoff, M.D.,[3] and Boris Chichkov, Ph.D.[1]

Laser printing based on laser-induced forward transfer (LIFT) is a new biofabrication technique for the arrangement of biological materials or living cells in well-defined patterns. In the current study, skin cell lines (fibroblasts/keratinocytes) and human mesenchymal stem cells (hMSC) were chosen for laser printing experiments due to their high potential in regeneration of human skin and new application possibilities of stem cell therapy. To evaluate the influence of LIFT on the cells, their survival rate, their proliferation and apoptotic activity, and the DNA damages and modifications of their cell surface markers were assessed and statistically evaluated over several days. The cells survived the transfer procedure with a rate of 98% ± 1% standard error of the mean (skin cells) and 90% ± 10% (hMSC), respectively. All used cell types maintain their ability to proliferate after LIFT. Further, skin cells and hMSC did not show an increase of apoptosis or DNA fragmentation. In addition, the hMSC keep their phenotype as proven by fluorescence activated cell sorting (FACS) analysis. This study demonstrates LIFT as a suitable technique for unharmed computer-controlled positioning of different cell types and a promising tool for future applications in the *ex vivo* generation of tissue replacements.

Introduction

Tissue engineering is a rapidly growing scientific field with an extremely high application potential. One important topic of tissue engineering is the production of skin substitutes for burn patients.[1] Since the possibility of autologous skin replacement is restricted and many different skin substitutes have not reached full success in burn regeneration, there is need for a better skin substitute, which fulfils the distinct criteria of tissue-engineered skin and might repair the respective skin defect without any complications. Further, the interest in mesenchymal stem cells (MSC) for research purposes and, in particular, for clinical applications continuously increased, which is related to the enormous potential of these cells to repair and support the regeneration process of specific tissues.[2] One major obstacle herein is the complex composition of very different but highly specific cells, which are arranged in defined three-dimensional (3D) structures representing the distinct functionality of the respective tissue or organ. To create such specific tissue, the different cell types might be arranged layer by layer in successive time intervals, so that each cell type can constitute a living cell sheet before the next cell type is deposited.[3] If more complex structures should be engineered with integrated vessels or glands, very precise deposition of small volumes of cells and biomaterials is required.

At present, different techniques, based on ink-jet printing technology[4–6] or on laser-induced forward transfer (LIFT),[7] also called laser printing, are under investigation to transfer small amounts of various materials—including living cells—in preset two-dimensional (2D) or 3D patterns. These techniques offer possibilities to control the process with existing computer-aided design and computer-aided manufacturing systems.[8] The ink-jet printing approach is the most commonly used for printing of biological materials.[9–11] The important benefit of this technique is the low investment cost, since nearly every ink-jet desktop-printer[9] can be reassembled for the print of biological materials.[12] The main drawback is the very high shear force at the ink-jet nozzle, which leads to significant cell impairment.[13] Therefore, only fluids with low viscosity and low cell density can be printed. Since the laser printing is nozzle free, high viscosity and high cell density solutions can be printed as well. By combining cell solutions with materials that can form stable gels[14] it would further be possible to print 3D tissues layer-by-layer. By using the LIFT approach, living cells have been

[1]Department of Nanotechnology, Laser Zentrum Hannover e. V., Hannover, Germany.
[2]Department of Plastic, Hand- and Reconstructive Surgery, Hannover Medical School, Hannover, Germany.
[3]Department of Cardiac Surgery, Research Center for Cardiac Tissue and Organ Regeneration, University of Rostock, Rostock, Germany.
*These four authors equally contributed to the work.

transferred in a 2D structure.[15–19] Further, Barron *et al*.[20] and Othon *et al*.[21] transferred single cells also in a 3D structure using layer-by-layer technique.

In the present study, LIFT with gold as a light absorbing layer was investigated to transfer skin cells (fibroblasts/keratinocytes) and human MSCs (hMSC) for the creation of well-defined patterns. Printing of more than one cell type and the generation of multicell patterns were demonstrated. The study was focused on the qualitative as well as quantitative investigation of cell survival, proliferation, apoptosis, and cell DNA damage of the used cell types as well as on phenotype changes of the stem cells after LIFT. The demonstrated laser printing of these cells is a promising step toward the fabrication of living tissue substitutes.

Materials and Methods

Laser printing

The laser printing technique, which is used for defined deposition of cells, is based on the principle of LIFT, as illustrated in Figure 1. The experimental setup consists of two coplanar glass slides. The upper, referred to as "donor-slide," is covered underneath with a light absorbing gold layer and a layer of the cell containing material to be transferred (Fig. 1). Laser pulses are focused through the glass slide into the gold layer, which is evaporated locally. Laser light absorption in the gold layer generates a high gas pressure that propels the subjacent cell compound toward the lower glass slide, referred to as "collector-slide." A thin layer of hydrogel or cell medium on the collector-slide provides a humid environment to prevent the cells from dehydration at longer processing times and cushions the impact. Note that the cells survive the impact even without this cushion layer. A hydrogel layer additionally keeps the cells positioned. All transfer experiments in this article are carried out under normal air conditions.

The achieved droplet size of the transferred cell compound depends on the laser pulse energy, the gap distance, the focused laser spot size, as well as the thickness of the energy absorbing layer and the cell compound layer. In our experiments, printed droplet sizes with a diameter in the range of 80 to 140 μm are used.

The applied laser is a Nd:YAG-laser (DIVA II; Thales Laser, Orsay, France) with 1064 nm wavelength, 8–9 ns pulse duration (FWHM), and 20 Hz repetition rate. The laser pulses are focused with a 60 mm achromatic lens, producing an ablation spot size of 45 μm in diameter. Depending on the cell/hydrogel layer thickness, the laser pulse energy, measured continuously during the ongoing process, is set between 100 and 190 μJ, corresponding to a laser fluence of 3 to 6 J/cm^2.

The cell deposition is controlled via a computerized scanning setup consisting of three high speed translation stages (M-414.1PD and M413.3PD; PI GmbH, Karlsruhe, Germany). On the XY-translation stages, two mirrors are mounted; on the Z-stage holding, the focusing optics as well as the camera for process visualization are mounted. The stages are synchronized with laser pulses over a computer-based real-time system (Adwin-4L-T400; Jaeger Messtechnik, Lorsch, Germany) to ensure equidistant positioning of the laser spots. This automated computer-aided manufacturing controlled stage setup allows the accurate positioning of a wide variety of patterns with a speed of 1200 printed cell droplets per minute, which is only limited by the laser repetition rate applied in this study.

The carrier for the donor-slide is structured modularly to allow quick replacement of the donor-slides coated with different cell compounds. The collector-slide is assembled on a Z-stage to provide controlled positioning with respect to the donor-slide. The gap between the donor- and collector-slide is set to a value in the range of 350 to 500 μm with an accuracy of 5 μm and is monitored through a camera looking parallel to the slides (see Fig. 1).

Preparation of donor- and collector-slides for laser printing experiments

The cultivated cells were trypsinized and centrifuged at $300\times g$. Then the supernatant was removed.

1. For all conducted cell assays, the cell pellet was resuspended in the respective cell medium. This cell suspension was pipetted on the gold-coated donor-slide. The square glass plates with a size of 26 mm and a thickness of 1 mm were coated with a 55 to 60 nm thick gold layer using plasma-enhanced sputter deposition. The cell suspension was dispersed on the gold surface with a blade coater to form a homogenous layer of approximately 50 μm thickness. Then the cell coated donor-slide was fixed in a metal frame and mounted upside-down in the setup. To collect the transferred cells, a sterilized square glass plate (the collector-slide) was mounted parallel to and under the donor-slide. The collector-slide was coated with a layer of cell medium for all the cell assays described here (except for comet assay). This coating was performed with a t-shape spreader. Directly after the LIFT experiments, the laser transferred cells were rinsed from the collector-slide with additional medium into a tube, counted, and distributed to the corresponding well plates for further analysis. The cells that remained on the donor-slide were also rinsed off and collected as control cells.
2. For the analysis of DNA damage, the collector-slide was coated with an agarose layer. The cells printed on the agarose layer were coated with a second layer of agarose and used for the comet assay.
3. For the printing of well-defined cell structures, the cell pellet was resuspended in a mixture of blood plasma and alginate hydrogel at a density of $1–2\times10^6$ cells in 30 μL. The obtained cell suspension was pipetted on the gold-coated donor-slide and dispersed on the gold surface with a blade coater to form a homogenous layer of approximately 50 μm thickness. To keep the printed cells in their position, the collector-slide was coated with Matrigel™ (BD Biosciences, Heidelberg, Germany). Note that the conducted Live/Dead-assays showed the same results in all studied cases, independent on the materials (cell medium, alginate, blood plasma, Matrigel) used for the preparation of donor- and collector-slides.

Cell culture of skin cell lines

NIH3T3 fibroblasts were cultured in Dulbecco's modified Eagle's medium (DMEM) with high glucose (4.5 g/L) (PAA, Pasching, Austria) supplemented with 10% fetal bovine

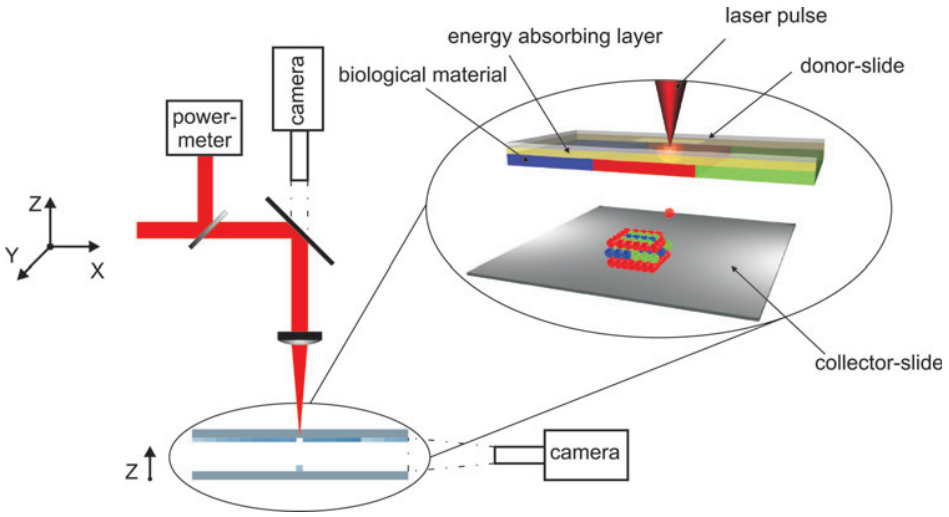

FIG. 1. Schematic sketch of the biological laser printing setup and a perspective figure of the principle of laser-induced cell transfer between two coplanar slides: The upper slide is coated underneath with an energy absorbing gold layer and materials to be transferred. Laser pulses are focused through the upper glass slide into the absorbing layer. By evaporating this layer, the material to be transferred is propelled toward the lower glass slide.

serum (FBS) (Biochrom, Berlin, Germany), 1% of 100 mM sodium pyruvate (Biochrom), and 1% of 10 mg/mL gentamycin (Biochrom). HaCaT keratinocytes were grown with DMEM/Ham's F12 medium (PAA) supplemented with 10% FBS and 1% of 10 mg/mL gentamycin.

Isolation and culture of hMSC

Bone marrow–derived hMSC. Collections of bone marrow (BM) aspirates of 12 patients ranging in the age from 68 to 84 years were obtained from the sternum of patients undergoing cardiac surgery at the Cardiac Surgery Department of the University of Rostock. The BM aspirates were received in accordance with the ethical standards of the local ethics committee. The aspirates were diluted 1:5 with 2 mM ethylenediaminetetraacetic acid-phosphate-buffered saline (PBS) (Merck, Whitehouse Station, NY; Nexell, Baxter, Unterschleissheim, Germany). The mononuclear cell fraction was isolated by density gradient centrifugation using Ficoll-Hypaque-Plus solution (GE Healthcare BioSciences, Piscataway, NJ) and seeded at a density of 1×10^6 cells/cm^2 into cell culture flasks (Greiner Bio-One, Frickenhausen, Germany). The expansion medium consisted of MSC basal medium (MSCBM; Lonza, Walkersville, MD). Cells were maintained in MSCBM until they reached 70% to 90% confluency. Cells were harvested at subconfluence using Trypsin (PromoCell, Heidelberg, Germany).

Adipose-derived hMSC. Adipose-derived hMSC (Ad-hMSC) were yielded from abdominoplastic surgery performed at the Department of Plastic Surgery at Hannover Medical School with written consent and approval of the ethics committee. Fat lobules were dissected with sterile scissors to lobules of approximately 1 cm^3 size. They were washed in equal volumes of sterile Hank's Balanced Salt Solution (HBSS) (PAA), and then their extracellular matrix was digested at 37°C for 1 h with 0.075% collagenase (Biochrom) in PBS under permanent shaking. Then, enzyme activity was neutralized with Hank's BSS containing 10% FBS, centrifuged at $1200\times g$ for 10 min, and incubated overnight at 37°C/5% CO_2 at a density of approximately 150,000/cm^2 in a medium (DMEM/Ham's F12) containing 10% FBS, 1% penicillin/streptomycin (Biochrom), and 0.1% ascorbat-2-phosphate. After incubation, the plates were washed with PBS to remove residual nonadherent blood cells. Finally, Ad-hMSC were plated in 150 cm^2 cell culture flasks and incubated at 37°C/5% CO_2 until they reached 60–70% confluence.

Cell staining

For cell staining, carboxy-fluorescein-diacetate (CFDA) (Invitrogen, Karlsruhe, Germany) and Hoechst 33342 (Invitrogen) were used. Cells were incubated for 15 min at 37°C and subsequently washed thrice in PBS (PAA).

Analysis of cell survival after LIFT

Survival of fibroblasts (NIH3T3), keratinocytes (HaCaT), and hMSC was studied directly after LIFT. Fibroblasts and keratinocytes were shown to be alive or dead after LIFT and this was attained while using the Trypan Exclusion Assay with 0.4% Trypan Blue (Invitrogen). Directly after, the LIFT process cells were rinsed off the collector-slide, counted with a haemocytometer (Fuchs-Rosenthal; Assistent, Sondheim, Germany), and compared to nontransferred cells from the gold layer (control). To evaluate cell membrane integrity of hMSC, fluorescein diacetate (FDA; Invitrogen) and propidium iodide (PI; Carl Roth, Karlsruhe, Germany) were used to differentiate between cells with intact membranes (live; FDA 5.5 μg/mL for 15 min) and membrane damaged cells (dead; PI 50 μg/mL for 15 min). After each stain, cells were washed with PBS, centrifuged, and finally fixed for 10 min with 4% paraformaldehyde for analysis. Live cells were identified by the presence of intracellular, green FDA staining. Red cells, stained by PI, were counted as dead cells.

Analysis of cell proliferation after LIFT

Proliferation of NIH3T3, HaCaT, and hMSC was analyzed using different methods. Proliferation of fibroblasts and keratinocytes was studied using the CellTiter-Blue Kit (Promega, Madison, WI). The test was carried out according to the description of the manufacturer in five replicates per LIFT process. Cells were distributed in a 96-well plate, starting with 500 viable cells in each well and measured with a Genios2 Tecan Reader (Tecan, Grödig, Austria). Proliferation was additionally measured by distributing 1000 transferred vital NIH3T3 cells as well as 860 HaCaT, respectively, in each well of 24-well plates. Over 6 days, every 24 h, 24 chosen samples were trypsinized and stained with Trypan Blue (0.4%) and vital cells were counted separately for each well. Nontransferred cells were used as controls.

To evaluate the influence of LIFT on hMSC proliferation, we assessed the proliferative activity using water-soluble tetrazolium salt (WST-1) assay (Roche Diagnostics, Mannheim, Germany). The WST-1 assay is a colorimetric method in which the dye intensity is proportional to the number of viable cells. HMSC were seeded into 96-well microtiter plates directly after LIFT at a concentration of 2×10^3 cells/well. Cells were then cultured in medium (MSCBM). After incubation of 24 h to 96 h, the cell proliferation reagent WST-1 was added with cell culture medium followed by incubation for 4 h. Sample absorbance was analyzed using a bichromatic enzyme-linked immunosorbent assay reader (Microplate Reader, Model 680; BioRad, Munich, Germany) at 450 nm.

Analysis of apoptosis after LIFT

For determination of apoptosis, fibroblasts, keratinocytes, and hMSC were lysed in ApoOne Buffer (Promega), and N-Acetyl-Asp-Glu-Val-Asp-7-amido-4-methylcoumarin (Sigma-Aldrich, Munich, Germany) was added as a substrate for caspases 3/7. Fluorescence was detected with a Genios2 Tecan Reader. As a positive control, HaCaTs treated for 7 h with 0,525 μM staurosporine (Merck, Darmstadt, Germany) were used.

Analysis of DNA damage through LIFT

To determine whether the LIFT procedure induces genotoxicity effects, a comet assay experiment was performed with fibroblasts (NIH3T3), keratinocytes (HaCaT), and hMSC right after the cell transfer and under control conditions, as previously described.[22] Genotoxicity can be studied by analyzing DNA damages, which are detected with the comet assay method according to single and double DNA strand breaks via a single-cell-gel electrophoresis. These DNA damage effects can be quantitatively described by the parameter tailmoment that characterizes the amount of damaged DNA.

Analysis of hMSC phenotype after LIFT

For characterization of changes in hMSC phenotype, which might be induced by LIFT, cell surface antigen phenotyping of Ad-hMSC was performed 4 days after the laser transfer using flow cytometry. The following cell-surface epitopes were marked with anti-human antibodies: CD90-PE-Cy5 (Becton Dickinson, Heidelberg, Germany), CD29-APC, CD44-FITC (Beckman Coulter, Krefeld, Germany), and CD105-PE (Immunokontakt; AMS Biotechnology, Wiesbaden, Germany). Mouse isotype antibodies served as controls (Becton Dickinson, Beckman Coulter). About 10,000 labeled cells were acquired and analyzed using an FACScan flow cytometer running with CellQuest-Software (Becton Dickinson).

Statistical analysis

To analyze, if a difference between the mean values of corresponding sets of measured values of laser printed cells and controls were real and not only due to statistical variations, Student's *t*-test ($\alpha = 0.05$) was performed with the program Origin 8 (Origin Lab, Northampton, MA).

In the case of the used skin cell lines, the "n" refers to the amount of samples in each experiment. The used skin cell lines have always been one strain (e.g., NIH3T3 and HaCaT), as these cells are commercially available cell lines. For the experiments using MSC, the "n" refers to the number of samples used out of 12 patients (1 sample = 1 patient).

Results

Printing of cells

All cells (fibroblasts, keratinocytes, and hMSC) used in this study were transferred successfully by LIFT. A local transfer efficiency of over 90% could be reached, considering the cells in the area wherein laser transfer was performed. In contrast, the overall efficiency also includes cell losses at the blade coater and considers coated areas at the edges of the donor-slide, which are not used for transfer on purpose. Therefore, the overall efficiency is lower than the local transfer efficiency.

Different 2D patterns consisting of one or more cell types were generated. Figure 2 shows a representative immuno-

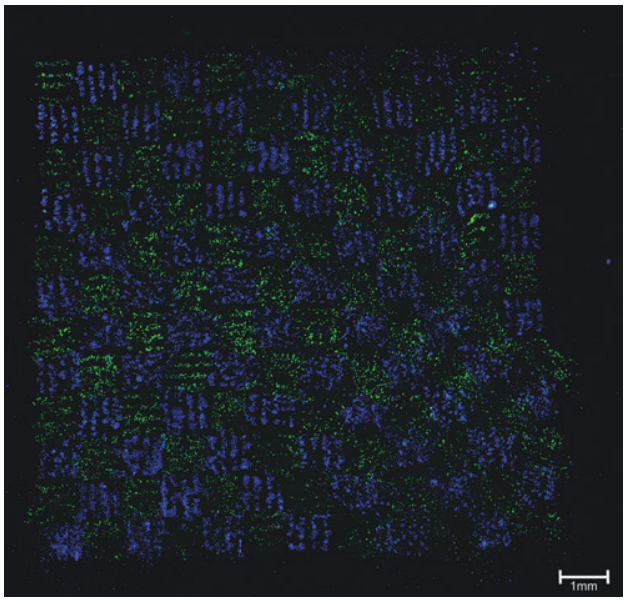

FIG. 2. Representative immunofluorescence microscopic image of fibroblasts (NIH3T3; green, stained with carboxyfluorescein-diacetate (CFDA)) and keratinocytes (HaCaT; blue, Hoechst33342) arranged in a chess board pattern by LIFT. LIFT, laser-induced forward transfer.

fluorescence microscopic image of fibroblasts (NIH3T3; green, stained with CFDA) and keratinocytes (HaCaT; blue, Hoechst33342) arranged in a chess board pattern by LIFT. The chess board pattern with a total size of 9.6×9.6 mm consists of four lines per square with a line width of 70 μm and a line spacing of 200 μm. This image (Fig. 2) shows the possibility of creating specific patterns consisting of two or even more different cell types, which could precisely be arranged by LIFT.

Cell survival after LIFT

Survival of cells was determined directly after the transfer. Compared to nontransferred control cells, 98% ± 1% (standard error of the mean [SEM]) of the skin cell lines survived the transfer. The Live/Dead staining of BM–derived hMSC (Bm-hMSC) immediately after transfer showed a survival rate of 90% ± 10% (SEM) versus control.

Cell proliferation after LIFT

To assess the effect of LIFT on cell growth, we analyzed the proliferation of the transferred cells in comparison to the respective control cells over a time period of several days. Proliferation was measured by two different methods. First, fibroblasts and keratinocytes were directly counted using a haemocytometer. Applying this method (with $n = 24$ samples each date), we could not detect any major differences in their ability to proliferate after LIFT. Skin cells showed exponential growth starting on day 1 and continuing up to day 6 with no significant differences compared with the control cells (Fig. 3a, b). Second, proliferation was tested by measurement of the metabolic activity, which is proportional to the amount of cells. Using the Celltiter-Blue method for fibroblasts and keratinocytes (each $n = 20$), transferred skin cells also showed nearly exponential cell proliferation (Fig. 3c), which could already be detected 24 h after LIFT. Albeit significant differences between transferred and control cells were measured at day 1 (fibroblasts, keratinocytes) and two (fibroblasts), the ongoing analysis presented similar curve gradients without statistical significant difference; thus, the difference at the beginning seems to be negligible from the biological point of view.

The proliferation of Bm-hMSC, analyzed by WST-1-assay ($n = 7$), showed a continuously increasing proliferation

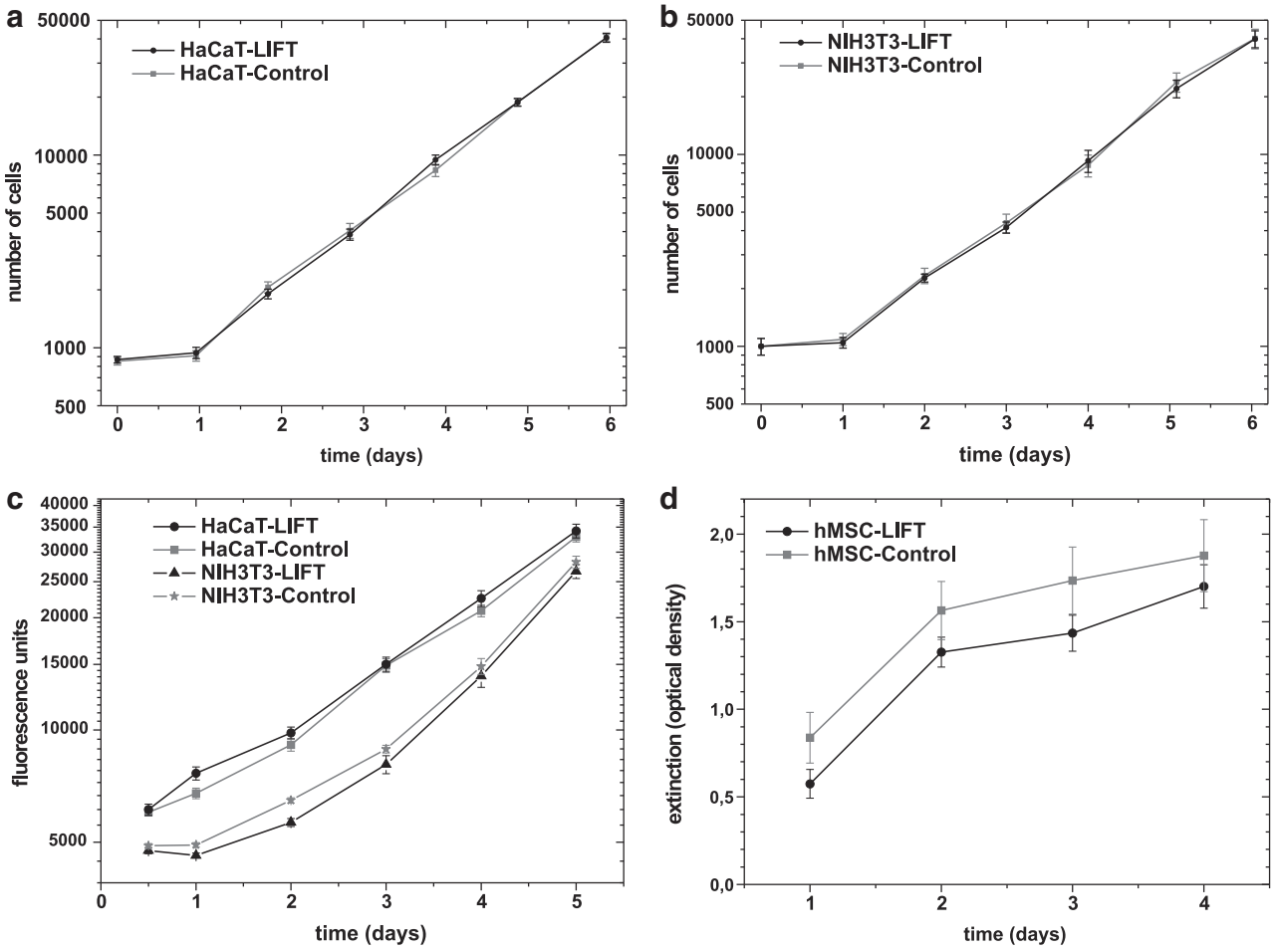

FIG. 3. (**a–d**) Assessment of proliferation of HaCaT keratinocytes (**a, c**), NIH3T3 fibroblasts (**b, c**), and human mesenchymal stem cells (hMSC) (**d**), which were printed by LIFT versus nontransferred cells (Control). Proliferation was assessed by cell counting in a haemocytometer (**a, b**) and metabolic activity with CellTiter-Blue (**c**). The water-soluble tetrazolium salt-1 assay (**d**) is a colorimetric method in which the dye intensity is proportional to the number of viable cells. Values are given as means ± standard error of the mean.

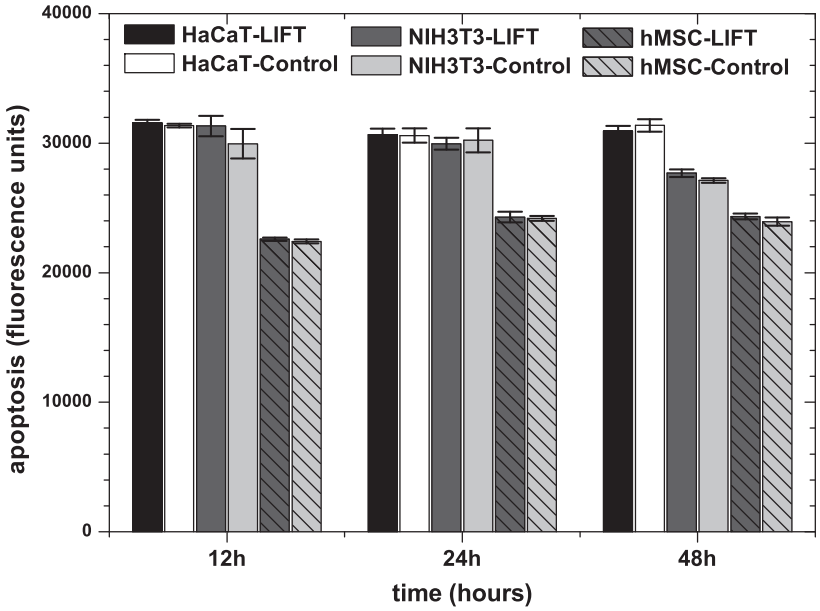

FIG. 4. Assessment of apoptosis of fibroblasts (NIH3T3), keratinocytes (HaCaT), and hMSC, which were printed by LIFT versus nontransferred cells (Control). Apoptosis was assessed by measurement of the activity of caspases 3/7. Values are given as means ± standard error of the mean.

without significant difference between transferred and nontransferred hMSC (Fig. 3d) until day 4 after LIFT.

Apoptosis of cells after LIFT

Transferred cells were tested for apoptosis as a parameter of possible cell death caused by LIFT. Fibroblasts, keratinocytes, and Bm-hMSC showed no significant differences in the fluorescence signal in the analysis of caspase 3/7 activity between the transferred cells and their respective controls (Fig. 4, each $n = 9$). This applies for the whole observation period from 12 h up to 48 h after laser transfer.

DNA damage through LIFT

Genotoxicity was investigated using the comet assay method. The parameter tailmoment characterizes the amount of damaged DNA. The results are given as mean of tailmoment ± SEM ($n = 4$). At least 1000 cells per treatment were evaluated. For fibroblasts, keratinocytes, and Bm-hMSC, it could be shown that the LIFT procedure did not significantly increase the incidence of DNA damages. As can be seen in Table 1, the tailmoments of all treatments were comparable with their controls.

Table 1. Analysis of DNA Damage Effects After Laser-Induced Forward Transfer of Fibroblasts (NIH3T3), Keratinocytes (HaCaT), and Human Mesenchymal Stem Cells Demonstrated by Comet Assay (each n = 4)

	Control	*LIFT*
NIH3T3	1.81 ± 0.33	1.72 ± 0.43
HaCaT	2.41 ± 0.38	2.31 ± 0.25
HMSC	1.27 ± 0.28	1.32 ± 0.28

At least 1000 cells per treatment were evaluated. The results are given as average of tailmoment as a marker of DNA damages ± standard error of the mean.

LIFT, laser-induced forward transfer; hMSC, human mesenchymal stem cell.

HMSC phenotype

For phenotype characterization of hMSC, surface protein expression of Ad-hMSC from five donors at passage 2 was examined by flow cytometry, 4 days after the laser transfer. Ad-hMSC, similarly to nontransferred control Ad-hMSC, expressed the typical stem cell marker proteins CD44, CD105, CD29, and CD90 without statistical significant difference (Fig. 5). This indicates that LIFT did neither change the immunophenotype of hMSC nor start the initiation of differentiation of stem cells after laser transfer.

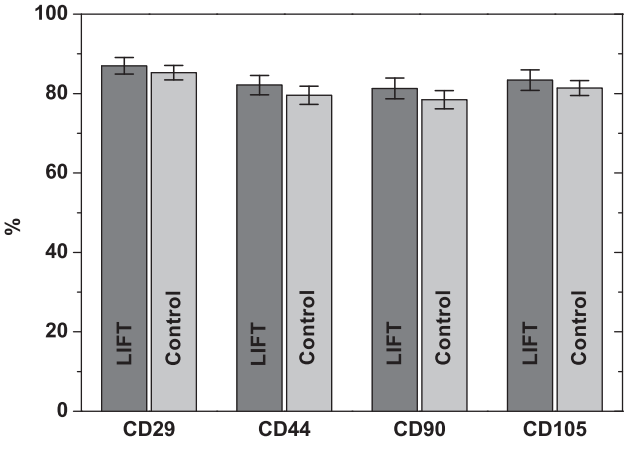

FIG. 5. Flow cytometric analysis of the phenotype of hMSC. The hMSC expressed the typical MSC-marker proteins CD44, CD105, CD29, and CD90. No significant difference in the ratio of expression between transferred cells and control cells was detected (mean values of %-positive cells ± standard error to the total number of cells analyzed).

Discussion

In the last few years, the ability to print biological material offered a revolutionary new technique for tissue engineering and functional genomics. With these printing techniques, it became possible to create multicellular constructs of arbitrary size with micrometer accuracy. The present study demonstrates LIFT of skin cells as well as hMSC to be a new promising printing method in tissue engineering. The following major findings have been obtained: (i) LIFT is a fast and reliable technique for printing living cells in predefined patterns; (ii) printed cells do not present major differences in survival, proliferation, apoptosis, and DNA-damage compared with respective control cells; and (iii) LIFT does not change the phenotype of the transferred hMSC, thus keeping their high potential for tissue regeneration.

As tissue engineering emerged, it provided many new therapeutic options in regenerative medicine. Besides all the advantages, major problems still exist with the preparation of pure and noncontaminated cells as well as the production of stable 3D-constructs. For this purpose, LIFT might offer the technical precondition for the production of complex 3D tissue-engineered constructs of multiple cell types with high precision, that is, skin or cardiovascular tissue.

In this context, many different skin substitutes have been created, varying in their utilization time (temporary, permanent) and composition (dermal, epidermal, both, with or without cells).[23–25] These are already available for clinical use (e.g., Biobrane®, Bertek Pharmaceuticals, Morgantown, WV; Integra®, Integra Life Science, Plainsboro, NJ; Matriderm®, Dr. Suwelack Skin & Health Care, Billerbeck, Germany; Apligraf®, Organogenesis, Canton, MA), offer decreased healing time and less pain, and result in an improved cosmetic outcome.[26–28] Regardless, current research still pursues further approaches to improve the quality of skin substitutes. Therefore, LIFT might offer a new procedure for the fast, precise, and reliable production of a ready-to-use skin equivalent.

The laser printing of fibroblasts, keratinocytes, and hMSC demonstrated high survival rates as one of the most important preconditions of this technique. Additionally, the assessment of cellular proliferation by two different methods and the possible induction of apoptosis studied by ApoOne did not present any biological significant changes compared with the respective control cells, which have not been transferred by LIFT.

Similarly to the used skin cells, laser transfer of hMSC also was studied and evaluated for the same parameters. MSC are found in many adult tissues and represent an attractive stem cell pool due to their self renewing ability, high differentiation capacity, and mesodermal differentiation potential.[29] Therefore, MSC are thought to regenerate many human tissues like bone, cartilage, adipose tissue, skin, cardiomyocytes, and even insulin producing tissue.[30] The printing of hMSC with a high survival rate demonstrates LIFT to be a very promising method for stem cell therapy. We could also not detect any differences in proliferation and apoptosis for hMSC. In addition, flow cytometric analysis demonstrated that LIFT does not induce differentiation of hMSC so that stem cells could be transferred safely.

In conclusion, the present study proved LIFT to be a reliable and safe technique for the unharmed computer-controlled positioning of different cell types. The standardized and statistical evaluation, as shown here, is an important precondition for the ongoing research in laser printed tissue-engineered constructs. Therefore, LIFT is a promising tool for future applications in the *ex vivo* generation of tissue replacements. The 3D printing of skin equivalents for burn patients or the production of cardiac tissue or even cardiac valves might be potential areas of application.

Acknowledgments

The authors kindly thank Mrs. M. Fritsche from the Department of Cardiac Surgery, University of Rostock, and Mrs. U. Fuhrmann and Mr. H. Naghilouy Hidaji from the Department of Plastic, Hand, and Reconstructive Surgery, Hannover Medical School, for their excellent technical assistance and organizational help.

This study has been supported by Deutsche Forschungsgemeinschaft, SFB TransRegio 37 and Rebirth Cluster of Excellence.

Disclosure Statement

No competing financial interests exist.

References

1. MacNeil, S. Progress and opportunities for tissue-engineered skin. Nature **445,** 874, 2007.
2. Summer, R., and Fine, A. Mesenchymal progenitor cell research: limitations and recommendations. Proc Am Thorac Soc **5,** 707, 2008.
3. Ng, K.W., and Hutmacher, D.W. Reduced contraction of skin equivalent engineered using cell sheets cultured in 3D matrices. Biomaterials **27,** 4591, 2006.
4. Nakamura, M., Kobayashi, A., Takagi, F., Watanebe, A., Hiruma, Y., Ohuchi, K., Iwasaki, Y., Horie M., Morita, I., and Takatani, S. Biocompatible inkjet printing technique for designed seeding of individual living cells. Tissue Eng **11,** 1658, 2005.
5. Cooley, P., Wallace, D., and Antohe, B. Applications of inkjet printing technology to BioMEMS and microfluidic systems. JALA Charlottesv Va **7,** 33, 2002.
6. Nakamura, M., Nishiyama, Y., and Henmi, C. 3D mircofabrication by inkjet 3D biofabrication for 3D tissue engineering. In: Micro-NanoMechatronics and Human Science. Piscataway, NJ: IEEE, 2008, p. 451.
7. Arnold, C.B., Serra, P., and Piqué, A. Laser direct-write techniques for printing of complex materials. MRS Bull **32,** 23, 2007.
8. Schiele, N.R., Koppes, R.A., Corr, D.T., Ellison, K.S., Thompson, D.M., Ligon, L.A., Lippert, T.K.M., and Chrisey, D.B. Laser direct writing of combinatorial libraries of idealized cellular constructs: biomedical applications. Appl Surf Sci **255,** 5444, 2009A.
9. Alper, J. Biology and the inkjets. Science **305,** 1895, 2004C.
10. Calvert, P. Printing cells. Science **318,** 208, 2007W.
11. Wilson, W.C., and Boland, T. Cell and organ printing 1: protein and cell printers. Anat Rec Part A **272A,** 491, 2003S.
12. Sun, W., Starly, B., Darling, A., and Gomez, C. Computer-aided tissue engineering: application to biomimetic modeling and design of tissue scaffolds. Biotechnol Appl Biochem **39,** 49, 2004B.
13. Born, C., Zhang, Z., Al-Rubeai, M., and Thomas, C.R. Estimation of disruption of animal cells by laminar shear stress. Biotechnol Bioeng **40,** 1004, 1992.

14. Fedorovich, N.E., Alblas, J., De Wijn, J.R., Hennink, W.E., Verbout, A.J., and Ddhert, W.J.A. Hydrogels as extracellular matrices for skeletal tissue engineering: state-of-the-art and novel application in organ printing. Tissue Eng **13,** 1905, 2007.
15. Hopp, B., Smausz, T., Antal, Zs., Kresz, N., Bor, Zs., and Chrisey, D. Absorbing film assisted laser induced forward transfer of fungi. J Appl Phys **96,** 3478, 2004.
16. Hopp, B., Smausz, T., Kresz, N., Barna, N., Bor, Z., Kolozsvári, L., Chrisey, D., Szabó, A., and Nógradi, A. Survival and proliferative ability of various living cell types after laser-induced forward transfer. Tissue Eng **11,** 1817, 2005.
17. Barron, J.A., Spargo, B.J., and Ringeisen, B.R. Biological laser printing of three dimensional cellular structures. Appl Phys A **79,** 1027, 2004.
18. Ringeisen, B.R., Kim, H., Barron, J.A., Krizman, D.B., Chrisey, D.B., Jackman, S., Auyeung, R.Y.C., and Spargo, B.J. Laser printing of pluripotent embryonal carcinoma cells. Tissue Eng **10,** 483, 2004.
19. Doraiswamy, A., Narayan, R.J., Lippert, T., Urecht, L., Wokaun, A., Nagel, M., Hopp, B., Dinescu, M., Modi, R., Auyeung, R.C.Y., and Chrisey, D.B. Eximer laser forward transfer of mammalian cells using a novel triazene absorbing layer. Appl Surf Sci **252,** 4743, 2006.
20. Barron, J.A., Wu, P., Ladouceur, H.D., and Ringeisen, B.R. Biological Laser Printing: A novel technique for creating heterogeneous 3-dimensional cell patterns. Biomed Microdevices **6,** 139, 2004.
21. Othon, C.M., Wu, X., Anders, J.J., and Ringeisen, B.R. Single-cell printing to form three-dimensional lines of olfactory ensheathing cells. Biomed Mater **3,** 1, 2008.
22. Schlie, S., Ngezahayo, A., Ovsianikov, A., Fabian, T., Kolb, H.A., Haferkamp, H., and Chichkov, B.N. Three-dimensional cell growth on structures fabricated from ORMOCER® by two-photon polymerisation technique. J Biomater Appl **22,** 275, 2007.
23. Vogt, P.M., Kolokythas, P., Niederbichler, A., Knobloch, K., Reimers, K., and Choi, C.Y. Innovative Wundtherapie und Hautersatz bei Verbrennungen. Chirurg **78,** 335, 2007.
24. Supp, D., and Boyce, S.T. Engineered skin substitutes: practices and potentials. Clin Dermatol **23,** 403, 2005.
25. Singer, A.J., and Clark, R.A.F. Cutaneous wound healing. N Engl J Med **341,** 738, 1999.
26. Boorboor, P., Vogt, P.M., Bechara, F.G., Alkandari, Q., Aust, M., Gohritz, A., and Spies, M. Toxic epidermal necrolysis: use of Biobrane or skin coverage reduces pain, improves mobilisation and decreases infection in elderly patients. Burns **34,** 487, 2008.
27. Nie, X., Zhang, J.Y., Cai, K.J., Yang, M.H., Xiao, A.H., Da Hu, H., Liu, L.Y., Wang, H.J., Wen, N., and Jin, Y. Cosmetic improvement in various acute skin defects treated with tissue-engineered skin. Artif Organs **31,** 703, 2007.
28. Lal, S., Barrow, R.E., Wolf, S.E., Chinkes, D.L., Hart, D.W., Heggers, J.P., and Herndon, D.N. Biobrane improves wound healing in burned children without increased risk of infection. Shock **14,** 314, 2000.
29. Pittenger, M.F., Mackay, A.M., Beck, S.C., Jaiswal, R.K., Douglas, R., Mosca, J.D., Moorman, M.A., Simonetti, D.W., Craig, S., and Marshak, D.R. Multilineage potential of adult human mesenchymal stem cells. Science **284,** 143, 1999.
30. Porada, C.D., Zanjani, E.D., and Almeida-Porad, G. Adult mesenchymal stem cells: a pluripotent population with multiple applications. Curr Stem Cell Res Ther **1,** 365, 2006.

Address correspondence to:
Lothar Koch, Ph.D.
Department of Nanotechnology
Laser Zentrum Hannover e. V.
Hollerithallee 8
30419 Hannover
Germany

E-mail: l.koch@lzh.de

Received: June 11, 2009
Accepted: November 2, 2009
Online Publication Date: December 15, 2009

Publication 2

Skin tissue generation by laser cell printing

Koch L[1], Deiwick A[1], Schlie S[1], Michael S[2], Gruene M[1], Coger V[2], Zychlinski D[3], Schambach A[3], Reimers K[2], Vogt PM[2], Chichkov B[1]

[1]Department of Nanotechnology, Laser Zentrum Hannover e.V., Hannover, Germany
[2]Department or Plastic, Hand and Reconstructive Surgery, Hannover Medical School, Hannover, Germany
[3]Department of Experimental Haematology, Hannover Medical School, Hannover, Germany

Published in

Biotechnol Bioeng, 2012, Jul, Vol 109 (7), p. 1855 - 1863
doi: 10.1002/bit.24455.

ARTICLE

BIOTECHNOLOGY and BIOENGINEERING

Skin Tissue Generation by Laser Cell Printing

Lothar Koch,[1] Andrea Deiwick,[1] Sabrina Schlie,[1] Stefanie Michael,[2] Martin Gruene,[1] Vincent Coger,[2] Daniela Zychlinski,[3] Axel Schambach,[3] Kerstin Reimers,[2] Peter M. Vogt,[2] Boris Chichkov[1]

[1]Department of Nanotechnology, Laser Zentrum Hannover e.V., Hannover, Germany; telephone: +49-511-2788-256; fax: +49-511-2788-100; e-mail: l.koch@lzh.de

[2]Department of Plastic, Hand- and Reconstructive Surgery, Hannover Medical School, Hannover, Germany

[3]Department of Experimental Haematology, Hannover Medical School, Hannover, Germany

Received 10 September 2011; revision received 21 December 2011; accepted 18 January 2012

Published online 13 February 2012 in Wiley Online Library (wileyonlinelibrary.com). DOI 10.1002/bit.24455

ABSTRACT: For the aim of ex vivo engineering of functional tissue substitutes, Laser-assisted BioPrinting (LaBP) is under investigation for the arrangement of living cells in predefined patterns. So far three-dimensional (3D) arrangements of single or two-dimensional (2D) patterning of different cell types have been presented. It has been shown that cells are not harmed by the printing procedure. We now demonstrate for the first time the 3D arrangement of vital cells by LaBP as multicellular grafts analogous to native archetype and the formation of tissue by these cells. For this purpose, fibroblasts and keratinocytes embedded in collagen were printed in 3D as a simple example for skin tissue. To study cell functions and tissue formation process in 3D, different characteristics, such as cell localisation and proliferation were investigated. We further analysed the formation of adhering and gap junctions, which are fundamental for tissue morphogenesis and cohesion. In this study, it was demonstrated that LaBP is an outstanding tool for the generation of multicellular 3D constructs mimicking tissue functions. These findings are promising for the realisation of 3D in vitro models and tissue substitutes for many applications in tissue engineering.

Biotechnol. Bioeng. 2012;109: 1855–1863.

KEYWORDS: cell printing; bioprinting; laser; 3D tissue generation; skin

Introduction

One major goal of regenerative medicine is manufacturing autologous replacement tissue by arranging vital cells in three-dimensional (3D) patterns mimicking the structure, characteristics and functionality of natural tissue. Such 3D cell patterns could also bridge the gap between common cell culture conditions and animal models, since two-dimensional (2D) cell culture models have significant limitations. It has become obvious (Cukierman et al., 2001, 2002; Edelman and Keefer, 2005) that cell behaviour differs dramatically in 3D. This is reflected in the complexity and architecture of the 3D-microenvironment in vivo, consisting of the extracellular matrix (ECM) and different cell types arranged in correlation to their specific function in tissue. Innovative 3D cell models could provide new insights in understanding of cell behaviour, tissue functions and regeneration. These facts point out that reproducible, controllable and well-defined 3D cell models are a key challenge for future progress in tissue engineering. Therefore, the ability to precisely position different cells in complex 3D patterns is of essential importance.

For this purpose, different techniques are under investigation (Hon et al., 2008). Since these techniques are related to printing technology, the terms 'bioprinting' or 'cell printing' are used. A detailed description of these techniques has been given by Ringeisen et al. (2006). From the biological and technical point of view, all these techniques have to fulfill several specifications: (a) achieve a high resolution similar to the heterogeneity of natural tissue ($\leq$100 μm), (b) printing of any desired cell density and (c) variable viscosities of cell suspensions, (d) controlled cell patterning and (e) the cell behaviour shall not be negatively affected by the printing procedure.

Modified ink-jet printers are used for ejecting small droplets of a biological material through a small nozzle (Alper, 2004). Printing of bacteria (Xu et al., 2004), DNA arrays (Okamoto et al., 2000), protein patterns (Phillippi et al., 2008) and living cells (Nakamura et al., 2005; Saunders et al., 2008) has been demonstrated. However, ink-jet printers are capable to handle cell suspensions only with low viscosities and low cell densities to avoid shear stress at the orifice or cell clogging (Born et al., 1992). To overcome these

Correspondence to: L. Koch

Contract grant sponsor: Braukmann-Wittenberg-Herz-Stiftung
Contract grant sponsor: Deutsche Forschungsgemeinschaft
Contract grant sponsor: SFB TransRegio 37
Contract grant sponsor: REBIRTH Cluster of Excellence (Exc62/1)

cell density limitations, printing of cell aggregates (Mironov et al., 2009) is now under investigation.

Microdispensing as another approach uses extrusion mechanisms (Khalil et al., 2005; Lee et al., 2009). The material is extruded under pressure out of a nozzle with about 50–1,000 μm diameter continuously or in droplets by switching a microvalve with a suitable frequency. With larger extrusion nozzle diameters, the disadvantages of the ink-jet printers (clogging and shear stress) can be avoided at the expense of resolution (Chang et al., 2008). However, all these techniques still have the potential for further development and it is still not sure, which technique will prevail.

In this study, Laser-assisted BioPrinting (LaBP) by laser-induced forward transfer is used to arrange cells in 3D structures, which also has been used for previous studies (Gruene et al., 2011a,b,c,d; Koch et al., 2010). LaBP is capable of positioning small volumes (down to a few hundred femtoliters) of cell suspensions with high resolution (Barron et al., 2005; Gruene et al., 2011a). Furthermore, high cell densities (up to 10^8 cells/mL; Ringeisen et al., 2006) and hydrogel precursors with any desired viscosity can be printed. An overview of the different realisations and denominations of this technique are given by Schiele et al. (2010).

It has been shown that cells are not harmed by the printing procedure (Barron et al., 2005; Hopp et al., 2005; Koch et al., 2010; Othon et al., 2008; Raof et al., 2011). Our own group has recently demonstrated that the differentiation potential of mesenchymal stem cells printed in grafts is not influenced with respect to osteogenic, chondrogenic (Gruene et al., 2011b) and adipogenic (Gruene et al., 2011c) differentiation.

Up to now, studies have concentrated on 3D arrangements (Barron et al., 2004; Gruene et al., 2011b; Othon et al., 2008) of single or 2D patterning of different cell types (Guillemot et al., 2010; Raof et al., 2011; Schiele et al., 2009). More complex multicellular 3D constructs generated via laser printing have not been described in literature. To serve as tissue substitutes or 3D cell models in the future, vital and functioning 3D cell constructs are required, which mimic natural tissue with respect to cell density and distribution of different cell types and wherein the cells form similar tissue. Whether LaBP can be used to build multicellular 3D patterns in natural matrix and whether the generated constructs are functioning and forming tissue, are the main focuses of our study.

Tissue formation is guided by intercellular junctions (Ko et al., 2000). Specific junctions can be found as cell–cell and cell–matrix connections in all kinds of tissue, abundantly in epithelium like the epidermis. Intercellular adherens junctions (Gumbiner, 1996; Niessen, 2007) are fundamental for tissue morphogenesis and cohesion. They are composed mainly of cadherins (calcium-dependent adherent proteins). Gap junctions (Mese et al., 2007; Simon and Goodenough, 1998) allow intercellular communication by chemical signals passing through these cell–cell channels. Gap junctions, consisting of connexins (Cx; Richard, 2000), are known to play a fundamental role in differentiation, cell cycle progression and cell survival (Fitzgerald et al., 1994; Schlie et al., 2010).

Thus, cadherin and Cx localisation followed by gap junction coupling are good parameters to study tissue properties. In this work, tissue formation of LaBP-generated 3D constructs was investigated with a focus on cadherins and Cx-43 (Cx43), which is the main Cx in human skin (Fitzgerald et al., 1994; Wiszniewski et al., 2000). The functionality of cell–cell communication via gap junction coupling was assessed with a dye-transfer, so-called scrape-loading method (Begandt et al., 2010).

In this study, fibroblasts (murine cell line NIH-3T3) and keratinocytes (cell line HaCaT from adult human skin) embedded in collagen were printed layer-by-layer in a 3D pattern as a simple example for skin tissue. Previously, we demonstrated that these cell types are not harmed by the printing procedure (Koch et al., 2010). These well-established cell lines were also combined in other studies (Bigelow et al., 2005; Delehedde et al., 2001). In the cultivation of keratinocytes 3T3 fibroblast cells are widely used, because they are secreting growth factors favorable for keratinocytes (Boehnke et al., 2007; Linge, 2004; Schoop et al., 1999). Collagen was employed as hydrogel, since it is the main component of ECM in skin, in order to approximate native skin as far as possible (Wisser and Steffes, 2003).

Our main focus was the arrangement of these skin cells under conditions (3D cell pattern, cell density, matrix material) comparable to native skin tissue for studying the tissue formation process. Therefore, the printed 3D cell constructs were analysed after different cultivation times by histological and immunohistological methods. The existence of cell–cell channels as an indication of tissue formation was investigated in vital 3D cell constructs.

Materials and Methods

Materials

Cell culture media and supplements were obtained from Lonza (Basel, Switzerland). Cell culture flasks and plates were purchased from TPP-Techno Plastic Products AG (Trasadingen, Switzerland). Chemicals and antibodies were purchased from Sigma–Aldrich (Deisenhofen, Germany), unless otherwise noted.

Cell Lines and Cell Culture

3D tissue formation experiments were performed with mouse NIH-3T3 Swiss albino fibroblasts (DSMZ Braunschweig, Germany) and the human immortalised keratinocyte cell line, HaCaT (DKFZ, Heidelberg, Germany). NIH-3T3 fibroblasts were cultured in

Dulbecco's modified Eagle's medium (DMEM) with high glucose (4.5 g/L) supplemented with 10% foetal bovine serum (FBS) and 1% antibiotic solution (100 U/mL penicillin, 100 μg/mL streptomycin). HaCaT keratinocytes were expanded in DMEM/Ham's F12 medium supplemented with 10% FBS and 1% antibiotic solution. The cells were cultured in a 37°C, 5% CO_2 humidified incubator and fed every 3 days. Cell passaging was performed with 0.05% trypsin/0.02% EDTA when the cells were at approximately 80% confluence.

Lentiviral Transduction

HaCaT human keratinocytes were transduced with lentiviral (pRRL.PPT.SF.FP.pre) or gammaretroviral (pSRS11.SF.FP.pre) expressing the fluorescent proteins (FP) green fluorescent protein (GFP) or mCherry. The lentiviral and gammaretroviral backbones have been previously described (Schambach et al., 2006a,b). Gammaretroviral and lentiviral supernatant production was performed as described in Schambach et al. (2006c). In brief, 293T cells were transfected with gammaretroviral/lentiviral vector, a gag/pol helper plasmid, a vesicular stomatitis virus glycoprotein (VSVg) expression plasmid and a Rev expression plasmid (the latter only for lentiviral production). 293T cells were maintained in DMEM supplemented with 10% foetal calf serum (FCS), 1% antibiotic solution and 2 mmol/L glutamine. Viral titers determined on HT1080 and SC-1 cells by flow cytometry were in the range of 10^7 IU/ml. HaCaT and NIH3T3 were transduced using an MOI of 3 to obtain nearly 100% positive cells containing the fluorescent marker gene. Transduced cells were used for Figures 1, 2c and 3f and g.

Laser Printing of Cells

Cells were arranged in 3D patterns via LaBP based on the principle of laser-induced forward transfer, using the setup described by Koch et al. (2010). Briefly, the experimental setup consists of two coplanar glass slides (Fig. 1, top). The upper one is covered underneath with a laser absorbing layer (here a 60 nm thin gold layer) and a layer of the cell containing material to be transferred (here cells embedded in collagen gel or a mixture of blood plasma and alginate). Laser pulses are focused through the glass slide into the absorption layer which is evaporated locally. This generates a high pressure that propels the subjacent cell compound towards the lower glass slide. A material sheet, scaffold or a layer of gel can be positioned on the lower glass slide to print cells onto or into it. In this study, a sheet of Matriderm™

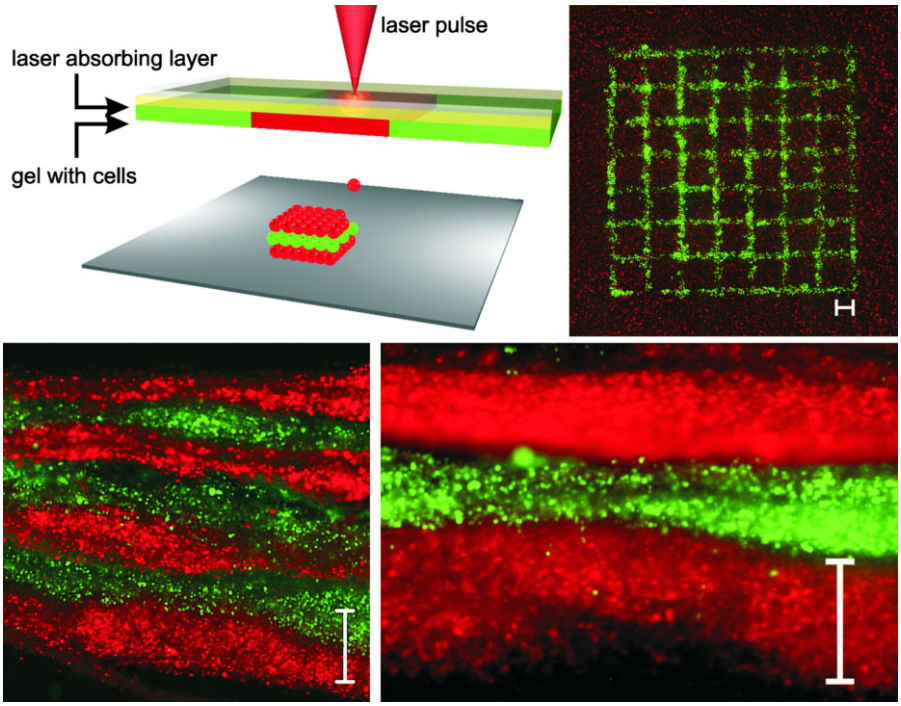

Figure 1. **Top**: Sketch of the laser printing setup. The cell–hydrogel compound is propelled forward as a jet by the pressure of a laser-induced vapour bubble. Layer-by-layer a 3D cell pattern is generated. A printed grid structure (top view) of fibroblasts (green) and keratinocytes (red) demonstrates micropatterning capabilities of the laser printing technique. **Bottom**: Seven alternating colour-layers of red and green keratinocytes (left; detail right). Each colour-layer consists of four printed sublayers. A histological section was prepared 18 h after printing. The whole structure has a height of about 2 mm and a base area of 10 mm × 10 mm. Scale bars are 500 μm. [Color figure can be seen in the online version of this article, available at http://wileyonlinelibrary.com/bit]

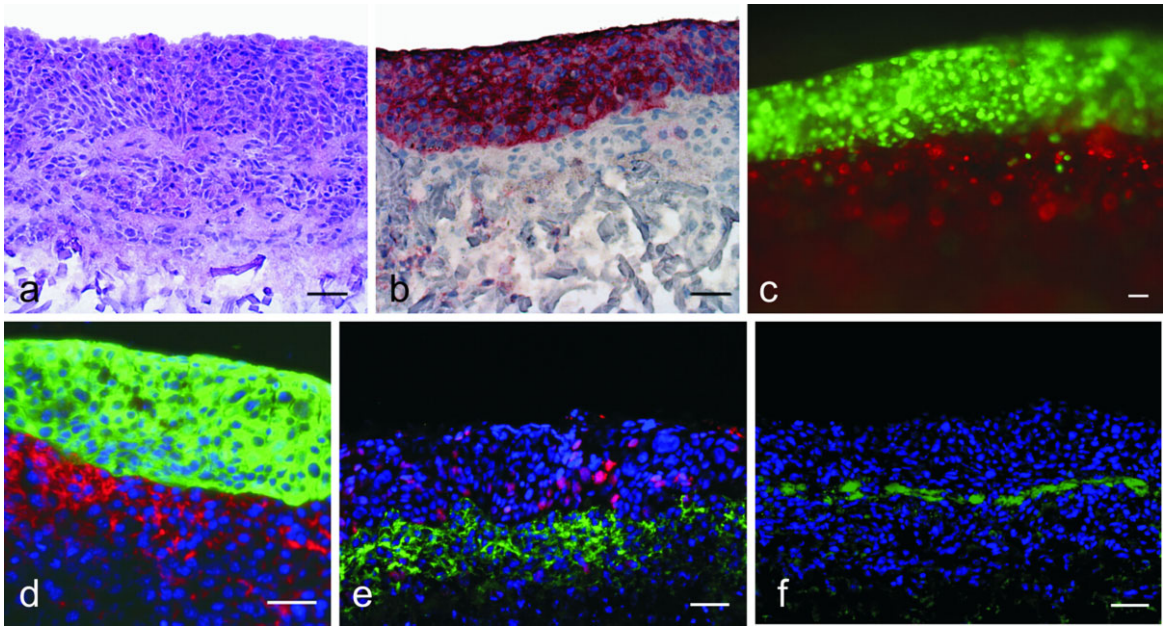

Figure 2. Skin mimicking bi-layered construct: 20 layers of murine fibroblasts (NIH-3T3) and 20 layers of human keratinocytes (HaCaT) embedded in collagen were printed subsequently on a sheet of Matriderm™. Cryostat sections were prepared 10 days after printing, except (**c**). All scale bars are 50 μm. Haematoxylin and eosin staining (**a**) show all printed cells in a tissue-like pattern. Immunoperoxidase staining of cytokeratin 14 in reddish-brown (**b**) depicts keratinocytes in the bi-layered structure while all cell nuclei (fibroblasts and keratinocytes) are counterstained in light blue with haematoxylin. Image (c) shows a section through the laser printed structure, prepared directly after the printing procedure, with transduced fibroblasts (red) and keratinocytes (green). In picture (**d**) the fibroblasts are stained in red (pan-reticular fibroblast), keratinocytes are stained in green (cytokeratin 14) and cell nuclei are stained in blue (Hoechst 33342). Especially the keratinocytes formed a compact cell organisation. In picture (**e**) all cell nuclei are stained with Hoechst 33342 (blue), the proliferating cell nuclei are stained with Ki-67 (red) and fibroblasts are stained in green. Fibroblasts and the keratinocytes above are still vital and proliferating. Image (**f**) depicts an anti-laminin staining in green and all cell nuclei in blue (Hoechst 33342). Laminin is a major constituent of the basement membrane in skin.

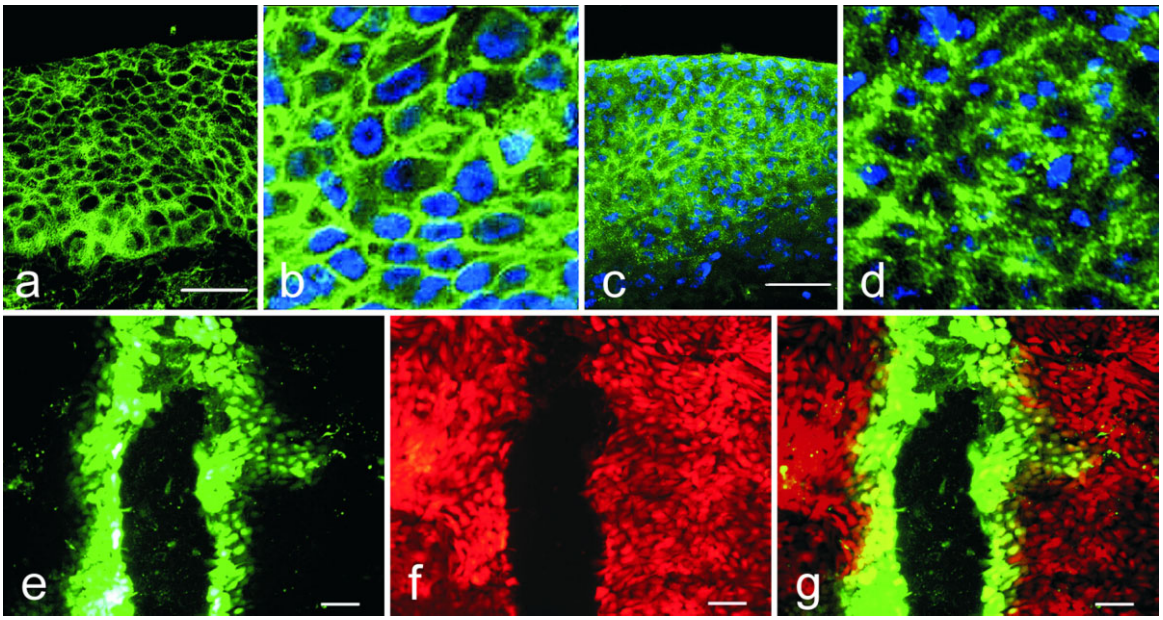

Figure 3. Qualitative analysis of adherens and gap junction formation essential for tissue function. Fluorescence microscopic images of 3D printed fibroblasts and keratinocytes: (**a**) pan-cadherin-staining depicts the adherens junctions consisting of cadherins, which are located between the membranes of neighbouring cells; (**b**) pan-cadherin-staining (green) and cell nuclei staining with Hoechst 33342 (blue); (**c**,**d**) connexin-43 (Cx43) staining (green) and Hoechst 33342 nuclei staining (blue), connexins are the constituents of the gap junctions; Picture **d** shows Cx43 distributed in a scattered, punctate fashion, which is a sign for the formation of gap junctions; (**e**–**g**) gap junction coupling visualised in green with lucifer yellow (e,g) after scrape-loading procedure, the keratinocytes, transfected with mCherry, are depicted in red (f,g). All scale bars are 50 μm.

(Dr. Suwelack Skin & Health Care, Billerbeck, Germany) was used (Golinski et al., 2009), which is porous and permeable for cell culture media.

The cell–gel compound is transferred as a jet (Duocastella et al., 2009; Unger et al., 2011). The transferred volume depends on the laser absorbing layer and the cell–gel layer as well as the laser pulse energy and the focused laser spot size. Volumes in the range of 0.1–1 nL were transferred in this study.

A Nd:YAG-laser (DIVA II; Thales Laser, Orsay, France) with 1,064 nm wavelength, approximately 10-ns pulse duration (FWHM) and 20-Hz repetition rate was applied. A 60 mm achromatic lens focussed the laser pulses into a 45-μm diameter ablation spot size. Depending on the cell–gel layer thickness (approx. 60 μm) and viscosity, the laser pulse energy was set between 30 and 60 μJ, corresponding to laser fluences between 1 and 2 J/cm^2. In Figure 1, a grid pattern consisting of green fibroblasts and red keratinocytes demonstrating the capability of the laser printing technique is shown.

Generating 3D Cell Structures With Layers of Green and Red Keratinocytes

To prove the ability of 3D cell arrangement, alternating layers of HaCaT keratinocytes labelled with GFP (green) and mCherry (red) were printed. For the printing process 1.5×10^6 cells were resuspended in 45 μL of a hydrogel composed of 50% 4 (wt.%) alginate and 50% ethylenediaminetetraacetic acid (EDTA) human blood plasma. Subsequently, this cell containing hydrogel was dispersed on the absorption layer on the upper glass slide with a blade-coater to form a homogenous layer of approximately 60 μm thickness. Then, the cell-coated glass slide was fixed in a metal frame and mounted upside-down in the setup for printing.

The lower glass plate was covered with an initial 60 μm layer of a mixture of 25% 4 (wt.%) alginate and 75% blood plasma and subsequently wetted with a 0.1 M $CaCl_2$ solution for gelation. Alternating layers of red and green keratinocytes were printed onto the lower glass plate. Each colour layer of cells consisted of four printed sublayers. When the colour layer was finished, it was cross-linked with the $CaCl_2$ solution. Altogether seven colour layers with 28 sublayers were printed. After cultivation submerged for 18 h, vertical sections were prepared with a scalpel and analysed by fluorescence microscopy, using an AxioImager A1.m microscope (Carl Zeiss Microimaging, Göttingen, Germany), equipped with AxioCam ICc1 camera and AxioVision Rel. 4.8 software.

3D Bi-Layered Tissue Formation Experiments With Collagen Hydrogel

For the transfer of cells by LaBP, type I collagen was isolated from rat tail tendons as described by Dunn et al. (1991) by a modified procedure of Elsdale and Bard (1972). For each cell–collagen layer a mixture consisting of collagen (3 mg/mL: 66.5% of the total volume), 10× DMEM/Ham's F12 (10% of the total volume), sodium hydrogencarbonate ($NaHCO_3$ 7.5% for neutralisation and gelification, 1% of the total volume) and 1.5×10^6 cells resuspended in 1× DMEM/Ham's F12 medium (22.5% of the total volume) was used. Subsequently, 45 μL of the cell containing collagen gel was dispersed on the absorption layer on the upper glass slide with a blade-coater to form a homogenous layer of approximately 60 μm thickness. Then the cell-coated glass slide was fixed in a metal frame and mounted upside-down in the setup for printing. To create 3D bi-layered cell constructs composed of fibroblasts and keratinocytes, 20 cell–collagen sublayers of NIH-3T3 fibroblasts were first printed onto a sheet of Matriderm^{TM} followed by 20 cell–collagen sublayers of HaCaT keratinocytes. The 3D cell constructs were further cultivated submerged in DMEM:Ham's F12 (3:1, v/v) supplemented with 10% FBS and 1% antibiotic solution at 37°C in a humidified atmosphere containing 5% CO_2 for 10 days. At the end of the experiment, the 3D bi-layered cell constructs were embedded in Tissue-Tek OCT (Science Services, München, Germany) and snap frozen in liquid nitrogen and stored at −80°C.

Immunohistochemistry of 3D Bi-Layered Cell Constructs

Immunohistochemical and immunofluorescence staining of frozen sections (7–10 μm) was performed by a two-step indirect method. Briefly, sections were fixed in 4% paraformaldehyde for 10 min. After blocking with 5% normal goat serum, sections were incubated overnight at 4°C with primary antibodies against keratin 14 (mouse monoclonal antibody, clone RCK 107, diluted 1:50; Acris Antibodies, Herford, Germany), fibroblasts (Pan Reticular; rat monoclonal antibody, clone ER-TR7, diluted 1:100; Acris Antibodies), Cx43 (rabbit polyclonal antibody, diluted 1:1,000), pan-cadherin (rabbit polyclonal antibody, diluted 1:250), laminin (rabbit polyclonal antibody, diluted 1:250) and Ki-67 (rabbit polyclonal antibody, diluted 1:50; Acris Antibodies). Following washing with Dulbeccós phosphate-buffered saline (DPBS), sections were incubated for 1 h at 37°C with peroxidase-conjugated or fluorescence-conjugated secondary antibodies at an appropriate dilution [horseradish peroxidase-conjugated goat anti-mouse IgG (H + L), diluted 1:100; Dianova, Hamburg, Germany] or for fluorescence staining with *Alexa Fluor® 488/Alexa Fluor® 555 F (ab') 2 fragment* goat anti-mouse, anti-rat or anti-rabbit IgG (H + L), diluted 1:500; Invitrogen, Karlsruhe, Germany). After that, sections were washed and cell nuclei in the immunofluorescence samples were stained with 10 μg/mL Hoechst 33342 (blue fluorescence staining). Immunostaining with horseradish peroxidase was developed by incubation with 3-amino-9-ethyl-carbazole substrate in sodium acetate puffer (0.1 mol/L, pH 5.2),

containing hydrogen peroxide, for 30 min. Cell nuclei were counterstained with haematoxylin. Following washing, sections were mounted in glycergel and analysed by microscopy. As negative control, primary antibody was replaced with an irrelevant primary antibody at the same concentration and of the same isotype. No significant staining was observed in the negative controls. For histological analysis, cryosections (10 μm) were stained with haematoxylin and eosin (H&E) following standard protocols.

Analysis of Gap Junction Coupling

Gap junction coupling, as a sign for tissue functions with respect to intercellular communication, can be estimated via scrape-loading method (Begandt et al., 2010). The confluently grown 3D printed cells were scratched and by this means, the added dye lucifer yellow (LY) could penetrate into the destroyed cells. As gap junctions are permeable for LY, the diffusion distance over channel-connected neighbouring cells correlating with gap junction coupling can be analysed. Twenty layers of keratinocytes embedded in collagen were printed on a glass slide and cultivated for 10 days at 37°C (5% CO_2). After washing with PBS, the slides were transferred into a DPBS solution including 0.25% LY. With the help of a razor blade one scratch along the whole sample was set. Following 5-min incubation time, the slides were washed four times with DPBS for 5 min each. At last the cells were fixed by 10-min incubation in DPBS containing 4% paraformaldehyde and conserved in DPBS. The diffusion distance of LY was documented via fluorescence microscopy.

Results

Generation of 3D Structures Consisting of Layers of Green and Red Keratinocytes

Seven alternating layers of red and green fluorescence labeled keratinocytes with four sublayers each (28 layers altogether) can be seen in the histologic cryo-section in Figure 1. The whole structure has a height of about 2 mm and base area of 10 mm × 10 mm. The red and green layers can be distinguished clearly; the individual layers do not intermix with each other.

Fibroblasts and Keratinocytes as a Simple Bi-Layered 3D Skin Structure

On a sheet of Matriderm™ 20 layers of NIH-3T3 fibroblast and subsequently 20 layers of HaCaT keratinocytes were printed to generate simple 3D skin equivalents with dermis- and epidermis-like structure. Collagen was used as the matrix material. After printing, cell structures were cultivated for 10 days. In Figure 2a, a H&E staining of a histological section depicts the cells on the Matriderm™ sheet. Cytokeratin 14 staining was used to distinguish the keratinocytes from the fibroblasts since the former have an abundant source of keratin, while the latter lacks the presence of keratin. Also a fibroblast pan-redicular red fluorescence staining combined with a cytokeratin 14 green fluorescence staining depicts the printed bi-layered structure. It can be seen that the fibroblast–collagen compound penetrates into the pores of the Matriderm™ sheet. However, the cell layers keep strictly separated over the whole observation period (Fig. 2b and d). The thickness of the printed structure decreases from 500 to 250 μm during the cultivation time as can be seen by comparing Figure 2c, taken directly after printing and 2b and d taken after 10 days in culture. This shrinkage of collagen gel by cultured fibroblasts is well known in literature (Bellows et al., 1982).

Post-Printing Cell Proliferation

To examine the vitality in the bi-layered 3D cell structures, the proliferation of the cells was studied in histologic sections prepared 10 days after printing. In Figure 2e, a Ki-67 staining shows the fraction of proliferating cells. The Ki-67 protein is present in cells during their active cell cycle phases, but it is absent in resting cells. In all regions proliferating cells can be found which verifies the vitality of the printed cells 10 days after printing.

Development of a Basement Membrane

Figure 2f illustrates the formation of a laminin layer between the fibroblasts and keratinocytes. Outside this layer, the laminin concentration is very low. Laminins are major proteins of the basal lamina, which is part of the basement membrane between epidermis and dermis in natural skin.

Analysis of Adherens Junctions

For tissue morphogenesis and maintenance adherens junctions mediated by cadherins are crucial, since they are connecting cells and their cytoskeleton mechanically with neighbouring cells and the ECM (Niessen, 2007). Immunostaining with pan-cadherin depicts in Figure 3a cadherin expression localised in the cell membrane 10 days after LaBP in all cells. In Figure 3b cadherin and the cell nuclei of keratinocytes are shown. While adherens junctions consisting of cadherins are formed extensively between the keratinocytes they are less between the fibroblasts.

Analysis of Gap Junctions

Tissue functions require intercellular communication over gap junctions consisting of Cx. Immunostaining of Cx43, the main Cx in human skin, pointed out that it is expressed

in all cells and localised within the cell membrane 10 days after LaBP procedure (Fig. 3c and d). It can be seen in Figure 3d that Cx43 is distributed in a scattered, punctate fashion, which is a sign for the formation of gap junctions (Morritt et al., 2007). Furthermore, the scrape-loading method proved that the gap junction channels generated by the cells are functional. The LY dye penetrated from the destroyed keratinocyte cells into neighbouring cells and further cells, which is only possible through functional gap junctions (Fig. 3e–g). The LY in the cells located furthest away from the scratch went through about 10 cells.

Discussion

Since more than 10 years different printing techniques are under investigation for applications in tissue engineering. By means of laser printing it has been shown that vital cells can be printed unharmed and that stem cells are not affected in their differentiation potential (Barron et al., 2005; Gruene et al., 2011b; Hopp et al., 2005; Koch et al., 2010; Othon et al., 2008; Raof et al., 2011). First 3D patterns have been presented (Barron et al., 2004; Gruene et al., 2011d; Othon et al., 2008). However, no printed tissue has been demonstrated so far.

This study is focused on the generation of 3D multicellular constructs resembling simple skin tissue as their native archetype. Vital skin cells were printed in 3D patterns, their vitality and tissue-formation behaviour was examined.

The alternating layers of red and green keratinocytes in Figure 1, printed with a blood–plasma/alginate mixture, demonstrate the ability to print 3D cell structures layer-by-layer, whereby the individual layers do not intermix with each other. Also, the fibroblasts and keratinocytes in Figure 2, printed with collagen (the main component of ECM in skin), did not intermix even after 10 days in culture. The cells remain in the printed pattern.

We have previously shown that the cells are not harmed by our printing procedure (Gruene et al., 2011b; Koch et al., 2010). Here, it was investigated if the printed cells kept their vitality also in the 3D structure. Therefore, proliferation after 10 days under 3D culture conditions was visualised by immunohistology. The Ki-67 staining and the Hoechst 33342 staining in Figure 2e showed that cells—fibroblasts and keratinocytes—in all areas of the printed construct proliferated and were vital.

The build-up of a basal lamina shown in Figure 2f is already a sign of the formation of skin tissue. To substantiate the tissue formation by laser printed cells, existence of cell–cell junctions was investigated. Adherens junctions assure the cohesion of tissue while gap junctions allow cell–cell communication (Ko et al., 2000). Therefore, the existence of these junctions and the functionality of the gap junctions were studied.

Tissue formation requires the adherence of cells to other cells and the ECM. Therefore, intercellular adhesion mediated by cadherin is an appropriate first measure for the tissue formation process. Figure 3a and b depict the extensive formation of intercellular adherens junctions between keratinocytes and their minor formation between fibroblasts. This difference is expected, since keratinocytes form the dermal epithelium (epidermis), where typically a higher level of junctions can be found (Niessen, 2007).

Since gap junction channels enable the direct exchange of metabolites, hormones, electric signals and second messengers needed for physiological activities (Mese et al., 2007), they are good candidates for analysis of tissue formation and its functionality. Gap junctions are associated hemichannels built out of tissue-specific Cx located within the cell membrane of neighbouring cells. To get a first insight whether gap junction channels are formed, analysis of Cx localisation (Morritt et al., 2007) is the primary step—hence a deficit of Cx localisation indicates a loss of function of gap junctions. Figure 3c and d reveal that Cx43, the main Cx in human skin, is still expressed in the membrane of the 3D printed cells. This result indicates that LaBP procedure and 3D cell arrangement does not affect Cx43 localisation providing gap junction formation. The Cx43 distribution in a scattered, punctate fashion is thereby a sign for the formation of gap junctions (Morritt et al., 2007).

In a second step, gap junction coupling via dye-transfer following scrape-loading method was documented. As the used dye LY can only diffuse via gap junctions, it cannot only be analysed whether the channels are formed in general, but also whether they are functional. In Figure 3e–g it is shown that the dye penetrated into parallel and vertical directions, meaning that the neighbouring cells in 3D setups build the channels and are connected in all 3D. Therefore, it can be concluded that the 3D printed skin grafts mimic tissue-specific functions with respect to gap junctions. Here, future research could concentrate on molecular procedure to quantify more detailed Cx expression levels or electrophysiological analysis with focus on gap junction conductance and second messenger exchange.

We demonstrated the 3D arrangement of vital cells by laser-printing as multicellular grafts analogous to native skin archetype. It could also be shown that these printed skin cells evolve intercellular adhesion and communication via adherens and gap junctions, which proves the tissue formation. To the best of our knowledge, these results are unique and have never been demonstrated so far.

The aim of the present study was to demonstrate that the laser printed cells are capable to generate real tissue. The applied tissue model, skin, has a layered configuration (dermis and epidermis), which was reproduced by printing fibroblasts and keratinocytes. This is an important step for future experiments where by integration of additional cell types, the printed cell construct complexity will be increased. For example, by printing endothelial cells we plan to generate capillaries inside the 3D structures. To illustrate further potential of our technique, a printed grid structure is shown in Figure 1.

The presented skin tissue constructs can serve as 3D cell-based models to study ex vivo cell and tissue functions or

milieu-/disease-dependent mechanisms. By integrating further cell types (e.g. melanocytes, Schwann cells, hair follicle cells) into the printed cell construct, the behaviour of these cells in a 3D in vitro microenvironment similar to their natural one can be analysed. Additionally, the generated tissue constructs might be used for in vivo testing by implanting them into animal models. The Matriderm™ substrates possess the required mechanical strength for suturing.

The tissue formation process needs also to be studied with different printed ECM and cell types to mimic other tissues, since our findings are demonstrated only for skin cells so far. Furthermore, with additional printing of endothelial cells also microvascularisation processes might be investigated. The here generated skin tissue with the collagen matrix is thin enough to supply the cells with oxygen and nutrients by diffusion, but the integration of a vascular network is crucial for printing bigger tissue grafts to assure the survival of the printed cells.

The LaBP technique offers promising potential for the future generation of different tissue engineered autologous grafts including skin substitutes. To cope with the challenge of producing tissue with an integrated vascular network, the LaBP technique might even enable the long-term goal of printing complete organs.

The authors kindly thank Dr. Suwelack Skin & Health Care, Billerbeck, Germany and Cornelia Kasper, Ph.D. from Institut für Technische Chemie, Leibniz Universität Hannover, Hannover, Germany for providing us with the Matriderm™ sheets. We would like to acknowledge the assistance of the Cell Sorting Core Facility of the Hannover Medical School supported in part by Braukmann-Wittenberg-Herz-Stiftung and Deutsche Forschungsgemeinschaft. This study has been supported by Deutsche Forschungsgemeinschaft, SFB TransRegio 37 and REBIRTH Cluster of Excellence (Exc62/1).

References

Alper J. 2004. Biology and the inkjets. Science 305:1895.

Barron JA, Wu P, Ladouceur HD, Ringeisen BR. 2004. Biological laser printing: A novel technique for creating heterogeneous 3-dimensional cell patterns. Biomed Microdevices 6:139–147.

Barron JA, Young HD, Dlott DD, Darfler MM, Krizman DB, Ringeisen BR. 2005. Printing of protein microarrays via a capillary-free fluid jetting mechanism. Proteomics 5:4138–4144.

Begandt D, Bintig W, Oberheide K, Schlie S, Ngezahayo A. 2010. Dipyriamole increases gap junction coupling in bovine GM-7373 aortic endothelial cells by a cAMP-protein kinase A dependent pathway. J Bioenerg Biomembr 42:79–84.

Bellows CG, Melcher AH, Aubin JE. 1982. Association between tension and orientation of periodontal ligament fibroblasts and exogenous collagen fibres in collagen gels in vitro. J Cell Sci 58:125–138.

Bigelow RLH, Jen EY, Delehedde M, Chari NS, McDonnell TJ. 2005. Sonic hedgehog induces epidermal growth factor dependent matrix infiltration in HaCaT keratinocytes. J Invest Dermatol 124:457–465.

Boehnke K, Mirancea N, Pavesio A, Fusenig NE, Boukamp P, Stark HJ. 2007. Effects of fibroblasts and microenvironment on epidermal regeneration and tissue function in long-term skin equivalents. Eur J Cell Biol 86:731–746.

Born C, Zhang Z, Al-Rubeai M, Thomas CR. 1992. Estimation of disruption of animal cells by laminar shear stress. Biotechnol Bioeng 40:1004–1010.

Chang R, Nam J, Sun W. 2008. Effects of dispensing pressure and nozzle diameter on cell survival from solid freeform fabrication-based direct cell writing. Tissue Eng Part A 14:41–48.

Cukierman E, Pankov R, Stevens DR, Yamada KM. 2001. Taking cell–matrix adhesions to the third dimension. Science 294:1708–1712.

Cukierman E, Pankov R, Yamada KM. 2002. Cell interactions with three-dimensional matrices. Curr Opin Cell Biol 14:633–640.

Delehedde M, Cho SH, Hamm R, Brisbay S, Ananthaswamy HN, Kripke M, McDonnell TJ. 2001. Impact of Bcl-2 and Ha-ras on keratinocytes in organotypic culture. J Invest Dermatol 116:366–373.

Dunn JCY, Tompkins RG, Yarmush ML. 1991. Long-term in vitro function of adult hepatocytes in a collagen sandwich configuration. Biotechnol Prog 7:237–245.

Duocastella M, Fernández-Pradas JM, Morenza JL, Serra P. 2009. Time-resolved imaging of the laser forward transfer of liquids. J Appl Phys 106:084907.

Edelman DB, Keefer EW. 2005. A cultural renaissance: in vitro cell biology embraces three-dimensional context. Exp Neurol 192:1–6.

Elsdale T, Bard J. 1972. Collagen substrata for studies on cell behaviour. J Cell Biol 54:626–637.

Fitzgerald DJ, Fusenig NE, Boukamp P, Piccoli C, Mesnil M, Yamasaki H. 1994. Expression and function of connexin in normal and transformed human keratinocytes in culture. Carcinogenesis 15:1859–1865.

Golinski PA, Zöller N, Kippenberger S, Menke H, Bereiter-Hahn J, Bernd A. 2009. Development of an engraftable skin equivalent based on matriderm with human keratinocytes and fibroblasts. Handchir Mikrochir Plast Chir 41(6):327–332.

Gruene M, Unger C, Koch L, Deiwick A, Chichkov B. 2011. Dispensing pico to nanolitre of a natural hydrogel by laser-assisted bioprinting. Biomed Eng Online 10:19.

Gruene M, Deiwick A, Koch L, Schlie S, Unger C, Hofmann N, Bernemann I, Glasmacher B, Chichkov B. 2011. Laser printing of stem cells for biofabrication of scaffold-free autologous grafts. Tissue Eng Part C 17:79–87.

Gruene M, Pflaum M, Deiwick A, Koch L, Schlie S, Unger C, Wilhelmi M, Haverich A, Chichkov B. 2011. Adipogenic differentiation of laser-printed 3D tissue grafts consisting of human adipose-derived stem cells. Biofabrication 3:015005.

Gruene M, Pflaum M, Hess C, Diamantouros S, Schlie S, Deiwick A, Koch L, Wilhelmi M, Jockenhoevel S, Haverich A, Chichkov BN. 2011. Laser printing of 3-D multicellular arrays for studies of cell–cell and cell–environment interactions. Tissue Eng Part C 17(10):973–982.

Guillemot F, Souquet A, Catros S, Guillotin B, Lopez J, Faucon M, Pippenger B, Bareille R, Rémy M, Bellance S, Chabassier P, Fricain JC, Amédée J. 2010. High-throughput laser printing of cells and biomaterials for tissue engineering. Acta Biomater 6:2494–2500.

Gumbiner BM. 1996. Cell adhesion: The molecular basis of tissue architecture and morphogenesis. Cell 84:345–357.

Hon KKB, Li L, Hutchings IM. 2008. Direct writing technology—Advances and developments. CIRP Ann 57:601–620.

Hopp B, Smausz T, Kresz N, Barna N, Bor Z, Kolozsvári L, Chrisey DB, Szabó A, Nógrádi A. 2005. Survival and proliferative ability of various living cell types after laser-induced forward transfer. Tissue Eng 11:1817.

Khalil S, Nam J, Sun W. 2005. Multi-nozzle deposition for construction of 3D biopolymer tissue scaffolds. Rapid Prototyping J 11:9–17.

Ko K, Arora P, Lee W, McCulloch C. 2000. Biochemical and functional characterization of intercellular adhesion and gap junctions in fibroblasts. Am J Physiol Cell Physiol 279:C147–C157.

Koch L, Kuhn S, Sorg H, Gruene M, Schlie S, Gaebel R, Polchow B, Reimers K, Stoelting S, Ma N, Vogt PM, Steinhoff G, Chichkov B. 2010. Laser printing of skin cells and human stem cells. Tissue Eng Part C 16:847–854.

Lee W, Debasitis JC, Lee VK, Lee JH, Fischer K, Edminster K, Park JK, Yoo SS. 2009. Multi-layered culture of human skin fibroblasts and kerati-

nocytes through three-dimensional freeform fabrication. Biomaterials 30:1587–1595.
Linge C. 2004. Establishment and maintenance of normal human keratinocyte cultures. In: Picot J, editor. Methods in molecular medicine, Vol. 107: Human cell culture protocols. 2nd edn. Totowa, NJ: Humana Press Inc. p. 1–11.
Mese G, Richard G, White TW. 2007. Gap junctions: Basic structure and function. J Invest Dermatol 127:2516–2524.
Mironov V, Visconti RP, Kasyanov V, Forgacs G, Drake CJ, Markwald RR. 2009. Organ printing: Tissue spheroids as building blocks. Biomaterials 30:2164–2174.
Morritt AN, Bortolotto SK, Dilley RJ, Han XL, Kompa AR, McCombe D, Wright CE, Itescu S, Angus JA, Morrison WA. 2007. Cardiac tissue engineering in an in vivo vascularized chamber. Circulation 115:353–360.
Nakamura M, Kobayashi A, Takagi F, Watanebe A, Hiruma Y, Ohuchi K, Iwasaki Y, Horie M, Morita I, Takatani S. 2005. Biocompatible inkjet printing technique for designed seeding of individual living cells. Tissue Eng 11:1658–1666.
Niessen CM. 2007. Tight junctions/adherens junctions: Basic structure and function. J Invest Dermatol 127:2525–2532.
Okamoto T, Suzuki T, Yamamoto N. 2000. Microarray fabrication with covalent attachment of DNA using bubble jet technology. Nat Biotechnol 18:438–441.
Othon CM, Wu X, Anders JJ, Ringeisen BR. 2008. Single-cell printing to form three-dimensional lines of olfactory ensheathing cells. Biomed Mater 3:034101.
Phillippi JA, Miller E, Weiss L, Huard J, Waggoner A, Campbell P. 2008. Microenvironments engineered by inkjet bioprinting spatially direct adult stem cells toward muscle- and bone-like subpopulations. Stem Cells 26:127–134.
Raof NA, Schiele NR, Xie Y, Chrisey DB, Corr DT. 2011. The maintenance of pluripotency following laser direct-write of mouse embryonic stem cells. Biomaterials 32:1802–1808.
Richard G. 2000. Connexins: A connection with the skin. Exp Dermatol 9:77–96.
Ringeisen BR, Othon CM, Barron JA, Young D, Spargo BJ. 2006. Jet-based methods to print living cells. Biotechnol J 1:930–948.
Saunders RE, Gough JE, Derby B. 2008. Delivery of human fibroblast cells by piezoelectric drop-on-demand inkjet printing. Biomaterials 29:193–203.
Schambach A, Galla M, Modlich U, Will E, Chandra S, Reeves L, Colbert M, Williams DA, von Kalle C, Baum C. 2006. Lentiviral vectors pseudotyped with murine ecotropic envelope: Increased biosafety and convenience in preclinical research. Exp Hematol 34(5):588–592.
Schambach A, Mueller D, Galla M, Verstegen MM, Wagemaker G, Loew R, Baum C, Bohne J. 2006. Overcoming promoter competition in packaging cells improves production of self-inactivating retroviral vectors. Gene Ther 13(21):1524–1533.
Schambach A, Bohne J, Chandra S, Will E, Margison GP, Williams DA, Baum C. 2006. Equal potency of gammaretroviral and lentiviral SIN vectors for expression of O6-methylguanine-DNA methyltransferase in hematopoietic cells. Mol Ther 13(2):391–400.
Schiele NR, Koppes RA, Corr DT, Ellison KS, Thompson DM, Ligon LA, Lippert TKM, Chrisey DB. 2009. Laser direct writing of combinatorial libraries of idealized cellular constructs: Biomedical applications. Appl Surf Sci 255:5444–5447.
Schiele NR, Corr DT, Huang Y, Raof NA, Xie Y, Chrisey DB. 2010. Laser-based direct-write techniques for cell printing. Biofabrication 2:032001.
Schlie S, Mazur K, Bintig W, Ngezahayo A. 2010. Cell cycle dependent regulation of gap junction coupling and apoptosis in GFSHR-17 granulosa cells. J Biomed Sci Eng 3:884–891.
Schoop VM, Mirancea N, Fusenig NE. 1999. Epidermal organization and differentiation of HaCaT keratinocytes in organotypic coculture with human dermal fibroblasts. J Invest Dermatol 112(3):343–353.
Simon AM, Goodenough DA. 1998. Diverse functions of vertebrate gap junctions. Trends Cell Biol 8:477–483.
Unger C, Gruene M, Koch L, Koch J, Chichkov BN. 2011. Time-resolved imaging of hydrogel printing via laser-induced forward transfer. Appl Phys Part A 103:271–277.
Wisser D, Steffes J. 2003. Skin replacement with a collagen based dermal substitute, autologous keratinocytes and fibroblasts in burn trauma. Burns 29(4):375–380.
Wiszniewski L, Limat A, Saurat JH, Meda P, Salomon D. 2000. Differential expression of connexins during stratification of human keratinocytes. J Invest Dermatol 115:278–285.
Xu T, Petridou S, Lee EH, Roth EA, Vyavahare NR, Hickman JJ, Boland T. 2004. Construction of high-density bacterial colony arrays and patterns by the ink-jet method. Biotechnol Bioeng 85:29–33.

Publication 3

The mouse dorsal skin fold chamber as a means for the analysis of tissue engineered skin

Michael S, Sorg H, Peck CT, Reimers K, Vogt PM

Department of Plastic, Hand and Reconstructive Surgery, Hannover Medical School, Hannover, Germany

Published in

Burns, 2013, Feb, Vol 39 (1), p. 82 - 88
doi: 10.1016/j.burns.2012.05.010

BURNS 39 (2013) 82–88

Available online at www.sciencedirect.com

SciVerse ScienceDirect

journal homepage: www.elsevier.com/locate/burns

The mouse dorsal skin fold chamber as a means for the analysis of tissue engineered skin

*Stefanie Michael, Heiko Sorg, Claas-Tido Peck, Kerstin Reimers *, Peter M. Vogt*

Department of Plastic, Hand- and Reconstructive Surgery, Hannover Medical School, Hannover, Germany

ARTICLE INFO

Article history:
Accepted 20 May 2012

Keywords:
Skin fold chamber
Tissue engineering
Mouse model
Skin substitute

ABSTRACT

The therapy of extensive and deep burn wounds is still a challenging task for reconstructive plastic surgery. The outcome is generally not satisfactory, neither from the functional nor from the aesthetic aspect. Several available skin substitutes are used but there is need for optimization of new skin substitutes which have to be tested *in vitro* as well as *in vivo*. Here, we show that the dorsal skin fold chamber preparation of mice is well suited for the testing of skin substitutes *in vivo*. Dermal skin constructs consisting of matriderm® covered with a collagen type I gel were inserted into full thickness skin wounds in the skin fold chambers. The skin substitutes integrated well into the adjacent skin and got epithelialized from the wound edges within 11 days. The epithelialization by keratinocytes is the prerequisite that also cell-free dermal substitutes might be used in the case of the lack of sufficient areas to gain split thickness skin grafts. Further advantage of the chambers is the lack of wound contraction, which is common but undesired in rodent wound healing. Furthermore, this model allows a sophisticated histological as well as immunohistochemical analysis. As such, we conclude that this model is well suited for the analysis of tissue engineered skin constructs. Besides epithelialization the mode and extend of neovascularization and contraction of artificial grafts may be studied under standardized conditions.

1. Introduction

The therapy of burns still displays a complex and challenging field due to the many difficulties arising from large and deep burns, *i.e.* the high risk of infections, the destruction of both epidermis and dermis and the only limited availability of autologous split-thickness skin grafts and keratinocytes for wound coverage. This leads to the need of skin substitutes for temporary or permanent wound closure. Several skin substitutes have already been used for years in the clinical application [1–3] but full success in burn regeneration has not been achieved yet. Although the available skin substitutes fulfil their very important goal of wound coverage, none is able to substitute all of the physiological functions of native skin on the functional and the aesthetic level.

Here, tissue engineered skin might be of a great benefit to these patients and many approaches are being followed to improve tissue engineered skin substitutes, *e.g.* by adding different cell types or growth factors. Nevertheless, following *in vitro* analysis, these skin constructs need to be tested *in vivo* before using them in humans. For this purpose the mouse displays one of the most ideal animal models due to several advantages, *i.e.* the easy and cheap breeding in large numbers,

* *Corresponding author at*: Department of Plastic, Hand- and Reconstructive Surgery, Hannover Medical School, Podbielskistr. 380, 30659 Hannover, Germany. Tel.: +49 511 532 8790; fax: +49 511 532 8795.
E-mail address: Reimers.Kerstin@mh-hannover.de (K. Reimers).

Abbreviations: SDS-PAGE, sodium dodecyl sulfate polyacrylamide gel electrophoresis; PBS, phosphate buffered saline; FBS, foetal bovine serum; DMEM, Dulbecco's modified Eagle's medium.

0305-4179/$36.00
http://dx.doi.org/10.1016/j.burns.2012.05.010

the known genetic background and the availability of different knock-out strains. For testing of new skin substitutes, the constructs can be inserted into full thickness skin wounds, mostly on the back of mice. This animal model can be performed on a standardized manner and already showed to be valid in the analysis of cells cultured in a bioreactor in contrast to cells cultured in normal cell culture [4,5], to examine the vascularization of transplants [6,7], to test the effect of mesenchymal cells and growth factors in addition to the skin constructs [8], to analyse constructs enriched with Schwann cells to enhance nerve migration [9] or constructs containing sweat gland cells [10], to assess constructs containing bone marrow mesenchymal stem cells [11], or to establish a humanized mouse model for psoriasis [12].

A disadvantage of the above-mentioned method, however, is the contraction of the wound due to the healing mechanism of rodents [13]. A solution may be the use of the dorsal skin fold chamber. In this case, the skin is fixed in a titanium frame avoiding tissue contraction [14]. Also, in the skin fold chamber the skin constructs can be monitored continuously without potential disturbances by wound dressing changes.

Here, we adapted the dorsal skin fold chamber for analysis of a tissue engineered skin construct. Therefore, we chose to insert a construct comprising a collagen type I gel on top of a matriderm® layer into a full thickness skin wound inside the skin fold chamber and analysed it for 11 days. Macroscopic changes were easily be assessed throughout the duration of the experiments with the chambers. Additionally, the ingrowth of the constructs as well as the migration of cells and possible neovascularization are parameters which can simply be analysed after the completion of the experiments.

2. Material und methods

2.1. Production of the transplant

Small round pieces of matriderm® sheet (Dr. Suwelack Skin & Health Care AG, Billerbeck, Germany), a collagen elastin matrix, were generated by using a biopsy punch of 6 mm diameter. After disinfection with isopropanol and washing with PBS, collagen type I gel was added on top of the matriderm® which was isolated from the tails of Sprague-Dawley rats (source: local animal care facility) as follows: The tails were washed with soap, cleaned with ethanol and each time four tendon bundles were prepared. The tendons were washed with NaCl 1% (J.T. Baker, Deventer, The Netherlands) and distilled water and subsequently incubated with acetic acid 3% (v/v) (J.T. Baker) at 4 °C over night. The solution was filtered through sterile gauze and centrifuged at 10,000 × *g* at 4 °C for 2 h. The supernatant was mixed dropwise with NaCl 30% (w/v) and centrifuged at 3300 × *g* at 4 °C for 30 min. The supernatant was discarded and the obtained pellet was resuspended in 5% (w/v) NaCl plus 0.6% acetic acid and centrifuged at 3300 × *g* for 10 min. The supernatant was discarded and the pellet resuspended in NaCl 5% (w/v) plus 0.6% acetic acid (v/v). This step was repeated with a final volume of 250 ml. The solution was dialysed against 5 l hydrochloric acid (pH 3, Roth, Karlsruhe, Germany) at 4 °C for 8 h, repeating the dialysis step five times. The solution was sterilized by addition and evaporation of chloroform (Sigma–Aldrich, Steinheim, Germany). The concentration of the obtained collagen was determined with absorbance spectroscopy at 280 nm with the mass extinction coefficient $\varepsilon_m = 0.9\ \mathrm{ml\ mg^{-1}\ cm^{-1}}$. The purity of the collagen was determined by electrophoretic separation with SDS-PAGE. To produce gels for testing the skin fold chamber, a mixture consisting of the collagen (66.5% of the total volume), 10× DMEM/Ham's F12 (10% of the total volume), sodium-hydrogencarbonate ($NaHCO_3$ 7.5% for neutralization and gelification, 1% of the total volume) and 1× DMEM/Ham's F12 medium (22.5% of the total volume) was used and gelified at 37 °C for 30 min.

2.2. Skin fold chamber

The dorsal skin fold chamber was used as a model for wound healing, according to Sorg et al. [14,15]. During anaesthesia with isoflurane the dorsal skin chamber was implanted, resulting in an extended double layer of back skin between the two titanium frames. A full thickness wound was created after marking a circle of 6 mm diameter by removing the complete skin inside the circle, down to the panniculus carnosus. The opposite side remained intact, still comprising the epidermis, dermis and the panniculus carnosus (Fig. 1). The respective skin constructs of 6 mm diameter were transferred into the wound with forceps and the wound area was covered with a glass coverslip, integrated into one of the frames (Figs. 1 and 2). After 11 days the mice were sacrificed. The constructs surrounded by normal skin were removed and saved for histological analyses (Fig. 1).

2.3. Animals

All animal experiments were evaluated and approved by the standing local animal care committee and the Hannover Medical School. The animals (5 male BALB/c-Nude mice, 8 weeks) were purchased from Charles River and kept in the local animal care facility with a day-night cycle of 12 h each, according to the institution guidelines. They received standardized food and water *ad libitum*. Animals were used for the experiments when they were at least 12 weeks old and weighed at least 25 g.

2.4. Histology

After fixation of the samples in 4% paraformaldehyde and subsequent embedding in paraffin, sections of 5 μm thickness were cut and haematoxylin/eosin and Masson's trichrome stainings were carried out following standard procedures. In the Masson's trichrome staining muscles are stained in red, connective tissue (containing collagen) appears green and cell nuclei are marked in black whereas cell nuclei appear dark blue in the haematoxylin/eosin staining, accompanied by pink cytoplasm.

2.5. Immunofluorescence

In order to detect blood vessels, deparaffinised and rehydrated paraffin sections were stained with anti actin smooth muscle (1:100, Millipore, Schwalbach, Germany) as first antibody followed by Alexa Fluor 488 chicken anti mouse (1:1000, Invitrogen, Darmstadt, Germany) as secondary antibody following standard protocols. After removing the

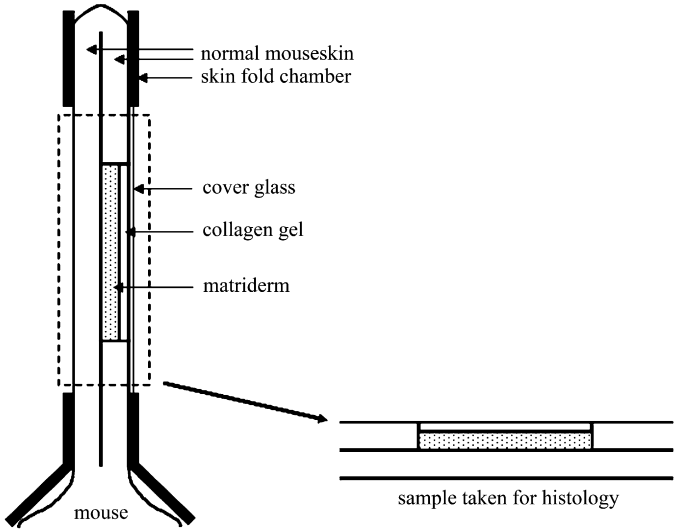

Fig. 1 – Cross section of the employed dorsal skin fold chamber in mice. The back skin of the mouse is pulled up and fixed by the chambers forming a sandwich like structure. In one side, a round full thickness wound is prepared into the skin and filled with a construct comprising collagen gel type I on top of matriderm®. The chamber is closed with a cover glass.

paraffin, the sections were treated with 0.1% Triton X 100 (Roth) in PBS (PAA, Pasching, Austria) for 4 min and subsequently blocked with 2% FBS (Biochrom, Berlin, Germany) in PBS for 30 min at room temperature. Both antibodies were incubated for 1 hour at 37 °C using 1% FBS in PBS. Signals were detected with a fluorescent microscope (Zeiss) equipped with the appropriate barrier filters.

3. Results

3.1. *Surgery of the mice*

In order to establish skin fold chambers as a means for investigation of tissue engineered skin constructs, we implanted skin fold chambers onto five mice. All of them survived the procedure and no problems occurred during the surgical procedure. The mice tolerated the chambers well and showed no signs of discomfort or changes in sleeping or feeding habits.

Constructs consisting of matriderm® with collagen type I gel on top were inserted into full thickness wounds in one half of the skin fold held by the skin fold chambers, while the opposite skin remained intact (for details see material and methods and Fig. 1). After introducing the constructs into the wounds, the borders of the constructs and the surrounding skin laid adjacent to each other (Fig. 2, left). We chose to analyse the described constructs because matriderm® plays an important role in burn or other wound treatment. Here, it serves as a carrier matrix to support the collagen, and in the long term may also support different cells types.

3.2. *Macroscopic observations*

Constructs were observed daily over a time period of 11 days. The transplants approximately kept their round form and at the

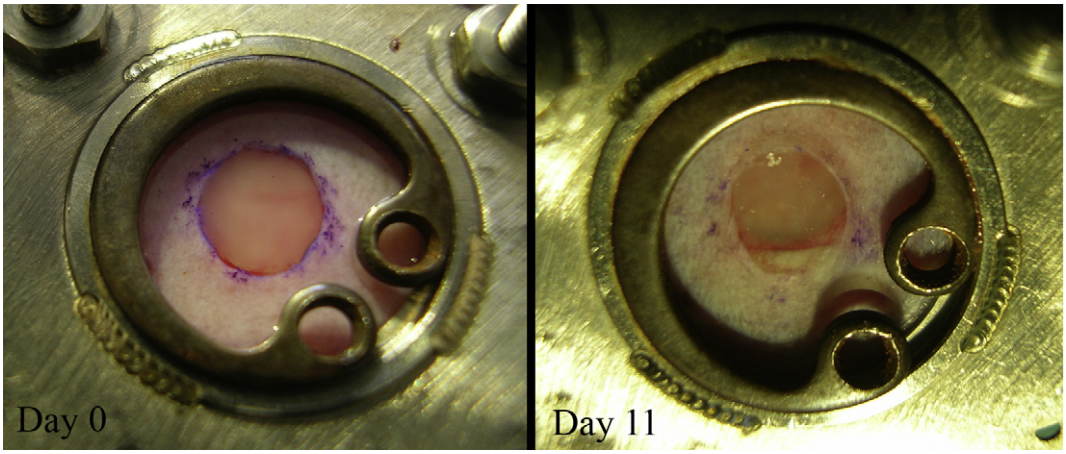

Fig. 2 – Pictures of a construct inserted into the wound directly after the operation (left) and on day 11 (right). The constructs contain collagen type I on top of matriderm® and fill the whole full thickness skin wounds.

end of the observation period the borders of the constructs seemed to be connected to the skin of the mice (Fig. 2, right). Meanwhile, the surface of the constructs tarnished increasingly during the course of time. After 11 days the tissue surrounding the skin substitute was still alive showing no inflammatory or necrotic processes. No contraction of the wounds could be detected (Fig. 2).

3.3. *Histological observations*

To assess the processes involved in the integration of the constructs, histological stainings were conducted (haematoxylin/eosin, Masson's trichrome). All constructs were well received in the wound beds and no gaps could be observed between the constructs and the surrounding skin (Fig. 3a and 4c). On the contrary, at the borders of the constructs, cells from the mouse skin started to grow onto the constructs. Single cells were also observed in the matriderm® layer and in the collagen. On the surface of the matriderm® keratinocytes migrated from the wound edges towards the middle of the constructs (Fig. 3b), but the centre of the surface remained free of cells (Figs. 3 and 4). There was no complete epidermis present on the matriderm®. In contrast, the inner part of the matriderm® was completely colonized by fibroblasts (Figs. 3 and 4).

After 11 days, the trichrome staining clearly showed collagen present on the surface of the matriderm® (Fig. 4b and d), leading to the conclusion that the collagen gel placed onto the matriderm® remained stable over the full observation period and was not degraded.

Also, on the histological level no contractions of the wound beds could be observed (Figs. 3 and 4). The intact skin opposite the wounds remained relaxed and showed all characteristics of normal skin.

To assess the formation of new blood vessels, the histological sections were stained with anti alpha smooth muscle actin antibody (Fig. 5). Several small and large blood vessels were present in the normal mouse skin and especially between the constructs and the opposite normal skin (Fig. 4a and 5). In contrast, in the matriderm® erythrocytes could be observed, but no blood vessels. This is probably due to bleeding during the surgical process.

4. Discussion

In our study we concentrated on the establishment of the dorsal skin fold chamber for the investigation of tissue engineered skin constructs. The skin fold chamber has already been used for many different purposes, *e.g.* in wound healing, angiogenesis, cancer, trauma research [14–21] and the evaluation of revascularization and angiogenesis of skin grafts [22,23]. But to our knowledge it has not been used for the testing of tissue engineered skin substitutes before.

A very important advantage of the skin fold chamber is the lack of wound contraction. In the chambers, the skin is safely secured by stitches to the frames and is therefore not able to close a wound by contraction *via* myofibroblasts [14] or the panniculus carnosus. A contraction leads to the reduction of the wound area and as such to an undesired sideward pressure onto the tissue engineered construct. Many skin substitutes have been tested by their integration into a normal full thickness wound onto the dorso-lateral region of the mouse [24–27], where a contraction can be seen. The avoidance of contraction is very important for the evaluation of the skin substitute as a major contraction of the wound is very typical for rodents but not for humans.

Additionally, in experiments with the chambers no need for wound dressings arise. This makes the experiments very easy to be carried out and reduces the failure rate of experiments due to problems with wound dressings and the respective dressing changes. This comprises the possible exsiccation of the wounds as well as the destruction or loss of

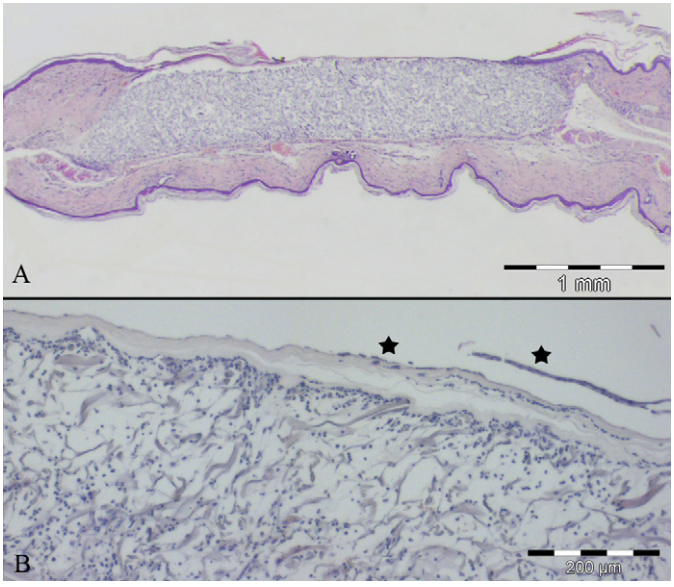

Fig. 3 – Histological cross sections stained with haematoxylin/eosin. An overview of a construct embedded in the surrounding skin is shown (A) as well as a detailed view of the keratinocytes (asterisks) migrating from the border regions onto the construct (B).

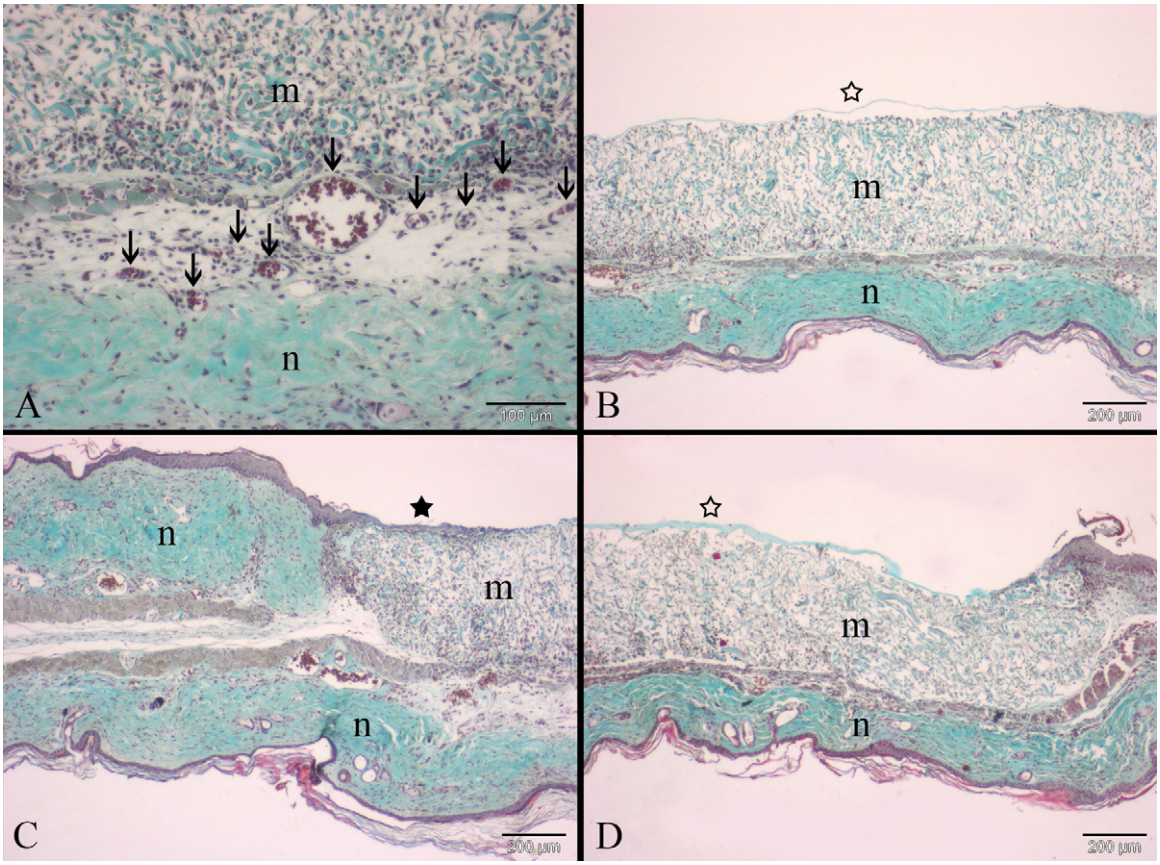

Fig. 4 – Histological cross sections stained with Masson's trichrome. The detailed view (A) shows one large and several small blood vessels (arrows) between the construct and the opposite skin. Many cells are seen in the matriderm® (m), but only few cells are present in the normal skin (n). In the border regions, the constructs and the adjacent normal skin are firmly connected (C) and some keratinocytes (filled asterisk) of the skin start to migrate onto the matriderm®. The collagen gel (empty asterisks) is still present after 11 days (B and D).

wound dressings due to the manipulation and removal by the mice themselves. Also, fixing the wound dressing neither too loosely, and as such risking the loss of the dressing, needs a lot of experience and care. The same holds true for fixing the dressings too tight, which could result in restriction of breathing as well as increased abdominal pressure.

In our experiments, the constructs were well received in the mice and fibroblasts migrated into the matriderm® from below. Additionally, keratinocytes started to migrate from the edges of the skin over the matriderm®, but did not suffice to form a complete epithelium within the chosen time frame of 11 days. This shows the integration of the skin substitute into the mouse skin, which is necessary for a skin substitute. Nevertheless, the time period was too short to form a new epidermis. Therefore, the next step would be to test a skin substitute already containing layers of fibroblasts and keratinocytes embedded in collagen on top of the matriderm®.

Furthermore, the fact that no necrosis could be detected is an additional sign for the acceptance of the construct by the mouse. However, no new vessel formation could be seen after 11 days. In studies comparing the vascularization rates of matriderm® and integra®, both kinds of matrices showed CD31 staining throughout the depth of the matrix after 2 and 3 weeks, respectively, in a rat model [28,29], but no shorter time points were described. In contrast, at least the border zones of matriderm® were vascularised after 10 days in a mouse model assessing the effect of low-pressure plasma treatment on the neovascularization of matriderm® [30].

In our study we show that the dorsal skin fold chamber is an appropriate tool to assess the behaviour of tissue engineered skin substitutes *in vivo*. The presented model is suited for cell-free and cell-seeded constructs, which is important for the testing of tissue engineered biomaterial. It offers the possibility to analyse and evaluate the skin constructs macroscopically as well as on the microscopic level [15,14]. Due to the transparent glass slide, the skin constructs can be monitored continuously without the need to change wound dressings [31]. The latter is especially advantageous for the animals as the animal stress response is massively reduced. On basis of the histological specimen, the integration of the skin constructs and the distribution of the cells in and on a matriderm® carrier can be shown by histological stainings. Also, the presence of collagen deposition can be determined by Masson's trichrome staining. This is important because collagen type I is a major

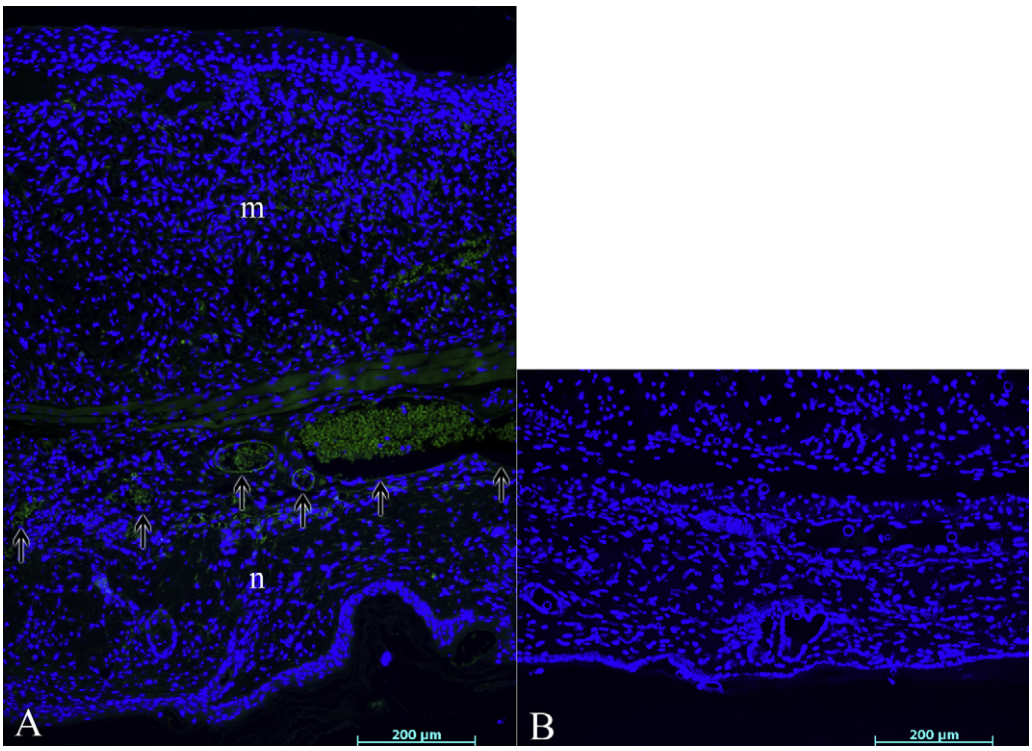

Fig. 5 – (A) Cross section stained with anti actin smooth muscle antibody (green fluorescence) to represent blood vessels (arrows). Cell nuclei are stained with DAPI (blue). Erythrocytes exhibit an autofluorescence (green/yellow). Vessels containing erythrocytes are present between the matriderm® (m) and the opposite normal mouse skin (n) as well as in the normal skin. No vessels are found in the matriderm®. (B) Negative control of the staining.

component of the dermis. Additionally, immunofluorescence offers the possibility to detect any blood vessels in the constructs. If available, also intravital microscopy can be applied to assess the vascularization of the skin constructs by time.

A skin substitute for burn patients needs to fulfil several criteria, among others the easy handling of the construct, the presence of a stable epithelium and the successful vascularization of the skin substitute. The first criterion is met by the use of matriderm® as a carrier matrix, which is already widely used in clinical applications. The other two criteria will be subject of further research and the here presented technique is as further contribution to the successful assessment of newly developed skin substitutes.

The second criterion can be met by the integration of keratinocytes into the skin substitute as a second step. Even further cells, such as fibroblasts or endothelial cells (to meet the third criterion) can be integrated and analysed. The long-term goal of many research groups is the development of a skin substitute for burn patients, which exhibits a structure close to real skin. This includes the presence of *e.g.* melanocytes and hair follicles for cosmetic improvement or the inclusion of perspiratory glands for the ability to control body temperature *via* sweat. Still, we have not reached our goal yet, but the here presented technique is a further contribution to the successful assessment of newly developed skin substitutes.

5. Conclusion

The use of the dorsal skin fold chamber in mice offers many possibilities in research. During the observation period the transplanted matriderm®/collagen skin construct integrated well into the surrounding tissue and no harmful effects occurred. Infiltration of single host cells indicates that the constructs are well-received in the wound bed while interference of transplanted cells with host cells has not to be feared. Due to the fact that the chamber avoids contraction of the wound area, it is a good model for wound research in rodents. Also, it helps to prevent difficulties connected to wound dressings. Therefore, it is an adequate and useful tool for the analysis of tissue engineered skin substitutes.

Conflict of interest statement

The authors declare there is no conflict of interest.

Acknowledgements

The authors kindly thank Sabine Braun for her excellent technical assistance and organizational help. This study has been supported by Deutsche Forschungsgemeinschaft, SFB

TransRegio 37. The authors thank Prof. Cornelia Kasper for providing us with matriderm®.

REFERENCES

[1] Vogt PM, Kolokythas P, Niederbichler A, Knobloch K, Reimers K, Choi CY. Innovative wound therapy and skin substitutes for burns. Chirurg 2007;4:335–42.

[2] Supp DM, Boyce ST. Engineered skin substitutes: practices and potentials. Clin Dermatol 2005;4:403–12.

[3] Singer AJ, Clark RA. Cutaneous wound healing. N Engl J Med 1999;10:738–46.

[4] Kalyanaraman B, Boyce ST. Wound healing on athymic mice with engineered skin substitutes fabricated with keratinocytes harvested from an automated bioreactor. J Surg Res 2009;2:296–302.

[5] Kalyanaraman B, Supp DM, Boyce ST. Medium flow rate regulates viability and barrier function of engineered skin substitutes in perfusion culture. Tissue Eng A 2008;5: 583–93.

[6] Shaterian A, Borboa A, Sawada R, Costantini T, Potenza B, Coimbra R, et al. Real-time analysis of the kinetics of angiogenesis and vascular permeability in an animal model of wound healing. Burns 2009;6:811–7.

[7] Egana JT, Condurache A, Lohmeyer JA, Kremer M, Stockelhuber BM, Lavandero S, et al. Ex vivo method to visualize and quantify vascular networks in native and tissue engineered skin. Langenbecks Arch Surg 2009;2:349–56.

[8] Egana JT, Fierro FA, Kruger S, Bornhauser M, Huss R, Lavandero S, et al. Use of human mesenchymal cells to improve vascularization in a mouse model for scaffold-based dermal regeneration. Tissue Eng A 2009;5:1191–200.

[9] Blais M, Grenier M, Berthod F. Improvement of nerve regeneration in tissue-engineered skin enriched with schwann cells. J Invest Dermatol 2009;12:2895–900.

[10] Huang S, Xu Y, Wu C, Sha D, Fu X. In vitro constitution and in vivo implantation of engineered skin constructs with sweat glands. Biomaterials 2010;21:5520–5.

[11] He L, Nan X, Wang Y, Guan L, Bai C, Shi S, et al. Full-thickness tissue engineered skin constructed with autogenic bone marrow mesenchymal stem cells. Sci China C Life Sci 2007;4:429–37.

[12] Carretero M, Guerrero-Aspizua S, Del Rio M. Applicability of bioengineered human skin: from preclinical skin humanized mouse models to clinical regenerative therapies. Bioeng Bugs 2011;4:203–7.

[13] Galiano RD, Michaels J5, Dobryansky M, Levine JP, Gurtner GC. Quantitative and reproducible murine model of excisional wound healing. Wound Repair Regen 2004;4:485–92.

[14] Sorg H, Krueger C, Vollmar B. Intravital insights in skin wound healing using the mouse dorsal skin fold chamber. J Anat 2007;6:810–8.

[15] Sorg H, Krueger C, Schulz T, Menger MD, Schmitz F, Vollmar B. Effects of erythropoietin in skin wound healing are dose related. FASEB J 2009;9:3049–58.

[16] Machado MJ, Watson MG, Devlin AH, Chaplain MA, McDougall SR, Mitchell CA. Dynamics of angiogenesis during wound healing: a coupled in vivo and in silico study. Microcirculation 2011;3:183–97.

[17] Lichtenbeld HC, Barendsz-Janson AF, van Essen H, Struijker Boudier H, Griffioen AW, Hillen HF. Angiogenic potential of malignant and non-malignant human breast tissues in an in vivo angiogenesis model. Int J Cancer 1998;3:455–9.

[18] Jewell AN, Swamydas M, Castillo CI, Wyan H, Allen LD, McDermott KA, et al. The endothelin axis stimulates the expression of pro-inflammatory cytokines and pro-migratory molecules in breast cancer. Cancer Invest 2010;9:932–43.

[19] Skala MC, Fontanella A, Lan L, Izatt JA, Dewhirst MW. Longitudinal optical imaging of tumor metabolism and hemodynamics. J Biomed Opt 2010;1:011112.

[20] Alexander S, Koehl GE, Hirschberg M, Geissler EK, Friedl P. Dynamic imaging of cancer growth and invasion: a modified skin-fold chamber model. Histochem Cell Biol 2008;6:1147–54.

[21] Knappe T, Mittlmeier T, Eipel C, Amon M, Menger MD, Vollmar B. Effect of systemic hypothermia on local soft tissue trauma-induced microcirculatory and cellular dysfunction in mice. Crit Care Med 2005;8:1805–13.

[22] Lindenblatt N, Calcagni M, Contaldo C, Menger MD, Giovanoli P, Vollmar B. A new model for studying the revascularization of skin grafts in vivo: the role of angiogenesis. Plast Reconstr Surg 2008;6:1669–80.

[23] Calcagni M, Althaus MK, Knapik AD, Hegland N, Contaldo C, Giovanoli P, et al. In vivo visualization of the origination of skin graft vasculature in a wild-type/GFP crossover model. Microvasc Res 2011.

[24] Boyce ST, Medrano EE, Abdel-Malek Z, Supp AP, Dodick JM, Nordlund JJ, et al. Pigmentation and inhibition of wound contraction by cultured skin substitutes with adult melanocytes after transplantation to athymic mice. J Invest Dermatol 1993;4:360–5.

[25] Xie JL, Li TZ, Qi SH, Huang B, Chen XG, Chen JD. A study of using tissue-engineered skin reconstructed by candidate epidermal stem cells to cover the nude mice with full-thickness skin defect. J Plast Reconstr Aesthet Surg 2007;9:983–90.

[26] Klingenberg JM, McFarland KL, Friedman AJ, Boyce ST, Aronow BJ, Supp DM. Engineered human skin substitutes undergo large-scale genomic reprogramming and normal skin-like maturation after transplantation to athymic mice. J Invest Dermatol 2010;2:587–601.

[27] Rasmussen CA, Gibson AL, Schlosser SJ, Schurr MJ, Allen-Hoffmann BL. Chimeric composite skin substitutes for delivery of autologous keratinocytes to promote tissue regeneration. Ann Surg 2010;2:368–76.

[28] Schneider J, Biedermann T, Widmer D, Montano I, Meuli M, Reichmann E, et al. Matriderm versus Integra: a comparative experimental study. Burns 2009;1:51–7.

[29] Bottcher-Haberzeth S, Biedermann T, Schiestl C, Hartmann-Fritsch F, Schneider J, Reichmann E, et al. Matriderm((R)) 1 mm versus Integra((R)) single layer 1.3 mm for one-step closure of full thickness skin defects: a comparative experimental study in rats. Pediatr Surg Int 2011.

[30] Ring A, Langer S, Schaffran A, Stricker I, Awakowicz P, Steinau HU, et al. Enhanced neovascularization of dermis substitutes via low-pressure plasma-mediated surface activation. Burns 2010;8:1222–7.

[31] Laschke MW, Harder Y, Amon M, Martin I, Farhadi J, Ring A, et al. Angiogenesis in tissue engineering: breathing life into constructed tissue substitutes. Tissue Eng 2006;8:2093–104.

Publication 4

Tissue engineered skin substitutes created by laser-assisted bioprinting form skin-like structures in the dorsal skin fold chamber in mice

Michael S[1], Sorg H[1], Peck CT[1], Koch L[2], Deiwick A[2], Chichkov B[2], Vogt PM[1], Reimers K[1]

[1]Department or Plastic, Hand and Reconstructive Surgery, Hannover Medical School, Hannover, Germany
[2]Department of Nanotechnology, Laser Zentrum Hannover e.V., Hannover, Germany

Published in

PLoS ONE, 2013, March, Vol 8 (3), e57741
doi: 10.1371/journal.pone.0057741

OPEN ACCESS Freely available online

PLOS ONE

Tissue Engineered Skin Substitutes Created by Laser-Assisted Bioprinting Form Skin-Like Structures in the Dorsal Skin Fold Chamber in Mice

Stefanie Michael[1]*, Heiko Sorg[1], Claas-Tido Peck[1], Lothar Koch[2], Andrea Deiwick[2], Boris Chichkov[2], Peter M. Vogt[1], Kerstin Reimers[1]

1 Department of Plastic, Hand- and Reconstructive Surgery, Hannover Medical School, Hannover, Germany, **2** Laser Zentrum Hannover e.V., Hannover, Germany

Abstract

Tissue engineering plays an important role in the production of skin equivalents for the therapy of chronic and especially burn wounds. Actually, there exists no (cellularized) skin equivalent which might be able to satisfactorily mimic native skin. Here, we utilized a laser-assisted bioprinting (LaBP) technique to create a fully cellularized skin substitute. The unique feature of LaBP is the possibility to position different cell types in an exact three-dimensional (3D) spatial pattern. For the creation of the skin substitutes, we positioned fibroblasts and keratinocytes on top of a stabilizing matrix (Matriderm®). These skin constructs were subsequently tested *in vivo,* employing the dorsal skin fold chamber in nude mice. The transplants were placed into full-thickness skin wounds and were fully connected to the surrounding tissue when explanted after 11 days. The printed keratinocytes formed a multi-layered epidermis with beginning differentiation and *stratum corneum*. Proliferation of the keratinocytes was mainly detected in the suprabasal layers. *In vitro* controls, which were cultivated at the air-liquid-interface, also exhibited proliferative cells, but they were rather located in the whole epidermis. E-cadherin as a hint for adherens junctions and therefore tissue formation could be found in the epidermis *in vivo* as well as *in vitro*. In both conditions, the printed fibroblasts partly stayed on top of the underlying Matriderm® where they produced collagen, while part of them migrated into the Matriderm®. In the mice, some blood vessels could be found to grow from the wound bed and the wound edges in direction of the printed cells. In conclusion, we could show the successful 3D printing of a cell construct *via* LaBP and the subsequent tissue formation *in vivo*. These findings represent the prerequisite for the creation of a complex tissue like skin, consisting of different cell types in an intricate 3D pattern.

Citation: Michael S, Sorg H, Peck C-T, Koch L, Deiwick A, et al. (2013) Tissue Engineered Skin Substitutes Created by Laser-Assisted Bioprinting Form Skin-Like Structures in the Dorsal Skin Fold Chamber in Mice. PLoS ONE 8(3): e57741. doi:10.1371/journal.pone.0057741

Editor: Andrzej T. Slominski, University of Tennessee, United States of America

Received October 18, 2012; **Accepted** January 24, 2013; **Published** March 4, 2013

Funding: This study has been supported by Deutsche Forschungsgemeinschaft, SFB TransRegio 37 and Rebirth Cluster of Excellence (Exc 62/1). The funders had no role in study design, data collection and analysis, decision to publish, or preparation of the manuscript.

Competing Interests: The authors have declared that no competing interests exist.

* E-mail: Michael.Stefanie@mh-hannover.de

Introduction

Major burn injuries often prove difficult in therapy due to their complexity, the high risk of infection, the large area which might be affected and the potential destruction of deeper skin layers including the dermis. Often, the availability of autologous split-thickness skin grafts and keratinocytes for wound coverage is limited, especially in case of large burned areas. Therefore, the need of skin substitutes for temporary or permanent wound coverage is high. Several skin substitutes like Integra® and Matriderm® are already employed in the clinical application, being complemented by the use of autologous split-thickness skin grafts [1–3]. While Integra® serves to prepare the wound bed in preparation for transplantation with autologous split-thickness skin three weeks later, Matriderm® is used in a single step procedure and must be covered immediately. Nevertheless, full success in burn wound regeneration has not been reached yet, neither under functional nor under aesthetic aspects. In nearly every case of treating large and deep burn injuries discolouring or scarring remains, the latter leading to undesirable contractions. Also, neither hair follicles nor sebaceous and perspiratory glands can be regenerated.

Tissue engineering promises to have high potential in the production of new skin. In this context, it remains a challenge to create a precise and complex new tissue comprising several cell types which are arranged in a specific 3D pattern. Furthermore, the different tissue functions strongly depend on its specific structure and on the cells which are influenced by their distinct microenvironment [4]. For example, the formation of vessels in a skin equivalent cultivated *in vitro* is thought to be dependent on the direct interaction of endothelial cells with fibroblasts and their secreted extracellular matrix proteins and growth factors [5]. Bioreactors are used for the *in vitro* cultivation of complex tissues offering the possibility to mimic and control the desired microenvironment [6].

One solution for the problem of creating complex 3D tissues might be the use of LaBP. It offers the possibility to produce specific high resolution two-dimensional (2D) as well as 3D patterns, incorporating different cell types like human osteosarcoma and mouse endothelial cells [7], human osteoprogenitor cells [8], rodent olfactory ensheathing cells [9], human endothelial cells

[10] and human adipose derived mesenchymal stem cells which can subsequently be differentiated to fat [11] as well as bone and cartilage [12]. Cells – including rat Schwann and astroglial cells, pig lens epithelial cells [13], Chinese hamster ovarian cells, human osteoblasts [14], murine embryonal carcinoma cells [15], and fibroblasts and kerationcytes [16] – survive the transfer without damage and alteration of cell phenotype. This represents a major prerequisite for the use of LaBP in tissue engineering. Commonly, also the terms cell printing or simply bioprinting are used. In advance of the *in vivo* testing of the here produced skin substitutes we could already show tissue formation and functional cell-cell contacts in corresponding 3D tissue constructs *in vitro* [17].

In this study, *via* the use of LaBP, we created a multi-layered, fully cellularized skin equivalent for the future treatment of burn patients. The transplanted skin equivalent was tested *in vivo* for its ability to form tissue as well as cellular behaviour of the printed cells, the differentiation of the keratinocytes and potential neovascularisation using the dorsal skin fold chamber in mice. *In vitro* controls supplemented the *in vivo* experiments.

Materials and Methods

Cell Culture

NIH3T3 fibroblasts (DSMZ, Braunschweig, Germany) and HaCaT keratinocytes (DKFZ, Heidelberg, Germany) have previously been labelled by stable transduction with lentiviral or gammaretroviral vectors encoding for either eGFP or mCherry [17]. In the following the four resulting cell lines are named accordingly: NIH3T3-eGFP, NIH3T3-mCherry, HaCaT-eGFP and HaCaT-mCherry. Fibroblasts were cultivated in Dulbecco's modified Eagle's medium (DMEM) with high glucose (4.5 g/L) (PAA, Pasching, Austria) supplemented with 10% fetal bovine serum (FBS) (Biochrom, Berlin, Germany), 1% of 100 mM sodium pyruvate (Biochrom), and 1% of penicillin/streptomycin (Biochrom) whereas keratinocytes were grown with DMEM/Ham's F12 medium (PAA) supplemented with 10% FBS and 1% of penicillin/streptomycin.

Cell Transfer and Production of the Transplant

Cells were arranged in 3D skin constructs using LaBP (as previously described in [16] [18–19]). Briefly, the setup consists of two co-planar glass slides. The upper one is coated with a thin layer of laser absorbing material (here 60 nm of gold) and a layer of biomaterial to be transferred (here 60 µm of cell containing collagen). This glass slide is mounted upside-down above a second (receiver) glass slide. The laser pulses are focused through the upper glass slide into the laser absorbing layer, which is evaporated locally. The vapor pressure propels a small amount of the subjacent biomaterial towards the receiver glass slide. By moving the glass slides relative to each other, arbitrary patterns of biomaterial can be produced. By repeating this procedure layer-by-layer also 3D patterns can be generated.

For the here presented skin substitutes the cells were trypsinized and centrifuged at 400 g. A pellet containing 1.5 million cells was resuspended in a mixture of 37 µl collagen (Collagen Type I, Rat Tail, BD Biosciences, Bedford, MA, USA), 5 µl phosphate buffered saline (10× PBS, Biochrom) and 0.85±0.5 µl sodium hydroxide (1N NaOH, Sigma-Aldrich) for neutralization (pH = 7.1±0.3) prior to the transfer. For the skin substitutes 20 layers of fibroblast-containing collagen and 20 layers of keratinocyte-containing collagen were printed subsequently onto a sheet of Matriderm® (2.3 cm×2.3 cm, Dr. Suwelack Skin & Health Care, Billerbeck, Germay), used as a stabilization matrix.

The printed cells were kept in the incubator under submerged conditions over night. The next day (defined as day 0), nine round pieces (diameter 6.0 mm) were removed from the large construct with a biopsy punch, three of which were implanted into the skin fold chambers *in vivo* (one per mouse). As four independent printing processes were conducted, altogether 12 animals were used. The remaining six pieces of each printing process served as *in vitro* controls. Two of them were directly fixed on day 0 to depict the situation at the beginning of the experiments, whereas the remaining four pieces were raised to the air-liquid-interface. *In vitro* controls were then fixed on days 5 and 11 (duplicates per time point) and *in vivo* specimen on day 11.

Cultivation of Constructs in vitro

Constructs were raised to the air-liquid-interface and cultivated with differentiation medium on top of plastic platforms. The latter consisted of cell strainers (BD Biosciences, Bedford, MA, USA) turned upside down. The medium was composed of DMEM high glucose medium (PAA) mixed with the same amount of DMEM/

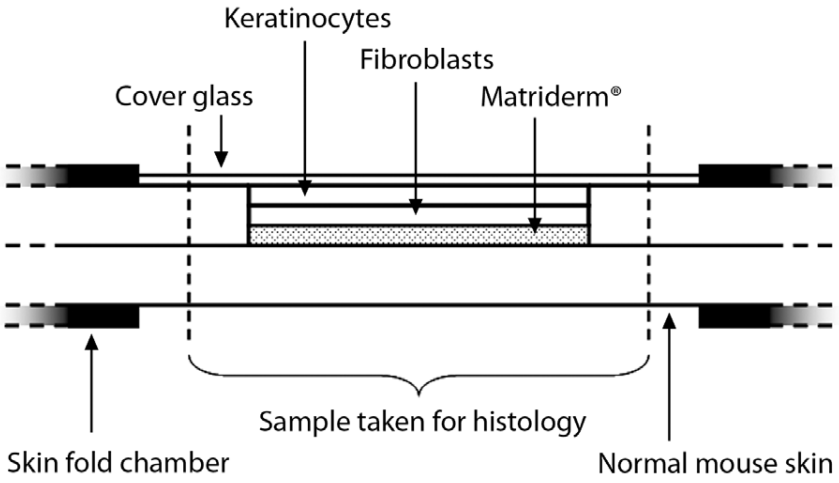

Figure 1. Scheme of the utilised dorsal skin fold chambers in mice. The chambers are attached to the back skin of the mice. The printed skin construct consisting of 20 layers of fibroblasts and 20 layers of keratinocytes on top of Matriderm® is placed into a round full-thickness wound in the mouse skin, while the opposite side remains intact. To close the chamber a cover glass is used.
doi:10.1371/journal.pone.0057741.g001

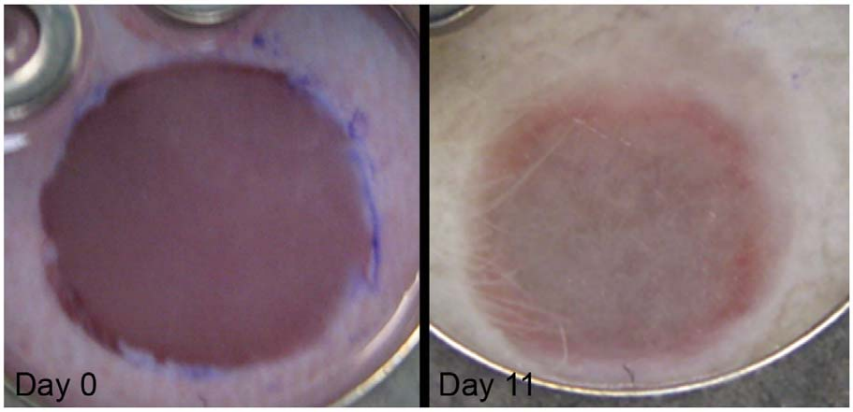

Figure 2. Tissue engineered skin construct in the dorsal skin fold chamber in nude mice. The pictures show a skin construct inserted into the wound directly after the implantation (left) and on day 11 (right). The implanted constructs were created *via* LaBP, consisting of 20 layers of fibroblasts and 20 layers of keratinocytes on top of Matriderm®. They fill the full-thickness wound completely.
doi:10.1371/journal.pone.0057741.g002

Ham's F12 medium (PAA), supplemented with 1% FBS, 1% penicillin/streptomycin, 10^{-7} mM isoprenaline hydrochloride (Sigma-Aldrich, Steinheim, Germany), 10^{-7} mM hydrocortisone (Sigma-Aldrich) and 10^{-7} mM insulin (insulin bovine pancreas, Sigma-Aldrich). The resulting calcium chloride concentration of the culture medium is 158.3 mg/L.

Animals and Ethics Statement

All animal experiments were evaluated and approved by the responsible animal care committee (Nds. Landesamt für Verbraucherschutz und Lebensmittelsicherheit) and the Hannover Medical School (Institut für Versuchstierkunde). The animals (male BALB/c-Nude mice, 8 weeks) were purchased from Charles River and kept in the local animal care facility according to the institution guidelines. They received standardized food and water, living with a day-night cycle of 12 hours each. Animals were used for the experiments when they were at least 12 weeks old.

Skin Fold Chamber

The dorsal skin fold chamber was used for the evaluation of tissue engineered skin *in vivo* as published previously [20]. The skin constructs were placed into full-thickness wounds, while the skin on the other side of the chamber remained intact. All surgery was performed under isoflurane anesthesia, and all efforts were made to minimize suffering. The mice were sacrificed on day 11 after implantation, preparing the constructs surrounded by normal skin for histological analyses (Figure 1). Analogous constructs - without cells - have already been assessed *in vivo* [20] and are used as a comparison in this study.

Histology

Samples were fixed in 4% paraformaldehyde, embedded in paraffin and subsequently cut to sections of 5 µm thickness. Masson's trichrome stainings were conducted following standard procedures.

Immunohistochemistry

In order to detect the presence of e-cadherin, collagen IV, cytokeratin 14 and Ki67, immunohistochemistry was carried out. For Ki67 (Thermo Fisher, RM9106_S0, 1:200) and e-cadherin staining (Santa Cruz, SC 7870, 1:300) the deparaffinised and rehydrated paraffin sections were incubated in a 99°C heated water bath for 25 min (Ki67) and 15 min (e-cadherin), respectively, before blocking. For cytokeratin 14 (Biozol, DBB-DB099-1, 1:300) and collagen IV (Abcam, Ab6586, 1:2000) stainings the sections were incubated in a 37°C warm water bath for 10 min, using 100 ml 0.2 N HCl solution with 100 mg pepsin. All sections were blocked with 2% FBS in PBS at room temperature for 30 min, followed by incubation with first antibody in 1% FBS in PBS at 4°C over night. After washing with PBS for all but the collagen IV staining a goat anti rabbit secondary antibody (Sigma-Aldrich, A3687, 1:1000) coupled to an alkaline phosphatase was employed. The samples were incubated at 37°C for 1 h. As a substrate nitro-blue tetrazolium-5-bromo-4-chloro-3'-indolyphosphate (Roche, Mannheim, Germany) was used. In case of the collagen IV primary antibody, a biotin coupled secondary anti rabbit antibody (Dako, E0432, 1:400) was used for 90 min at room temperature. Subsequently, the Vectastain ABC Kit (Vector Laboratories, Peroxidase Standard PK-4000) was employed for 60 min at room temperature to enhance the signal. The latter was then visualised with diaminobenzidine tetrahydro chloride (ICN98068). Staining of all antibodies was detected with a light microscope (Olympus).

Results

Operations and Macroscopic Evaluation

To evaluate skin constructs *in vivo* generated *via* LaBP, we printed 20 layers of a keratinocyte cell line (HaCaT) on top of 20 layers of a fibroblast cell line (NIH3T3) by an established laser-assisted bioprinting procedure. Using stable transduction, cell lines were labelled with genes encoding for green or red fluorescent proteins, respectively: NIH3T3-eGFP, NIH3T3-mCherry, HaCaT-eGFP and HaCaT-mCherry. Matriderm® was used as a carrier matrix to enhance stability of the constructs for transplantation (Figure 1). The skin constructs were placed into full-thickness skin wounds in the dorsal skin fold chamber preparation in mice in such a way that the constructs and the surrounding skin laid in close contact to each other. Uninjured skin from the opposite side of the back fold served as a control for all experiments. Analogous constructs without the cells [20] serve as a comparison to this study.

All animals survived the surgical intervention and implantation procedure and tolerated the chambers well, showing no signs of discomfort or changes in sleeping and feeding habits. After 11

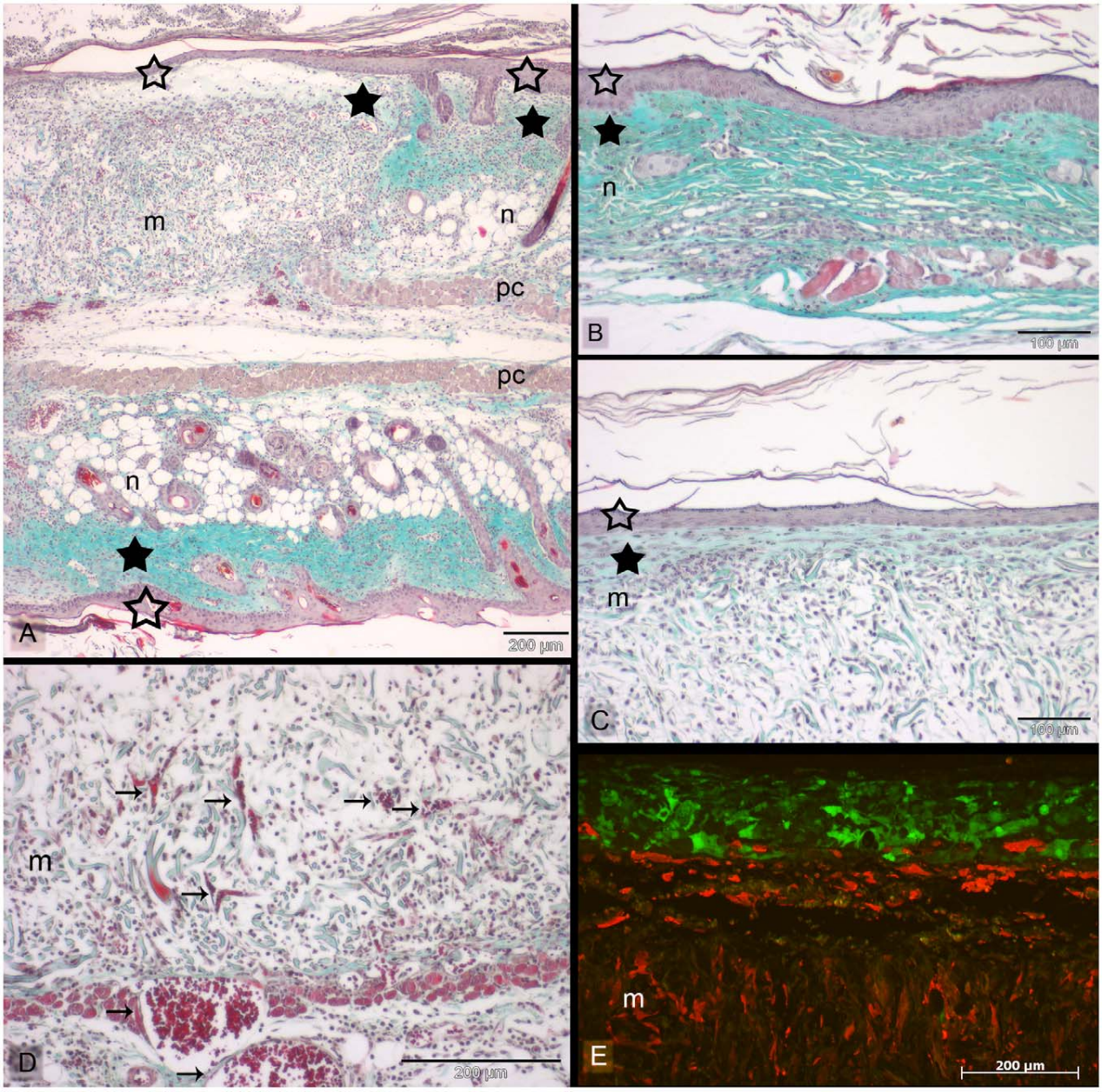

Figure 3. Histological sections of the tissue engineered skin constructs *in vivo*. Skin constructs were implanted in dorsal skin fold chambers in mice for 11 days. Sections were stained with Masson's trichrome (A–D) or analyzed with fluorescence microscopy (E), respectively. (A) illustrates an overview with the junction between the inserted skin construct (m = Matriderm®) and native mouse skin (n) at the wound edge after 11 days in the dorsal skin fold chamber in mice. The intact mouse skin opposite of the skin construct can be seen in the lower part of the picture (n) (see also Figure 1). The skin construct and the intact skin part in the sandwiched skin are separated by the *panniculus carnosus (pc)*. Both in native mouse skin (B) and the printed skin construct (C) a dense epidermis (empty asterisks) and a corneal layer can be observed. In case of the skin construct, the epidermis is formed by the printed keratinocytes (E). This can clearly be seen by the green fluorescence emitted by the used HaCaT-eGFP cells. The fibroblasts (NIH3T3-mCherry) partly migrated into the Matriderm® (yellowish fibres). The fibroblasts, which stayed on top of the Matriderm®, display an outstretched morphology (C), being accompanied by collagen deposition (filled asterisks). Blood vessels (arrows) can be detected in the skin constructs (D). Scale bars depict 200 µm (A, D, E) and 100 µm (B, C).
doi:10.1371/journal.pone.0057741.g003

days, the borders of the skin constructs and the surrounding mouse skin were tightly grown together so that no sharp linings were visible between the two tissue types any more (Figure 2). During the course of time, the previously shining surface of the constructs became matt. Neither inflammatory/necrotic processes nor contraction of the wounds could be detected.

Formation of Skin-like Tissue in vivo by Printed Skin Constructs

First of all, the survival and tissue formation of the printed skin cells was of particular interest. On top of the fibroblasts and the Matriderm®, the keratinocytes (HaCaT-eGFP) developed a dense stratified tissue (Figure 3E), similar to normal epidermis as can be

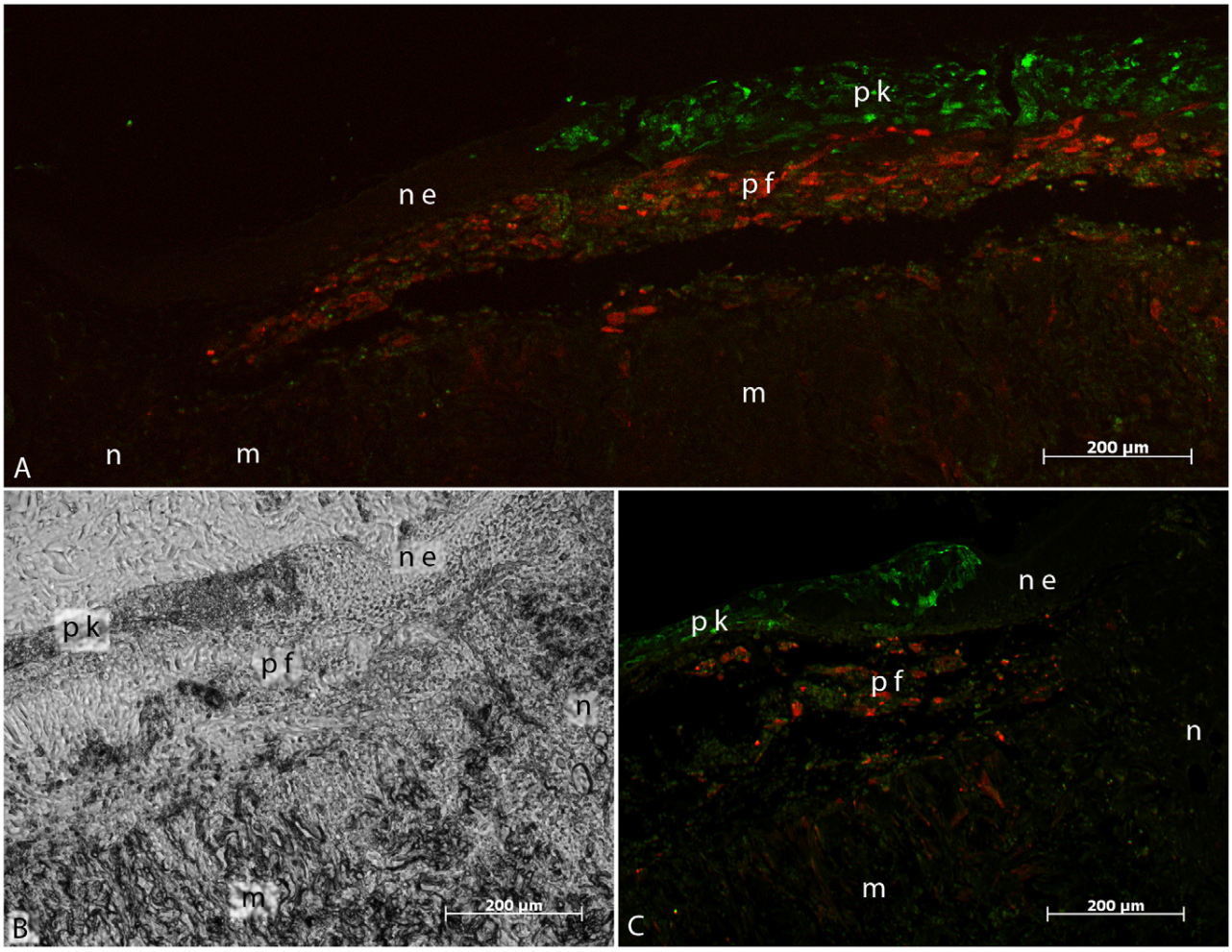

Figure 4. Fluorescent pictures of the tissue engineered skin constructs *in vivo*. Skin constructs were implanted in dorsal skin fold chambers in mice for 11. The sections show an overview of the junction between the inserted skin construct (m = Matriderm®) and native mouse skin (n) with either fluorescence microscopy (A, C) or transmitted light microscopy (B). Two different situations concerning the epidermis were observed during analysis of the junction zones: In some cases, as depicted in (A), the normal mouse epidermis (ne) started to grow on top of the Matriderm®, where it connected to the epidermis formed by the printed keratinocytes (pk). The latter were labelled in green by stable transduction (HaCaT-eGFP). In other cases, as depicted in (B) and (C), the epidermis formed by the printed keratinocytes ended at the border of the Matriderm®, synchronous to the presence of the printed fibroblasts (pf) labelled in red (NIH3T3-mCherry). As can be seen by comparing (B) and (C) - which depict the same location - the keratinocytes even partly grew on top of the normal mouse epidermis. In both cases, the printed fibroblasts formed a multi-layer tissue underneath the printed keratinocytes. Partly, they also migrated into the Matriderm®. All scale bars depict 200 µm.
doi:10.1371/journal.pone.0057741.g004

seen in the Masson's trichrome staining (Figure 3A, C). In some samples, this was followed by a corneal layer (Figure 3A, C). However, the epidermis in the skin constructs was less thick than in native mouse skin. Besides, no rete ridges could be found in the skin constructs. After 11 days the tissue developed by the printed cells was connected to the surrounding native mouse skin tissue at the wound edges. Neither an interruption of the epidermis nor a gap between the dermis and the Matriderm® could be observed at the junction between the skin constructs and the mouse skin (Figure 3A, Figure 4). In this context, two different situations could be observed: In some cases, the normal mouse epidermis started to grow on top of the Matriderm®, becoming connected to the epidermis which was formed by the printed keratinocytes (Figure 4A). In other cases, the epidermis formed by the printed keratinocytes ended simultaneously with the printed fibroblasts (NIH3T3-mCherry), directly at the border of the Matriderm®. Partly, the keratinocytes even grew on top of the normal mouse epidermis (Figure 4B, C).

Furthermore, the migration pattern of the printed fibroblasts was assessed. As can be seen in the histological sections, the fibroblasts partly migrated into the Matriderm®, closely following the fibres of the latter (Figure 3E, Figure 4). Some fibroblasts remained on top of the Matriderm®, composing a multi-layer sheet of tissue (Figure 3C) and secreting collagen as can be seen in the trichrome staining. As such, the printed skin cells survived well and formed a multi-layer, keratinized skin equivalent.

One important issue in respect of the use of skin substitutes is their vascularisation. Here, small blood vessels could be found in the skin constructs which seem to grow in from the depth of the wound bed as well as from wound edges into the Matriderm® in the direction of the printed cell layers (Figures 3D and 5).

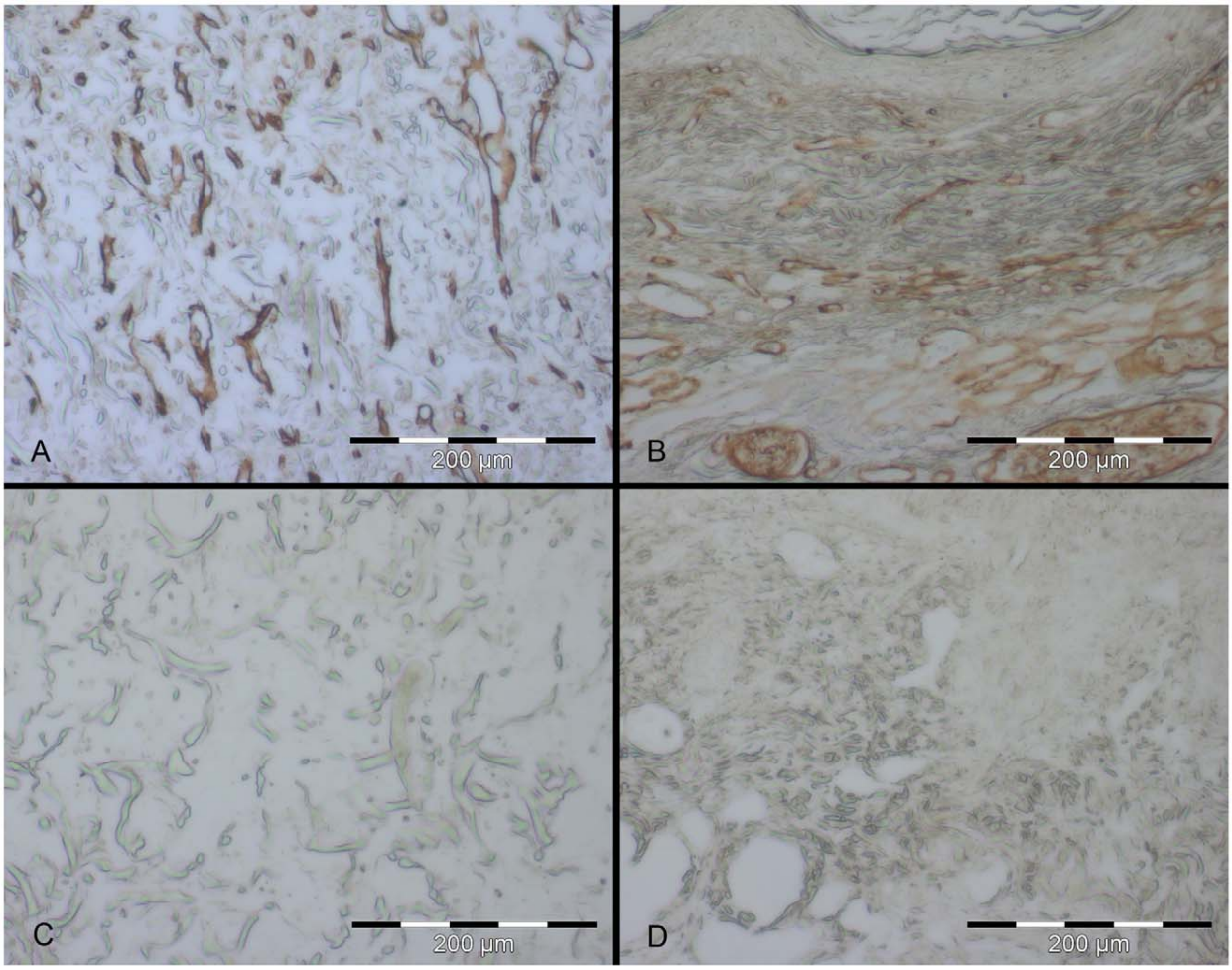

Figure 5. Blood vessel detection *via* immunohistochemistry in skin constructs cultivated *in vivo* for 11 days. Skin constructs were cultivated *in vivo* for 11 days in the dorsal skin fold chamber in mice. Collagen IV expression (brown) – indicating blood vessels/capillaries – can be detected in the Matriderm® as small tubes reaching from the wound bed in the direction of the cells (A). Small and large blood vessels are present in the normal mouse skin (B). Matriderm® (C) and normal mouse skin (D) without first antibody serve as the respective negative controls. Scale bars depict 200 µm each.
doi:10.1371/journal.pone.0057741.g005

Adherens junctions – containing especially e-cadherin - are essential for stable cell-cell contact and can abundantly be found in epithelia like skin. Therefore, e-cadherin can be used as a hint for epithelia formation and consequently for tissue development. By means of immunostaining, e-cadherin could be detected between the keratinocytes of the skin constructs inserted into the wounds. Here, the pattern of the e-cadherin localisation is the same as in native skin and can be found in the whole epidermis (Figure 6).

One important characteristic of an epidermis is the differentiation of the keratinocytes. Cytokeratin 14 is a marker for undifferentiated keratinocytes. The corresponding immunostaining revealed the presence of cytokeratin 14 in the whole epidermis of the skin constructs (Figure 7A–C). In native skin cytokeratin 14 staining could be found in only the suprabasal layers.

In contrast, Ki67 as a proliferation marker, showed a signal mainly in the suprabasal layer of the skin constructs (Figure 7D–F), indicating that only those keratinocytes maintained their proliferating state. Note that in the skin constructs only a few cells showed a positive signal for Ki67 whereas in the normal mouse skin nearly all suprabasal cells were stained. Fibroblasts in the dermis showed proliferation in the skin constructs as well as in the native mouse skin.

In vitro Controls of Printed Skin Constructs

As a control, printed skin constructs were also cultivated *in vitro* with the addition of differentiation medium. Samples were taken for histology on day 0-at the same time point as the corresponding transplants were inserted into the chambers of the mice – to demonstrate the starting conditions of the experiments. Further on, samples were also secured on day 11, corresponding to the end of the *in vivo* experiments and in between (on day 5).

On day 0 the two multi-layers of different cell types on top of the Matriderm® could clearly be seen (Figure 8A, D, G). The keratinocytes were still round and embedded in the collagen gel without contact to each other and with quite large spacing between the cells. In contrast, the fibroblasts already began to stretch out and to migrate into the Matriderm®. While the keratinocytes formed a dense tissue during the course of time, part of the fibroblasts migrated into the Matriderm®, following the

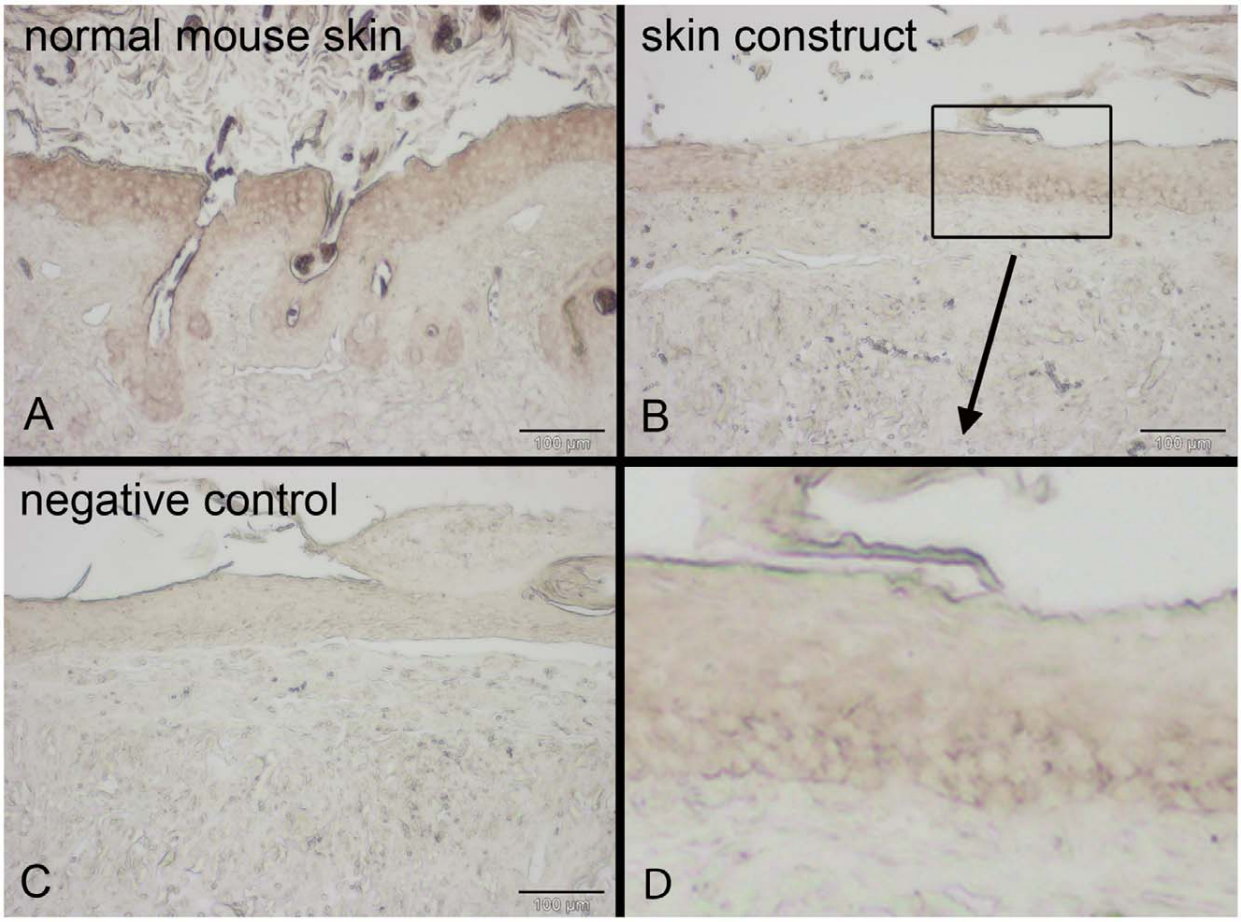

Figure 6. E-cadherin detection *via* immunohistochemistry in skin constructs cultivated *in vivo* for 11 days. Skin constructs were cultivated *in vivo* for 11 days in the dorsal skin fold chamber in mice. E-cadherin expression (dark brown) can be found throughout the epidermis in both normal mouse skin (A) and the skin constructs (B). Normal mouse skin without first antibody serves as a negative control (C). All scale bars depict 100 µm.
doi:10.1371/journal.pone.0057741.g006

fibres closely (Figure 8, brown cells beside green Matriderm® fibres, especially clear in Figure 8H and I).

A thickening of the epidermis-like tissue formed by the keratinocytes could be observed comparing day 11 to day 5 (Figure 8). Surprisingly, trichrome staining revealed the presence of a horizontal line of collagen in the lower part of the epidermis-like tissue and some globular collagen accumulations in the upper part. These probably are the remnants of the collagen used for the printing process.

Also in the *in vitro* cultures, immunostaining was carried out. The presence of e-cadherin increased during time from none on day 0 to its detection in the whole epidermis-like tissue on day 11, (Figure 9A–C). This is in accordance with the trichrome stainings, where a dense tissue can be observed on days 5 and 11 (Figure 8).

Also *in vitro*, cytokeratin 14 could be detected evenly distributed throughout all layers of the epidermis-like tissue (Figure 9D–F). This indicates a lack of differentiation. Proliferation could be found in all examined stages of the *in vitro* cultures (Figure 9G–I). While nearly all of the just printed cells showed proliferation on day 0, only some of the cells did so on days 5 and 11. But in contrast to the *in vivo* situation, the proliferating cells were found in the whole epidermis-like structure, more or less evenly distributed. No special spatial pattern could be observed.

Discussion

The development of newly generated skin substitutes for burn therapy is very important. Here, we present the *in vivo* assessment of a simple skin equivalent created *via* LaBP. The printed cells form a tissue which is quite similar to native skin, including collagen producing fibroblasts and presumably differentiating keratinocytes, forming a dense epidermis. Although 11 days of cultivation is too short for a complete differentiation of keratinocytes, the distribution of Ki67 (as a marker for proliferation) mainly in the suprabasal layers hints at the beginning differentiation of the keratinocytes. In native skin, only the keratinocytes in the *stratum basale* maintain proliferation, whereas the differentiating keratinocytes in the other skin layers cease proliferating. Furthermore, the Matriderm® carrier becomes populated by the printed fibroblasts (presented in this work) as well as murine host fibroblasts (presented in previous work [20]). This leads to the integration and ingrowth of the skin construct into the wound. However, the absence of rete ridges and the thinner epidermis in the skin constructs may result in less stability of the constructs compared to native mouse skin. This may be solved by printing rete ridges and a thicker epidermis in future experiments, though.

As skin is a complex organ consisting of different cell types and substructures arranged in defined spatial patterns, LaBP is suited

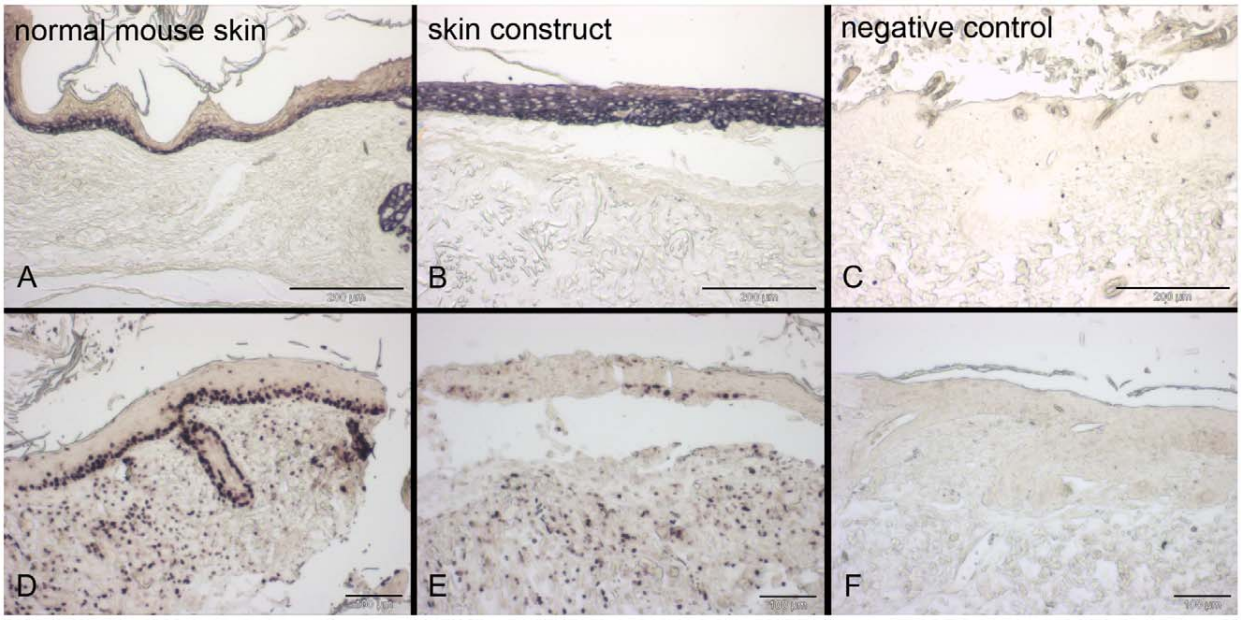

Figure 7. Detection of cytokeratin 14 and proliferation *via* immunohistochemistry in skin constructs cultivated *in vivo*. Skin constructs were cultivated *in vivo* in the dorsal skin fold chamber in mice for 11 days. The left column shows normal mouse skin, the middle column the skin construct and the right column the respective negative controls (normal mouse skin without first antibody) of the immunohistochemistry stainings. Cytokeratin 14 expression is limited to the suprabasal layers of the epidermis in mouse skin (A) but present in the whole epidermis in the skin constructs (B). Proliferation *via* Ki67 can be detected in the suprabasal layers of the epidermis and in the dermis in both normal mouse skin and skin constructs (D, E). Scale bars depict 200 μm (A–C) and 100 μm (D–F).
doi:10.1371/journal.pone.0057741.g007

for the production of tissue engineered skin substitutes. It offers many possibilities and is a very promising technique for the fabrication of other kinds of tissues as e.g. bone or cartilage [8] [10]. [12]. Different levels of tissue generation have been investigated using bioprinting techniques. As we have previously shown *in vitro*, printed epidermal cells develop a dense epidermis including the expression of adherens and gap junctions [17]. In this manuscript, the next step has been carried out and tissue formation also *in vivo* could be documented. In a different setting, a pie-shaped multi-layered construct produced by inkjet printing (see below) and consisting of different cell types (stem cells, smooth muscle cells, endothelial cells) has already been analysed *in vivo* as a technical prerequisite to develop vascularised bone tissue in the future. The implanted cells could be detected several weeks after implantation indicating good survival rates. Interestingly, the used stem cells were able to differentiate into bone *in vivo* and endothelial cells formed a network of blood vessels in the implants after six weeks [21].

Concerning maintenance of cellular phenotype, human chondrocytes were found to express cartilage specific genes after being printed into cartilage lesions by inkjet printing and being cultivated *ex vivo*. They maintained their deposited positions due to simultaneous photopolymerization of a surrounding biomaterial scaffold, and attached firmly to the enclosing cartilage tissue [22]. These findings are in accordance with our own experiences [16] and that of others [7] [9] [13–14] as LaBP does not seem to impair cellular phenotype and behaviour. Even the differentiability of transferred mesenchymal stem cells [11–12] and pluripotent murine embryonal carcinoma cells [15] is maintained.

In the *in vitro* samples, a horizontal stripe of collagen without cells could be observed in the lower part of the epidermis-like structure. Obviously, the fibroblasts did not degrade the circumjacent collagen - which has been used as a hydrogel during the printing process - but started to migrate into the Matriderm® right away. During the printing, the cells are mixed with a hydrogel (in general called printing matrix) to serve four different purposes. Firstly, the matrix is necessary to achieve a uniform coverage of the donor glass slide with the biomaterial to be transferred. This is important as only then a consistency and uniformity of the printing process is possible. Secondly, the matrix helps the cells to survive, providing a moist environment preventing drying. Thirdly, it presents a specific surrounding for the printed cells and thereby acts as a biomimetic gel to create the desired micro-environment. In our case, collagen is already present in physiological skin and therefore is very suited as a printing matrix. Fourthly, a matrix like collagen enables the formation of a 3D construct due to its gelling effect. While in the *in vitro* controls the collagen is left by the fibroblasts, in the *in vivo* situation outstretched fibroblasts can be found in the collagen, probably also expressing and producing collagen by themselves. As this is similar to the situation in physiological skin, this process is much desired.

Very important for the take of a grafted skin or skin substitute is its fast vascularisation. It is a major prerequisite for the successful clinical use of a skin substitute. In our experiments, blood vessels could be found to start growing into the Matriderm® from the wound bed and the wound edge mostly in the direction of the transplanted cells. In a previous study, in skin constructs consisting of Matriderm® covered with collagen type I but without cells [20] no vessels could be detected growing into the Matriderm®. This suggests that the neovascularisation might be induced or supported by the printed cells on top of the Matriderm®. Actually, keratinocytes were found to produce vascular endothelium growth factor (VEGF) [23], the expression of which is regulated by several growth factors and cytokines [24] as well as by insulin in a diabetic mouse model [25]. Furthermore, keratinocytes in a tissue engineered skin substitute regulate the size of newly growing

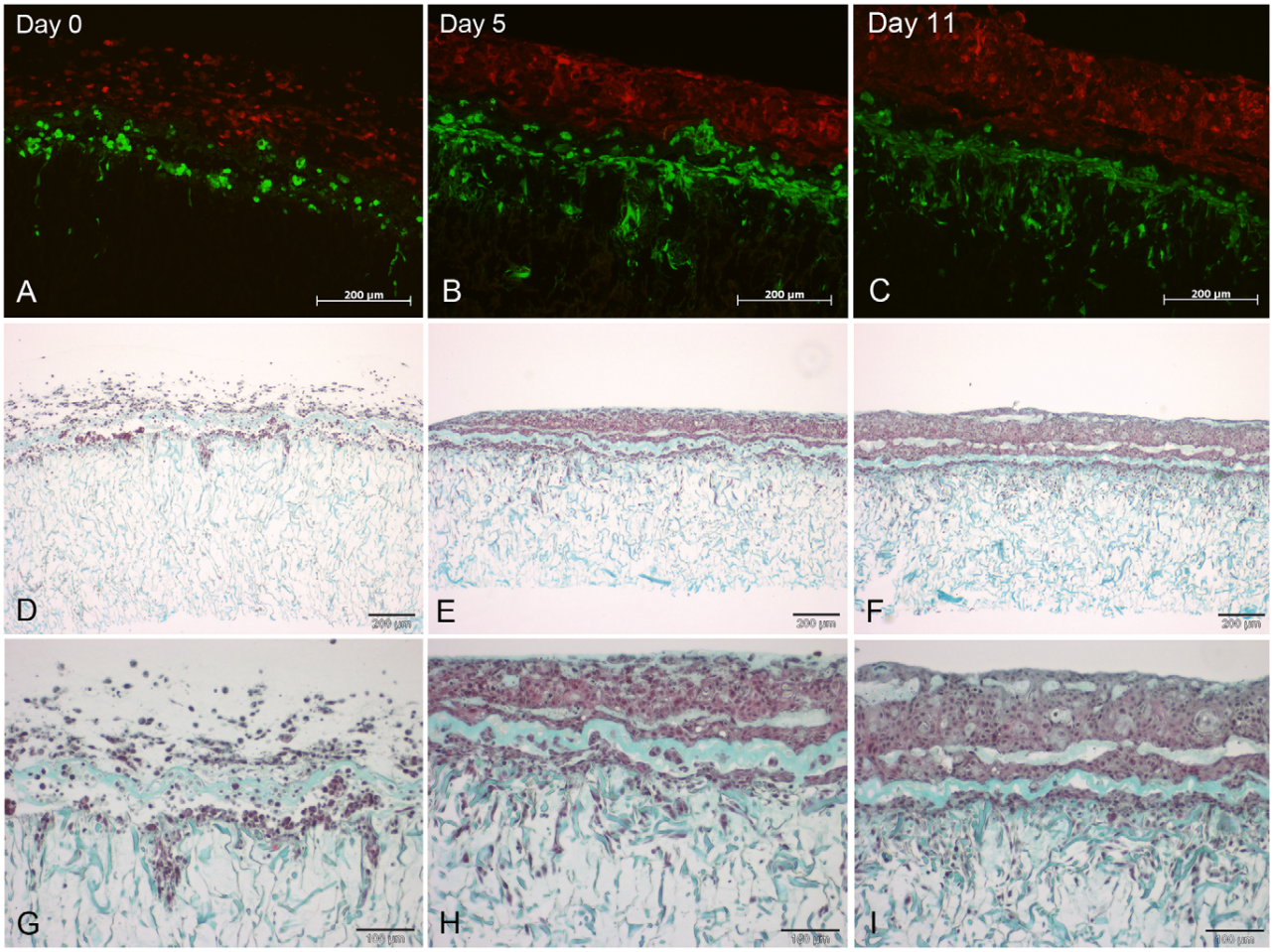

Figure 8. Histological sections of the tissue engineered skin constructs *in vitro*. Skin constructs were cultivated at the air-liquid-interface with differentiation medium for 11 days. Sections show cells using fluorescent microscopy and Masson's trichrome staining, respectively. The time points indicated in A–C are valid for the whole respective columns. The skin constructs were cultivated at the air-liquid-interface. The keratinocytes (HaCaT-mCherry) exhibit red fluorescence while the fibroblasts (NIH3T3-eGFP) appear in green (A–C). Masson's trichrome staining reveals the connective tissue containing collagen (green) and the cells (reddish) (D–I). The fibroblasts already start to grow into the Matriderm® underneath one day after printing (A, D, G). The keratinocytes, which still are rounded and are not connected to each other on day 0 (A, D, G), already form a dense tissue on day 5 (B, E, H). The thereby formed epidermis increases in height until day 11 (C, F, I). Scale bars depict 200 µm (A–F) and 100 µm (G–I).
doi:10.1371/journal.pone.0057741.g008

vessels in the dermis *in vitro*, resulting in small vessels similar to capillaries present in the skin's microcirculation [26]. The same effect could be observed in the absence of keratinocytes when adding keratinocyte-conditioned medium or VEGF. Therefore, we assume that the printed keratinocytes in our skin substitutes might enhance vessel formation by VEGF production.

In our experiments no complete vascularisation of the printed skin equivalents could be achieved under the current conditions. Probably, the period was too short for complete vascularisation of the skin equivalent. Following the idea of improving graft vascularisation, Black *et al.* integrated human umbilical vein endothelial cells (HUVEC) into tissue engineered skin equivalents containing fibroblasts and keratinocytes in combination with a collagen chitosan scaffold [5] [27]. According to their study, the HUVEC were shown to form capillary-like tubules in the dermis *in vitro*. In a similar approach, skin equivalents constructed by seeding acellular dermis with keratinocytes and Bcl-2-transduced HUVEC showed perfusion through HUVEC-lined microvessels two weeks after implantation into mice [28]. This highlights the necessity but also the probable success to incorporate endothelial cells into our printed constructs as a next step.

In contrast to the *in vivo* situation, our *in vitro* controls formed a multi-layered tissue with collagen producing fibroblasts, but did not show any differentiation of the keratinocytes (HaCaT). This might be due to the culturing method *in vitro*. Although differentiation aiding supplements were added to the culture medium and the skin constructs were raised to the air-liquid-interface, this might not have been appropriate enough to trigger the differentiation. Also, the culturing period of 11 days is quite short and induction of differentiation *in vitro* might have been observed at a later time point. However, the beginning differentiation of the keratinocytes *in vivo* could be due to the growth factors present in mice but absent *in vitro*.

Summing up, LaBP offers the possibility to place cells of a specific type wherever in the tissue they are needed. This is a unique feature of bioprinting techniques and it may be used to print skin supplemented with endothelial cells, hair follicle cells, peripheral nerve cells, Schwann cells, melanocytes or cells present

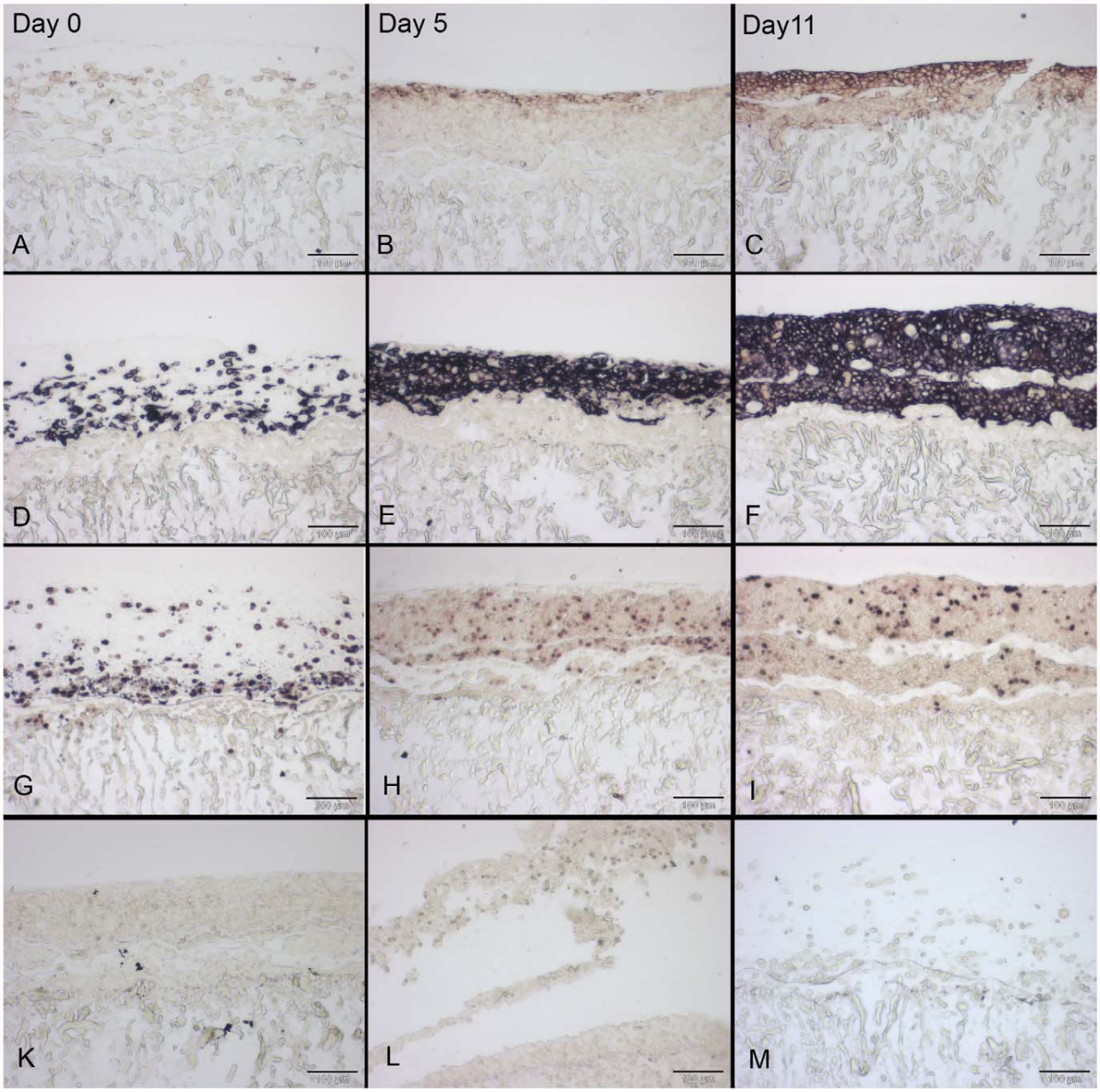

Figure 9. Sections of immunohistochemically stained skin constructs cultivated *in vitro*. Skin constructs were cultivated *in vitro* at the air-liquid-interface with differentiation medium for 11 days. The indicated time points in A–C are valid for the whole respective column. E-cadherin expression is absent on day 0 but can be detected on days 5 and 11 (A–C) while cytokeratin 14 expression is clearly visible at all time points in the whole epidermis (D–F). While nearly all cells exhibit Ki67 staining on day 0, only few cells do so at days 5 and 11 (G–I). The corresponding negative controls of the stainings (skin constructs without first antibody) are shown below (K – e-cadherin, L – cytokeratin 14, M – Ki67). All scale bars depict 100 μm.
doi:10.1371/journal.pone.0057741.g009

in perspiratory and sebaceous glands. Therefore, we hope to be able to produce a much more similar skin construct to native skin compared to other current approaches. This is especially important for the future patients as they gain a much more functional and aesthetic skin substitute. This in turn would lead to a major increase of their quality of life, on the physical as well as on the mental level.

As an alternative to LaBP, a similar technique called inkjet printing is available, which has already been used to print 2D protein arrays [29], endothelial cells, smooth muscle cells [29–30], a 3D construct containing HeLa cells [31], or a 3D composite construct containing muscle cells, endothelial cells and stem cells [21]. Also, inkjet printing can be used to create antimicrobial assays [32] or to transfect cells with relatively large molecules [33]. The major disadvantage of this technique, however, is the high shear force of the nozzle, leading to severe cell impairment [34]. With LaBP – which is nozzle free – cells can be printed with a much higher density [10]. This is very important for the printing

of skin, which is a tissue with a very high density of cells present. Therefore, for our purposes, LaBP remains the technique of choice.

To further improve the use of LaBP for the creation of (skin) tissue, an adaptation to automation would be of advantage. Our setup is not suited for the high throughput production of skin substitutes yet, but in principal an automation of the whole process - including the printing process as such as well as the cultivation of the skin substitutes - is conceivable.

We used the dorsal skin fold chamber in mice for the assessment of the tissue engineered skin constructs. This approach exhibits different advantages as well as drawbacks. The common approach of dorso-lateral full-thickness wounds without a chamber allows for the cultivation of a tissue engineered skin constructs for a long period of time. While two to eight weeks are the most frequently used time intervals [35–38], animals can be kept up to six months [39]. Using the chambers and the small nude mice, the observation period is quite limited as the mice would not be able to bear the weight of the chambers for several weeks. In our study, we demonstrated that skin constructs produced by LaBP are viable *in vivo*, forming a tissue similar to simple skin within the time frame of 11 days. As a further limitation, compared to the common approach of simple full-thickness wounds in the dorso-lateral region of mice with an area of 2 cm×2 cm to 2 cm×3 cm [35] [38–40], the wound area in the chambers is very small (round hole with 6 mm diameter). This, however, is partly compensated by the lack of wound contraction. The latter is the major way of wound healing in rodents [41], opposed to the main mechanisms in human wound healing, i.e. granulation tissue formation and subsequent reepithelialisation [3] [42]. In the chambers, the skin constructs are safely secured in the wound by the glass slide while the surrounding and opposite skin is firmly attached to the titanium frames [20]. Therefore, no contraction of the wound area occurs. This is very important since we aim at assessing the situation in humans and not in rodents. A further advantage of the skin fold chamber is the lack of customary wound dressings. Thereby, no changes of the dressings are necessary, which reduces the stress for the animals considerably [20]. Furthermore, the transparent glass slide allows for a continuous observation of the wound closure, without any stress for the animals due to the removal of wound dressings [43].

In conclusion, we could show LaBP to be an adequate technique for the creation and *in vivo* formation of a 3D tissue like skin. Therefore, LaBP represents a major promise for the improvement of burn therapy and thus for a raised quality of life for the patients.

Acknowledgments

The authors kindly thank Sabine Braun, Vincent Pritzel, Annika Köhler und Viktor Maurer for their excellent technical assistance and organizational help.

Author Contributions

Conceived and designed the experiments: SM LK AD HS BC PMV KR. Performed the experiments: SM HS CTP AD LK. Analyzed the data: SM HS CTP KR. Contributed reagents/materials/analysis tools: AD LK BC PMV KR. Wrote the paper: SM HS KR.

References

1. Vogt PM, Kolokythas P, Niederbichler A, Knobloch K, Reimers K, et al. (2007) Innovative wound therapy and skin substitutes for burns. Der Chirurg; Zeitschrift Fur Alle Gebiete Der Operativen Medizen 78: 335–342.
2. Supp DM, Boyce ST (2005) Engineered skin substitutes: Practices and potentials. Clinics in Dermatology 23: 403–412.
3. Singer AJ, Clark RA (1999) Cutaneous wound healing. The New England Journal of Medicine 341: 738–746.
4. Jakab K, Norotte C, Marga F, Murphy K, Vunjak-Novakovic G, et al. (2010) Tissue engineering by self-assembly and bio-printing of living cells. Biofabrication 2: 022001.
5. Black AF, Berthod F, L'heureux N, Germain L, Auger FA (1998) In vitro reconstruction of a human capillary-like network in a tissue-engineered skin equivalent. The FASEB Journal : Official Publication of the Federation of American Societies for Experimental Biology 12: 1331–1340.
6. Couet F, Mantovani D (2012) Perspectives on the advanced control of bioreactors for functional vascular tissue engineering in vitro. Expert Review of Medical Devices 9: 233–239.
7. Barron JA, Wu P, Ladouceur HD, Ringeisen BR (2004) Biological laser printing: A novel technique for creating heterogeneous 3-dimensional cell patterns. Biomedical Microdevices 6: 139–147.
8. Catros S, Fricain JC, Guillotin B, Pippenger B, Bareille R, et al. (2011) Laser-assisted bioprinting for creating on-demand patterns of human osteoprogenitor cells and nano-hydroxyapatite. Biofabrication 3: 025001.
9. Othon CM, Wu X, Anders JJ, Ringeisen BR (2008) Single-cell printing to form three-dimensional lines of olfactory ensheathing cells. Biomedical Materials (Bristol, England) 3: 034101.
10. Guillotin B, Souquet A, Catros S, Duocastella M, Pippenger B, et al. (2010) Laser assisted bioprinting of engineered tissue with high cell density and microscale organization. Biomaterials 31: 7250–7256.
11. Gruene M, Pflaum M, Deiwick A, Koch L, Schlie S, et al. (2011) Adipogenic differentiation of laser-printed 3D tissue grafts consisting of human adipose-derived stem cells. Biofabrication 3: 015005.
12. Gruene M, Deiwick A, Koch L, Schlie S, Unger C, et al. (2010) Laser printing of stem cells for biofabrication of scaffold-free autologous grafts. Tissue Engineering.Part C, Methods.
13. Hopp B, Smausz T, Kresz N, Barna N, Bor Z, et al. (2005) Survival and proliferative ability of various living cell types after laser-induced forward transfer. Tissue Engineering 11: 1817–1823.
14. Ringeisen BR, Kim H, Young HD, Spargo BJ, Auyeung RCY, et al. (2001) Cell-by-cell construction of living tissue. 698.
15. Ringeisen BR, Kim H, Barron JA, Krizman DB, Chrisey DB, et al. (2004) Laser printing of pluripotent embryonal carcinoma cells. Tissue Engineering 10: 483–491.
16. Koch L, Kuhn S, Sorg H, Gruene M, Schlie S, et al. (2010) Laser printing of skin cells and human stem cells. Tissue Engineering.Part C, Methods 16: 847–854.
17. Koch L, Deiwick A, Schlie S, Michael S, Gruene M, et al. (2012) Skin tissue generation by laser cell printing. Biotechnology and Bioengineering 109: 1855–1863.
18. Unger C, Gruene M, Koch L, Koch J, Chichkov BN (2011) Time-resolved imaging of hydrogel printing via laser-induced forward transfer. Applied Physics A: Materials Science & Processing 103: 271–277.
19. Gruene M, Unger C, Koch L, Deiwick A, Chichkov B (2011) Dispensing pico to nanolitre of a natural hydrogel by laser-assisted bioprinting. Biomedical Engineering Online 10: 19.
20. Michael S, Sorg H, Peck CT, Reimers K, Vogt PM (2012) The mouse dorsal skin fold chamber as a means for the analysis of tissue engineered skin. Burns : Journal of the International Society for Burn Injuries.
21. Xu T, Zhao W, Zhu JM, Albanna MZ, Yoo JJ, et al. (2013) Complex heterogeneous tissue constructs containing multiple cell types prepared by inkjet printing technology. Biomaterials 34: 130–139.
22. Cui X, Breitenkamp K, Finn MG, Lotz M, D'Lima DD (2012) Direct human cartilage repair using three-dimensional bioprinting technology. Tissue Engineering.Part A 18: 1304–1312.
23. Ballaun C, Weninger W, Uthman A, Weich H, Tschachler E (1995) Human keratinocytes express the three major splice forms of vascular endothelial growth factor. The Journal of Investigative Dermatology 104: 7–10.
24. Hacker C, Valchanova R, Adams S, Munz B (2010) ZFP36L1 is regulated by growth factors and cytokines in keratinocytes and influences their VEGF production. Growth Factors (Chur, Switzerland) 28: 178–190.
25. Goren I, Muller E, Schiefelbein D, Gutwein P, Seitz O, et al. (2009) Akt1 controls insulin-driven VEGF biosynthesis from keratinocytes: Implications for normal and diabetes-impaired skin repair in mice. The Journal of Investigative Dermatology 129: 752–764.
26. Rochon MH, Fradette J, Fortin V, Tomasetig F, Roberge CJ, et al. (2010) Normal human epithelial cells regulate the size and morphology of tissue-engineered capillaries. Tissue Engineering.Part A 16: 1457–1468.
27. Black AF, Hudon V, Damour O, Germain L, Auger FA (1999) A novel approach for studying angiogenesis: A human skin equivalent with a capillary-like network. Cell Biology and Toxicology 15: 81–90.
28. Schechner JS, Crane SK, Wang F, Szeglin AM, Tellides G, et al. (2003) Engraftment of a vascularized human skin equivalent. The FASEB Journal:

Official Publication of the Federation of American Societies for Experimental Biology 17: 2250–2256.
29. Wilson WC Jr, Boland T (2003) Cell and organ printing 1: Protein and cell printers. The Anatomical Record.Part A, Discoveries in Molecular, Cellular, and Evolutionary Biology 272: 491–496.
30. Boland T, Mironov V, Gutowska A, Roth EA, Markwald RR (2003) Cell and organ printing 2: Fusion of cell aggregates in three-dimensional gels. The Anatomical Record.Part A, Discoveries in Molecular, Cellular, and Evolutionary Biology 272: 497–502.
31. Arai K, Iwanaga S, Toda H, Genci C, Nishiyama Y, et al. (2011) Three-dimensional inkjet biofabrication based on designed images. Biofabrication 3: 034113.
32. Zheng Q, Lu J, Chen H, Huang L, Cai J, et al. (2011) Application of inkjet printing technique for biological material delivery and antimicrobial assays. Analytical Biochemistry 410: 171–176.
33. Owczarczak AB, Shuford SO, Wood ST, Deitch S, Dean D (2012) Creating transient cell membrane pores using a standard inkjet printer. Journal of Visualized Experiments : JoVE (61). pii: 3681. doi:10.3791/3681.
34. Born C, Zhang Z, Al-Rubeai M, Thomas CR (1992) Estimation of disruption of animal cells by laminar shear stress. Biotechnology and Bioengineering 40: 1004–1010.
35. Klingenberg JM, McFarland KL, Friedman AJ, Boyce ST, Aronow BJ, et al. (2010) Engineered human skin substitutes undergo large-scale genomic reprogramming and normal skin-like maturation after transplantation to athymic mice. The Journal of Investigative Dermatology 130: 587–601.
36. Xie JL, Li TZ, Qi SH, Huang B, Chen XG, et al. (2007) A study of using tissue-engineered skin reconstructed by candidate epidermal stem cells to cover the nude mice with full-thickness skin defect. Journal of Plastic, Reconstructive & Aesthetic Surgery : JPRAS 60: 983–990.
37. Egana JT, Fierro FA, Kruger S, Bornhauser M, Huss R, et al. (2009) Use of human mesenchymal cells to improve vascularization in a mouse model for scaffold-based dermal regeneration. Tissue Engineering.Part A 15: 1191–1200.
38. Kalyanaraman B, Boyce ST (2009) Wound healing on athymic mice with engineered skin substitutes fabricated with keratinocytes harvested from an automated bioreactor. The Journal of Surgical Research 152: 296–302.
39. Boyce ST, Medrano EE, Abdel-Malek Z, Supp AP, Dodick JM, et al. (1993) Pigmentation and inhibition of wound contraction by cultured skin substitutes with adult melanocytes after transplantation to athymic mice. The Journal of Investigative Dermatology 100: 360–365.
40. Rasmussen CA, Gibson AL, Schlosser SJ, Schurr MJ, Allen-Hoffmann BL (2010) Chimeric composite skin substitutes for delivery of autologous keratinocytes to promote tissue regeneration. Annals of Surgery 251: 368–376.
41. Galiano RD, Michaels J, Dobryansky M, Levine JP, Gurtner GC (2004) Quantitative and reproducible murine model of excisional wound healing. Wound Repair and Regeneration : Official Publication of the Wound Healing Society [and] the European Tissue Repair Society 12: 485–492.
42. Kirfel G, Herzog V (2004) Migration of epidermal keratinocytes: Mechanisms, regulation, and biological significance. Protoplasma 223: 67–78.
43. Laschke MW, Harder Y, Amon M, Martin I, Farhadi J, et al. (2006) Angiogenesis in tissue engineering: Breathing life into constructed tissue substitutes. Tissue Engineering 12: 2093–2104.

4 Discussion

4.1 General aspects of LIFT in skin tissue printing

The establishment of the LIFT process for the creation of a skin substitute for burn patients - which is the aim of this thesis - comprised several steps. First, the LIFT setup was planned and arranged according to the needed parameters. Subsequently, the basics of the transfer were tested with hydrogels alone and in combination with living cells. In this context, the creation of different 2D patterns was successfully conducted. One impressive example is a high resolution chessboard pattern, consisting of keratinocytes and fibroblasts. Having mastered the mechanical and physical aspects of the transfer, the influence of LIFT on the cells was of central interest, as only unimpaired cells are of use in tissue engineering. Our investigations showed no harmful effects of LIFT on different cell types. Neither morphological nor behavioural changes occured. Therefore, the necessary prerequisites for the application of LIFT in the field of tissue engineered were fulfilled. All the above described experiments are part of the first publication [82] (page 36).

After all aspects of the 2D printing were successfully established, the 3D printing of tissue, i.e. skin tissue, became the next step. In this context, the choice of a suitable printing matrix (hydrogel) was a big challenge. Our studies demonstrated, that neither alginate nor fibrinogen/thrombin - which are very adequate for the printing process as such - were suitable for the printing of skin tissue. Finally, using collagen as a matrix, skin equivalents consisting of 20 layers of fibroblasts followed by 20 layers of keratinocytes were printed via LIFT and cultured *in vitro*. Histological analysis showed tissue formation by the printed cells, which was confirmed by the detection of adherens junctions and functional gap junctions. To be able to track the printed cells *in vitro*, as well as *in vivo*, skin cell lines were marked with fluorescent proteins by stable transduction of the according genes. All of these data can be found in the second publication [81] (page 45).

Following the assessment of the printed skin constructs *in vitro*, as the next logical step the *in vivo* evaluation took place. As a preparation, the use of the dorsal skin fold chamber in mice was adapted to this purpose and shown to be a suitable and sophisticated tool. The use of the skin fold chambers offers several advantages: no contraction of the wound developes, the skin constructs can be observed during the whole cultivation period without the need to change wound dressings, and after the end of the experiment the specimen can easily be taken for histological analysis, being surrounded by native skin as a control. These findings are described in the third publication [104] (page 55).

The *in vivo* experiments showed the tight connection between the skin constructs and the surrounding native skin as well as the development of tissue by the printed cells. The tissue formation was observed by histological analysis and

even more evident by the direct detection of the fluorescently labelled printed cells. The presence of adherens junctions could be identified in the epidermis. Moreover, a beginning differentiation of the keratinocytes occured. Also, the presence of capillaries sprouting from the host tissue towards the printed cells could be detected. This is especially important with respect to the successful integration of even larger skin equivalents in clinical applications. All of these results are the content of the fourth publication [103] (page 63).

Thus, the four publications which are part of this thesis describe the different steps to achieve the generation of a skin substitute by laser based bioprinting. While at first the technical aspects of the LIFT setup and the transfer of the cell were the central aspects, in the course of time the biological considerations came to the fore. Altogether, the inter-disciplinary approach towards tissue engineering used in this thesis proved to be very successful.

4.2 Scaffold-free bioprinting - possibilities and problems

As explained in section 1.5, bioprinting is an example of scaffold-free tissue engineering. While this is not the common approach, it displays a major advantage. Normally, it is difficult to seed scaffolds with cells in exactly the desired location. Although they tend to migrate through present pores, the creation of a defined seeding pattern would be very difficult - even if chemokinces would be used - since the migration of cells is influenced by a complex set of parameters. An unoriented distribution of cells, however, is especially undesired in complex tissues like the skin. Here, different cell types reside close to each other in a defined 3D distribution to achieve functional cell structures. As one example, a network of endothelial cells preparing blood vessels can be created by bioprinting but never be pipetted into a simple collagen gel following the hitherto existing approaches.

In the process of laser based bioprinting, hydrogels are needed to realise scaffold-free tissue engineering. They serve mainly three different purposes: First, the hydrogels enable an even coating of the donor glass slide with the cell-matrix-solution (bioink). This is a major prerequisite for the uniform transfer of the cells as the needed laser energy is directly dependent on the thickness of the bioink layer (see section 1.6). Second, the hydrogels serve as a protection for the cells against dehydration by providing a highly hydrated protective surrounding. This is especially important if the printed constructs are large, because then the printing process is quite time consuming. Third, a 3D construct can only be printed if the employed hydrogel forms a stable network, providing the needed rigidity to stably print layer on top of layer. Even so, in case of a skin substitute, the formed gel needs to be flexible enough to provide the elasticity found in physiological skin.

Many different hydrogels exist and are being used in tissue engineering and bioprinting, either naturally occurring substances or chemically designed polymers. They have to allow for the desired mechanical support as well as for sufficient transport of nutrients, an appropriate degradation, and a good biocompatibility [48], [87]. Furthermore, the chosen hydrogel must be suitable for the required cell type(s). This means, that the desired interactions of the cells with the hydrogel must be possible, i.e. support of growth, adhesion, migration, proliferation, and

differentiation. For this purpose, hydrogels complemented with growth factors, biomimetic alterations or appropriate ECM molecules can be used. Thereby, different desired and specific cellular responses may be elicited [48], [151]. This is the fourth purpose a chosen hydrogel may serve in bioprinting, apart from the other three basic ones.

Several different matrices may be used to achieve the printing of various cell types in different situations. Nevertheless, each hydrogel has its advantages and drawbacks, either concerning the printing process or the needs of the cells. Those do not have to be congruent, though. Each newly printed cell type may require a different gel, which has to be found by the according experiments. In any case, cell vitality and behaviour of the cells need to be assessed and the selected hydrogels should maintain, or induce, the desired functions of the included cells as well as exhibit the needed mechanical properties [30], [48]. In the end, the used matrix must be suitable for the printing process as well as for the specific cell type. To find the appropriate hydrogel, sometimes elaborate experiments are needed, as e.g. in case of the skin cells (see the next section 4.2.1).

4.2.1 Matrices used for skin tissue printing - occurring problems and challenges

In the process of printing skin tissue, several different hydrogels and stabilising agents were tested. Three of them were the most promising: alginate, fibrinogen/thrombin, and collagen type I. In the following, the respective results are discussed.

4.2.1.1 Alginate

Alginate is a polysaccharide originating from algae and bacteria. Sodium-alginate gels in the presence of bivalent cations like calcium chloride and forms an ionic network (ionic cross-linking) [48]. It has been used for drug delivery [158] and cell encapsulation [160], [162], [76] as well as for tissue engineering [94], [87], treatment of vesicoureteral reflux [9] or myocardial infarction [161]. Furthermore, it is employed as wound dressing [5], [43] and as an impression material in dentistry [114], [6].

The major advantage of alginate with regard to bioprinting is the fact that its viscosity is very easily adapted and controlled, which is especially important for the even coverage of the donor glass slide and thereby an optimal and uniform LIFT process. Moreover, alginate can easily be gelled and hardened after transfer by the addition of simple calcium chloride solution. This, in turn, leads to the simple creation of stable 3D constructs. Furthermore, it displays high biocompatibility, low toxicity, and very low cost and is already used in clinical applications.

Mainly we used it for the transfer of ASC, which were subsequently differentiated to bone, cartilage, and fat tissue [58], [59]. Furthermore, alginate has been used to study the influence of parameters like viscosity, cell density, printing speed, and laser energy in case of laser based bioprinting [62]. In case of inkjet printing, alginate has been employed to successfully arrange a variety of different cell types [119], [112] including HeLa cells [7] in diverse 2D and 3D patterns. Therefore, it seems to be a promising hydrogel with respect to bioprinting.

Nevertheless, it is not suitable for the production of tissue using skin cells. A large 3D construct consisting of different fluorescently labelled keratinocytes arranged in several layers was successfully created (see figure 1 on page 48) to show the possibility of 3D printing by LIFT. Unfortunately, skin cells (fibroblasts and keratinocytes) were not able to degrade the alginate gel, maintaining a round appearance even after two weeks of cultivation and as such failing to form a normal tissue (see picture A.1 in appendix A). As can be seen in the live dead staining, the cells remained viable in the alginate, though (see picture A.2 in appendix A). Similar results were obtained when fibroblasts were treated with an alginate solution in the sol phase. Proliferation was strongly reduced, adherence was impaired, but cytotoxicity was very low [110].

Different concentrations of alginate were tested to see if lower concentrations were more compatible with the cells (see picture A.3 in appendix A). Nevertheless, this did not result in success, as even in very low concentrations (0.5 %), the cells remained rounded. This, however, is of no use in the context of skin tissue generation. In contrast, the deposition of stem cells with alginate and the subsequent differentiation to bone and cartilage proved to be successful [58], which is probably due to the fact that the stem cells did not need to form a dense tissue with cell-cell-contacts, but just produced their specific ECM at their deposited position.

As has been shown before, protein adsorption and therefore adherence of the cells to alginate is low due to its hydrophilic properties [87]. Therefore, as a remedy for the above described situation, one solution might be to chemically alter the alginate and introduce respective signalling peptides. This might be possible, since modification of alginate has been shown before [87], [157]. Indeed, when GRGDY peptides were covalently coupled to alginate, myoblasts were able to adhere to and spread on disk-shaped alginate gels *in vitro*. The cells subsequently proliferated and formed myofibrils. Controls, which consisted of non-modified alginate, showed neither cell attachment nor proliferation [143]. However, this would probably not solve our problem since when printing skin tissue, the cells are encapsulated in the alginate gel. Even if they were able to adhere, they would probably not be able to degrade the alginate to stretch out and proliferate. We suppose that mammalian skin cells lack the necessary enzyme to degrade the alginate (alginate lyase). In the literature, only algae, fungi, marine invertebrates, and microorganisms are described to produce alginate lyases [171]. Moreover, a search for alginate lyase in the human genome did not produce any hits (nucleotide database of NCBI). Nevertheless, alginate is often described as a biocompatible and biodegradable hydrogel. Its degradation in mammals is realised by the leakage of the bivalent Ca^{2+} ions from the alginate gel, which ultimately leads to its dissolution [118]. In our experiments, this leakage was apparently not strong enough to dissolve the alginate.

4.2.1.2 Fibrinogen and thrombin

Another very useful hydrogel is the combination of fibrinogen and thrombin. Fibrinogen-like proteins are already present in gastropodes [175] and fibrinogen and thrombin are both involved in blood coagulation in the mammalian body. In this context, fibrin is formed by enzyme-catalyzed crosslinking of fibrinogen in the presence of thrombin, calcium chloride, and factor XIIIa [48].

Fibrin has already been used for different purposes *in vitro* and *in vivo*: In research, human umbilical cord stem cells were encapsulated into fibrin for myogenic differentiation, with the goal of achieving tissue engineered muscles [92]. Fibrin in combination with collagen and chitosan was also used for the creation of a specific ECM microenvironment within a dermal wound healing model [115]. Furthermore, a fibrin-chitosan composite substrate was developed for the *in vitro* culture of chondrocytes [54].

In clinical surroundings, fibrin is often applied as a biocompatible sealant [87]. This comprises the use of fibrin for the sutureless wound healing of inner organs after operations [100], its application as a sealant for pneumothorax [74] as well as its usage in inguinal hernia repair with meshes [117]. Furthermore, fibrin glue is employed in facelifts [154] and was tested for its ability to improve graft adherence in a porcine burn wound model [22]. Similarly, its use resulted in an increase of skin graft take in patients with diabetes mellitus type II or smoking history [136].

A major advantage of this hydrogel is the possibility of using autologous fibrin from the patients [87]. This in turn, drastically reduces the risk of infection and the rejection connected to allogeneic material. Moreover, no toxic degradation or inflammatory reactions are to be expected. The major disadvantage of the fibrinogen/thrombin approach is the short storage life of both substances.

In general, cells can easily and evenly be deposited with this hydrogel, forming very stable 3D constructs. The cells are mixed with fibrinogen and hyaluronic acid before transfer, while stiffening of the printed 3D construct is effected by the addition of a thrombin and calcium chloride containing solution. This results in a very precise positioning of the printed cells and the accurate formation of a 3D pattern. Precisely this characteristic was appreciated and utilized by our group when creating a 3D migration assay. MSC and endothelial colony forming cells (ECFCs) were printed as a spot array in several layers above each other [60]. Thereby, cell-cell and cell-environment interactions could easily be assessed.

When used for the production of a skin equivalent by LIFT, transfer of skin cells resulted in the specific deposition of fibroblasts forming a multi layer dermal part and keratinocytes residing in a multi layer epidermal part on top of the fibroblasts, which was very promising. However, after a few days the keratinocytes started to migrate into the dermal part (see picture A.4 in appendix A). In some cases, a continuous epidermis was formed, but in other cases mushroom-like formations were produced by the keratinocytes. This is not unexpected as keratinocytes are initiated by e.g. fibrin to migrate during wound healing from the wound edges towards the wound to conduct reepithelialisation [55], [42]. Therefore, this hydrogel is not suitable for the creation of a skin substitute.

4.2.1.3 Collagen

As a major constituent of skin, collagen type I has finally been used by us for the bioprinting of skin equivalents [81], [103]. It is a major constituent of connective tissue [4, chapter 19] and can already be found in simple life forms like sponges [108]. Collagen serves as a structural protein in the ECM and gives cells structural support from the outside [87]. In skin, it plays an important role not only for the flexibility of the tissue but also for the survival of endothelial cells and vessel formation [17].

Being a fibrous protein, collagen contains a triple-helix structure which is stabilised by hydrogen bonds. Connected via covalent bonds, these helices form elongated fibrils which are found in fibrous tissues like tendon, ligament, fascia, and skin, but also in cornea, cartilage, bone, blood vessels, the gut, and intervertebral discs. Collagen is mainly synthesised by fibroblasts and exhibits a great tensile strength. Being located in the dermis, in co-operation with elastin and other molecules, collagen type I is responsible for skin strength and elasticity, while collagen types IV and VII are part of the basement membrane. Ligament and tendon comprise collagen types I and III, whereas cartilage mainly contains collagen type II. Also in bone collagen type I can be found, being the main component of the organic part [19], [4, chapter 19]. Collagen type V is present on cell surfaces, in hair, and the placenta.

The major advantage of the application of collagen in tissue engineering is its natural occurrence in the human body. Therefore, collagen is very biocompatible and biodegradable and does not elicit a rejection reaction. However, collagen also possesses some disadvantages. Although collagen is a natural hydrogel it cannot - like fibrin - be used as an autologous biomaterial from the patients. Therefore, the risk of infection and rejection remains. Normally, collagen isolated from bovine skin or rat tails is used.

In tissue engineering, collagen type I forms a thermally reversible gel, providing good cell adhesion [48]. It can often be found as an ingredient of compound matrices comprising a natural occurring and an artificially created polymer. For instance, poly ethylene glycol (PEG) can be mixed with collagen to produce a hydrogel system which can be used as a scaffold for viscoelastic tissue engineering [29]. While the PEG is mainly responsible for the mechanical properties, the collagen enables the bioactiveness of the matrix, i.e. the interaction with the cells and biological molecules. Another example of a compound matrix is the combination of collagen with amphiphile nanofibres and bone morphogenetic protein 2 (BMP-2) with the aim to enhance bone regeneration [89]. Moreover, collagen sponges were used to provide a scaffold for cartilage regeneration in combination with MSC and stromal cell-derived factor-1 (SDF-1) [176].

Collagen is often used in skin tissue engineering (see sections 1.3 and 1.4). It can be degraded by cells [87] and resulting gels are contracted by fibroblasts [4, chapter 19]. In the field of bioprinting - apart from skin tissue formation - collagen has also been used to transfer endothelial cells and smooth muscle cells [170], [18].

Regarding the printing process, the inconsistency of different batches is a major drawback [87] (and our own experiences). This is especially problematic for the printing process as with every new batch the printing parameters need to be tested anew. This is very time consuming and according to our own experiences not all batches work well for printing if they work at all. In this context, we tried many different collagens from different companies, complemented by rat tail collagen isolated ourselves, until we found a feasible commercial collagen.

A further disadvantage of collagen is the inconsistency of the printing. The gelification of collagen is difficult to control and uneven gelification will negatively affect the spatial accuracy of the printing process [75] (and our own experiences). To compensate for the inconsistency of the printing process, I tried a combination of alginate and collagen to create a 3D cell construct, thereby making use of the

advantages of both hydrogels. These experiments were only conducted *in vitro* by pipetting, without the use of LIFT. The idea was to first utilize the alginate to achieve a stable and accurate 3D gel very quickly, while the collagen needs more time to gel. Then, as a second step, the alginate should have been dissolved enzymatically by alginate lyase, leaving the stable collagen with the cells behind to form a skin-like tissue without the inhibiting alginate. Unfortunately, this approach did not work as either both hydrogels dissolved at the same time or the cells were damaged by the used solutions.

As no other hydrogel worked for the printing of the skin cells and since collagen type I is present in normal skin, we chose to use collagen for the creation of the skin substitutes by bioprinting. To further improve skin tissue generation and to mimic physiological skin even closer, we may add elastin to our bioprinted skin constructs to enhance elasticity. Nevertheless, this would need appropriate testing systems and probably it is not necessary as the printed fibroblasts quickly start to synthesize their own ECM.

4.2.2 Further matrices used for bioprinting

Apart from the above mentioned matrices, further hydrogels were used for bioprinting of different tissues/constructs by other groups. Subsequently, some of these hydrogels and their applications are discussed.

For instance, Pluronic F127 was employed to print a 3D hollow diamond shape. Pluronic F127 is a poloxamer, consisting of hydrophilic poly(ethylene oxide) and hydrophobic poly(propylene oxide) [41]. It has already been applied in different situations, e.g. for bone [73] or cartilage [77] tissue engineering or for cardiovascular applications. Advantages are its biocompatibility, reversible temperature-sensitive gelling, adhesion to surfaces, and broad range of viscosities at room temperature [30]. Furthermore, Pluronic F127 has been approved by the Food and Drug Administration (FDA) of the USA [48]. From the biological/medical viewpoint, especially its biocompatibility and its approval by the FDA are major assets for its application in tissue engineering. Its easy and adaptive gelling characteristics, on the other hand, are very suitable for the printing process. Although tissues with characteristics of bone and cartilage were successfully formed by cells seeded into Pluronic F127, the development of skin tissue might be more difficult due to similar reasons as in case of alginate. Pluronic molecules are not degraded by the body [10], but instead are cleared after intravenous administration by renal and biliary excretion in a rat model [166]. Therefore, it is doubtful that a dense epithelium would be able to form in case of skin tissue engineering.

Matrigel® is a hydrogel which is often used in the context of endothelial cells as it stimulates complex cell behaviour and formation of networks on Matrigel® by endothelial cells [111]. When endothelial cells were printed into a layer of Matrigel® as a specific 2D pattern they remained viable after printing [170]. Nevertheless, Matrigel® does not seem to be the optimal hydrogel to use (regardless of the cell type) due to its very heterogeneous composition, which also varies from batch to batch. This hydrogel is gained from the basement membrane of a mouse sarcoma and contains among others laminin, collagen type IV, entactin, heparin sulphate proteoglycans and a variety of growth factors which occur naturally in this tumour and may promote differentiation and proliferation of many cell types [48]. The use of such a matrix is surely not optimal for tissue

engineering, as material and growth factors derived from a tumour might not be safe to use in humans (or animals) since induction of cancer growth in the tissue engineered or the surrounding host cells cannot be excluded.

In a different approach, agarose was used for the printing process. It is a thermo sensitive polysaccharide originating from red algae and gels via hydrogen bond formation [48]. Apart from its gelatinous properties, which are utilised in the food industry, it is also employed for gel electrophoresis and as an ingredient for agar in laboratories. Here, it was used as a stabilizing matrix for the production of vasculature by printing multiple cell types to form vessels [75], [120]. Even a branched vessel construct could successfully be printed as well as a double-layered vascular tube containing smooth muscle cells and fibroblasts. In this context, agarose proved to be an inert and biocompatible hydrogel which the cells neither invaded nor rearranged. This was important, since only due to the inertness of the agarose, the cells were forced to stay in the printed place and to form the desired vessel structure. After the cells were grown together, the excessive agarose was removed to free the vessel lumen of the now superfluous hydrogel. The biocompatibility and natural occurrence of agarose certainly are advantageous. Nevertheless, if used for skin tissue creation, its stability and inertness are not expedient since the skin cells need to form a dense tissue and would probably not be able to do so when encapsulated by agarose.

For the creation of bone or cartilage, a much harder scaffold is needed than for the production of skin or blood vessels. Bone tissue engineering was e.g. realised by the transfer of osteoprogenitor cells along with nano-hydroxyapatite [28]. Thereby, a 3D construct was created, which remained stable and contained cells expressing osteoblastic phenotype markers. A similar approach was used to transfer chondrocytes together with poly(ethylene glycol) dimethacrylate (PEGDMA) for the production of cartilage [34]. This resulted in the creation of a cartilage-like construct with the printed cells remaining at their deposited positions due to simultaneous photopolymerization of the PEGDMA. When this tissue engineered 'cartilage' was directly printed into a real cartilage defect, the printed construct bound firmly to native cartilage tissue. This especially emphasises the necessity to adapt the chosen hydrogel to the tissue, which should be engineered. In this context, both approaches seemed to be successful under biological and technical aspects. Moreover, the described approach for the creation of cartilage utilised two major advantages of the bioprinting: the defined and even distribution of the printed cells and the defined and accurate shaping of the cartilage construct.

Further hydrogels used for bioprinting are reviewed in [48]. They include the above described gels as well as starch, dextran, gelatin, methylcellulose, and chitosan and are used for different approaches.

4.2.3 Final conclusions about matrices used for bioprinting

Both, the section about skin tissue printing as well as the overview of different hydrogels used for bioprinting of other tissues, emphasise the same conclusions, i.e. that the selection of the adequate matrix for the printing of different cell types and tissues is of utmost importance. While one matrix might be suited for one specific aim, it might not be appropriate for another purpose. Moreover,

even if one matrix is suitable from the technical point of view it is not necessarily optimal concerning the biological aspects and *vice versa*. This is especially true for the printing of skin tissue, since only collagen allowed good tissue formation by the printed skin cells. On the other hand, collagen is disadvantageous for the printing process.

4.3 Clinical applicability

4.3.1 Challenges and solutions for tissue engineering of skin for clinical application

One major challenge is posed by the step from research to clinical application, the step from bench to bedside. In this case, several issues need to be considered. The first issue is the scale-up from printing a few small pieces of skin for research to the serial production of large skin constructs for clinical use in e.g. burn patients (see also section 5). The second concern is the functional and aesthetical enhancement of the tissue engineered skin by addition of different supplemental cell types. Bioprinting - specifically laser based bioprinting like LIFT - is able to successfully solve this quest. The possibility of transferring special types of cells to exactly the desired 3D position in a (skin) tissue is the unique feature of bioprinting and as such its major strength. As we [81], [58], [60] and others [14], [125], [30], [34], [7], [28] could show, already now 3D constructs and 3D patterns of different cell types can be printed by laser or inkjet printing. Still, the printing process and the selection of the appropriate matrix need to be optimized for the different cell types until their inclusion is possible (see also section 4.2).

4.3.2 Alternative cell sources for tissue engineered skin

4.3.2.1 Vascularisation of tissue engineered skin

When thinking about clinical applications of LIFT, among others the question about the source of all the above described cell types needs to be considered. In case of extensive burn injuries, autologous cells for biopsies to produce skin sheets or similar are very scarce. Nevertheless, autologous cells are the best source of cells for transplantation or the production of skin substitutes as they are not rejected by the immune system of the patient and do not bear the risk of infectious diseases. Also, the use of genetically modified cells for the treatment of humans still is a controversial issue. Therefore, other cell sources are being searched for by researchers and clinicians. In this context, the use of stem cells may represent a solution. They can be found in nearly every organ as tissue must be capable of self-renewal [102]. Adult stem cells can be found e.g. in bone marrow, adipose tissue, blood, and skin and may be used according to the desired differentiated cell type. Especially ASC may prove to be of major advantage as they are of bountiful occurrence in humans.

Since fast vascularisation is one of the most important prerequisite for the take of a graft, major research has been focusing on the quick vascularisation of tissue engineered skin or other organs (see also section 1.3). In this context, ASC from lipoaspirates could be amplified to obtain endothelial progenitor cells,

which were then differentiated into endothelial cells. A skin equivalent was constructed *in vitro* by seeding a collagen-glycosaminoglycan-chitosan scaffold with those differentiated endothelial cells, also adding fibroblasts and keratinocytes. In this setting, the endothelial cells formed capillary-like tubular structures. In contrast, in skin constructs seeded with endothelial progenitor cells instead of already differentiated cells no tubular structures were formed [12]. Also another group demonstrated the possibility of differentiating MSC to endothelial cells using endothelial growth medium supplemented with vascular endothelial growth factor (VEGF) [129]. These cells may be used to create a vascularised tisse engineered skin equivalent. While these approaches might be feasible regarding the clinical aspects, the fact still remains that a long time for the differentiation of stem cells to endothelial cells is needed. However, in burn injuries a quick coverage of the burned skin is essential. Therefore, a temporary coverage with allogeneic cadaveric skin - as is already common in the clinic - could be used to bridge the time until the skin equivalent would be ready for use. This is also true for the further described approaches.

Sweat gland derived stem cells represent another cell source, displaying the feature of being quite abundant in the human body. They can be isolated easily and exhibit a high proliferation rate *in vitro* as well as *in vivo*. When seeded onto Integra® (an acellular dermal substitute consisting of collagen and glycosaminoglycan) and cultured *in vitro*, the cells released molecules involved in angiogenesis, immune response and tissue remodelling. After seeding the stem cells onto Matrigel® they formed capillary-like structures. *In vivo* they significantly enhanced vascularisation during dermal regeneration in a full skin defect model in mice. The exact mechanism is not known yet, but the stem cells might differentiate into endothelial cells or they might act as mediators to create a proregenerative microenvironment in the wound area [37]. Although - according to the authors of this publication - these stem cells are plentiful in the body, the question remains if enough of them can be isolated and cultured to print a skin equivalent for burn patients.

Apart from stem cells, endothelial cells can be used. In one approach, transduced human umbilical vein endothelial cells (HUVEC) overexpressing Bcl-2 were seeded onto human acellular dermis grafts. Upon subcutaneous implantation in immunodeficient mice the transduced grafts contained a significantly higher density of perfused HUVEC-lined microvessels than the controls (unseeded human acellular dermis) after one month. Following this approach, a skin equivalent was produced by seeding the apical surface of the acellular dermis with keratinocytes and the basal surface with Bcl-2-transduced HUVEC. Already two weeks after implantation into a full-thickness skin wound, perfusion through HUVEC-lined microvessels could be detected. The vessels showed signs of progressive maturation and increased the speed of graft vascularisation. In contrast, murine vessels could only be detected at the edges of the implants. The latter was also true for unseeded controls. Therefore, the very quick successful vascularisation by the human endothelial cells already present in the grafts is of major importance. Inosculation of the human vessels with the murine ones also occurred quickly. Even after six weeks, the human vessels could still be detected [146]. Despite these promising results, this approach has two drawbacks concerning its clinial application. First, HUVEC are allogenic cells, which bear the risk of infection

and may elicit rejection. Second, the use of genetically modified cells in human therapy may be risky.

Another approach to seed Integra® or Matriderm® with cells as a dermal skin substitute utilizes ECFCs derived from cord or adult blood. The idea is to establish pre-formed vessel networks in the dermal substitutes prior to implantation. Thereby, the vascularisation time decreases from two weeks (in case of the scaffold without cells) to only five days (in case of the scaffold already containing a vessel network). Using an *in vitro* vasculogenesis assay, the cells originating from cord blood were found to form more vessels than the cells originating from adult blood. Further, bmMSC as well as fibroblasts could enhance vessel formation of the ECFCs derived cells. To test the same parameters in a 3D model, ECFCs were seeded together with either bmMSC or fibroblasts on Integra® or Matriderm® scaffolds and cultured *in vitro* for 14 days. Here, also vessel formation could be detected, after the cells migrated into the scaffolds. The vessels contained lumens, were lined with endothelial cells connected with tight junctions, and showed typical capillary walls. No differences with respect to the cell type or the scaffold could be found [11]. The idea to use autologous cells from adult blood seems feasible and sensible for the clinical application. Nevertheless, proliferation and propagation of those cells and the subsequent creation of pre-formed vessel networks *in vitro* before implantation still needs time. This, however, is scarce for burn patients. Therefore, as mentioned before, coverage with a temporal skin substitute like cadaveric allogeneic skin may be a solution.

As a further alternative cell source, fibroblasts were used and transformed into endothelial cells by genetic reprogramming. The reprogrammed fibroblasts showed endothelial cell (EC) morphology and expressed endothelial markers *in vitro*, confirming their transformation. Moreover, when seeded onto decellularized aortic grafts and cultured in a bioreactor, the grafts displayed normal vessel morphology while the cells expressed EC markers. Furthermore, the reprogrammed cells expressed VE-cadherin and improved neovascularization and blood flow recovery in a hindlimb ischemic model in mice. Thereby, they formed a typical vascular architecture. Concerning their safety, the reprogrammed cells did not induce tumour formation *in vivo* after subcutaneous injection into SCID mice [98]. Since no hint for their tumourigenesis is present and fibroblasts are quite abundant, they might represent a feasible and good cell source for tissue engineering of artificial skin. Nevertheless, genetically modified cells are still considered as problematic regarding their application in human therapies.

An even more feasible way to enhance vascularisation may be the use of the stromal vascular fraction (SVF), which contains heterogeneous cells of the adipose tissue, including ASC, endothelial progenitor cells (EPCs), hematopoietic progenitors, T cells, and anti-inflammatory cells. The major advantages are the abundance of adipose tissue in the human body as well as the quick access to the SVF during the operation and the lack of cultivation time of cells *in vitro*. To compare the ability of SVF to promote vascularisation to that of bone marrow derived mononuclear cells (BM-MNCs), both were used in a skin flap model in rats. BM-MNCs were already shown to promote neovascularisation of random skin flaps. Two days prior to lifting the flaps, either SVF or BM-MNCs were injected subcutaneously in the area of the flap. Seven days after the flap surgery, in both treated groups blood perfusion and capillary density were higher than

in the control group (injection of PBS without cells) and VEGF and basic fibroblast growth factor (bFGF) expression was increased. Altogether, the SVF acted similar to the BM-MNCs. Therefore, in case of flap surgery, the use of SVF seems to be a feasible and quick manner to achieve increased vascularisation and increased flap survival [150]. Whether this technique represents a possibility in burn therapy still needs to be assessed.

In summary it can be said that several approaches are being followed to enhance vascularisation of tissue engineered skin constructs and that many different cell types were proposed to achieve this goal. Some seem to be more feasible in the clinical applications than others due to their abundant/scarce availability and their autologous/allogeneic origin.

4.3.2.2 Skin equivalents and wound healing

Many research groups propose to use stem cells, originating from different tissues in the body. They seem to be abundant enough to be used as autologous cells and display hope inspiring behaviour with respect to tissue engineered organs. Especially in case of skin regeneration and chronic wounds, MSC were shown to improve wound healing [109]. Cutaneous wound repair comprises a well-coordinated interaction of inflammation, neovascularisation, ECM formation, and epithelialisation. In chronic wounds, however, the cells are thought to be intrinsically impaired and therefore no physiological skin regeneration occurs. Treatment with bone marrow derived MSC showed promising results in animal studies as well as in humans. In mice and rat models, it led to an accelerated wound closure, being accompanied by an increase in the inflammatory response, granulation tissue, angiogenesis, collagen composition, and wound burst strength [109]. Note that these experiments also included diabetic animal strains. This is especially important since they represent circumstances in which chronic wounds are likely to appear. Also in human trails containing chronic wounds, the administration of MSC resulted in an increased inflammatory response, increased angiogenesis and decreased wound size if not complete wound closure. This, in turn, led to an improvement of life quality for the patients, as e.g. in an increased pain-free walking distance [109]. A similar approach utilized EPCs originating from BM-MNCs, which were topically applied to full-thickness skin wounds in diabetic mice. Wound healing and wound vascularity were increased compared to wounds treated with BM-MNCs or PBS alone (controls). The seeded EPCs were shown to express VEGF and basic fibroblast growth factor [8].

Apart from MSC originating from bone marrow or adipose tissue, amniotic mesenchymal stem cells (AMM) were shown to enhance cutaneous wound healing in a diabetic mouse model [80]. The AMM integrated into the forming tissue and partly differentiated towards a keratinocyte-like phenotype. Already *in vitro* wound closure induced by AMM conditioned medium was enhanced compared to closure rates due to ASC conditioned medium. Also *in vitro* AMM showed a significantly higher expression of angiogenic cytokines like insulin-like growth factor 1 (IGF-1), epidermal growth factor (EGF), and interleukin 8 (IL-8) compared to ASC. While EGF plays a role in keratinocyte migration and angiogenesis, IL-8 promotes skin re-epithelialisation.

In a burn wound model in pigs, tissue engineered skin consisting of collagen-GAG scaffolds seeded with porcine bmMSC resulted in a better healing, better

keratinisation, less wound contraction, and more vascularisation compared to controls (scaffolds without cells). To be able to track the seeded cells, they were stained with a fluorescent dye. Since single fluorescent signals were detected throughout the whole wound area after four weeks, the bmMSC were thought to accelerate wound healing and to contribute to the formation of the new dermis and epidermis of the wound area [95]. Nevertheless, no information was given concerning the question how exactly the seeded cells contributed to the wound healing. They might have differentiated to e.g. keratinocytes, they might have hybridised with host cells, or/and they might have provided special chemokines or the like.

The way of action of the MSC still has to be studied in more detail, but paracrine effects on keratinocytes and fibroblasts could be detected *in vitro*. ASC conditioned medium increased proliferation of HaCaT cells as well as primary human fibroblasts. Furthermore, *in vitro* wound healing of HaCaT was improved and contraction of a fibroblast-seeded collagen lattice was increased, while the transcription of the type I procollagen alpha 1 chain was upregulated [88]. Paracrine factors also stimulated migration of inflammatory cells, endothelial cells and keratinocytes as well as the secretion of collagen from dermal fibroblasts. They include among others VEGF, EGF, and erythropoietin [109]. *In vivo* experiments also hint at the incorporation of ASC into the new skin tissue, when scaffolds seeded with MSC were implanted into wounds in a rat model [152].

In search for still another, abundant cell source, human amniotic mesenchymal stem cells and human amniotic epithelial cells were suggested [90]. They possess properties of stem cells and are easy to isolate, at the same time exhibiting a huge availability. The cells were used to create a tissue engineered skin construct, by seeding the cells into/onto a collagen type I matrix and culturing them at the air-liquid-interface for 2 weeks. No cornified layers could be detected but a stratified epidermis developed. Proliferation of the cells as well as the secretion of collagen type I could be perceived. *In vivo*, the skin constructs could successfully repair full-thickness skin defects in a mouse model. They exhibited a morphology similar to normal skin with a stratified epidermis and an underlying dermis after 18 days. Here, amniotic cells were present in the epidermis as well as the dermis. As feasible as this approach might be due to the large availability of the cells, their allogeneic origin might pose severe problems in case of transplantation.

For the function of skin not only a stratified and cornified epidermis and a sufficient vascularisation are needed, but also the innervation of the skin equivalent is necessary. In a porcine model it could be shown that vascularisation precedes innervation and that the development of nerves is dependent on the nutritional and trophic factors supplied by the vascular network [49]. Therefore, a quick vascularisation by the addition of appropriate cells and growth factors in the bioprinted skin substitutes might also lead to a faster and better innervation of the skin equivalent.

4.3.2.3 Possible dangers concerning the use of stem cells

In spite of those promising results, the use of stem cells might also pose danger to the patients. These cells might differentiate into very many other (unwanted) cell types or may secrete factors which enhance the formation or growth of other cells like cancer cells. The risk of tumour formation is dependent on the origin of the

cells, the extent *ex vivo* expansion, the induced differentiation, and the site/route of administration. Large differences exist between embryonic stem cells, which are pluripotent, and adult/somatic stem cells (e.g. MSC), which are multipotent [46]. Also, the interaction between the tumour cells and their microenvironment is very important concerning tumour development and prognosis. Corresponding examples will be presented in the following:

In e.g. pancreatic tumours so-called cancer stem cells (CSC) were found. These cells play a major role in the malignancy of tumours due to contributing to the resistance of tumours towards chemotherapeutics as well as to the establishment of metastasis and tumour growth/proliferation [63]. CSC have been shown to be partially independent from their stem cell niche, adding to their migration and metastatic activity. Moreover, cancer cells interact with surrounding cells, stromal cells, and MSC, resulting in the establishment of a suitable microenvironment for their survival and growth. In this context, MSC were found to be recruited to and accumulate in the tumours from the bone marrow, therefore adding to the protective role of CSC towards tumour development. Furthermore, they contribute to the angiogenesis and desmoplasia of the tumours and suppress anti-tumour immune responses [35]. The immunosuppressive role of MSC and its dangerous consequences have also been indicated by the fact that only in the presence of coinjected MSC, B16 melanoma cells led to tumour growth in an allogeneic mouse model [40].

Further evidence along similar lines indicates that cancer cells are able to induce malignant transformation of MSC *in vitro* by paracrine effects. In a co culture experiment of rat bmMSC and malignant rat glioma cells without direct cell-cell contact, MSC became phenotypically malignant cells after seven days [93]. They showed a decreased wildtype p53 expression while increasing the expression of a mutant p53, being accompanied by an aneuploid karyotpye. Therefore, the exposure of MSC to a tumour microenvironment resulted in the conversion of normal MSC to tumour-promoting, malignant cells. Furthermore, MSC were found to be transformed into carcinoma-associated fibroblasts-like cells *in vitro* by exposing them to tumour-conditioned medium over a period of 30 days [105]. The resulting cells showed the ability to promote tumour growth *in vitro* as well as *in vivo* in a co implantation model. Carcinoma-associated fibroblasts (CAF) were shown to enhance tumour growth, angiogenesis, and metastasis in epithelial solid tumours. Thus, also by transformation to CAF, MSC are thought to be involved in the formation and maintenance of tumours.

Taking the above mentioned into account, the selection of suitable cells for tissue engineering needs to be made with utmost prudence and care. While MSC may be transformed to malignant cells in the context of tumours, they may also be of immense value in the formation of tissue engineered skin. Therefore, for each combination of application and cell type, the benefits and drawbacks as well as potential dangers have to be assessed.

4.3.3 From bench to bedside - legal framework and use of Matriderm®

Since tissue engineered skin substitutes contain living cells and are destined for use in humans, they have to be produced, processed, and applied according to

the corresponding legal requirements. In case of Germany, European (EU) law in form of different directives and regulations is in effect, which is then implemented in according German laws.

Regulation (EC) 726/2004 specifies procedures for the authorisation and supervision of medicinal products for human and veterinary use on the Community level (meaning on the EU level). Furthermore, to provide Community institutions and Member States with the best possible scientific knowledge, the European Medicines Agency (EMA) is established [134]. Medicinal products comprising gene therapy, somatic-cell therapy, or Tissue Engineering are subsumed under the term 'advanced therapies medicinal products' (ATMP). ATMP may contain biological materials (e.g. tissues or cells), chemical structures (e.g. metal implants), or polymer scaffolds [99]. For the evaluation of ATMP and the according counsel, a special committee within the EMA is present, the Committee for Advanced Therapies (CTA). The CTA centres the highest available expertise concerning the advanced therapies, with the aim to ensure the highest quality of the medicinal products and the highest safety of the patients (Regulation (EC) 1394/2007). This regulation specifies particular rules concerning authorisation, supervision and pharmacovigilance of ATMP. This includes for example the free movement and facilitation of access to the EU market by the Member States [133]. Special attention to the application of stem cells in human treatment and corresponding advanced therapies is given by the EMA and the CTA, due to potential harmful risks. The risk depends on the origin of the stem cells (e.g. embryonal or adult stem cell) as well as the status of differentiation (e.g. proliferation or terminally differentiated). In this context, undifferentiated and proliferative stem cells possess a relatively high potential risk of tumour formation. New regulations need to be developed for the assessment of risk factors concerning stem cells [46].

Further considerations comprise the donation, procurement, testing, processing, preservation, storage, and distribution of human tissue and cells. The according standards of quality and safety to ensure a high protection of human health are laid down in Regulation 2004/23/EC [130]. This regulation is amended and augmented by Commission Directives 2006/17/EC and 2006/86/EC, which describe the implementation of e.g. the technical requirements with the aim of preventing disease transmission, and the technical aspects of traceability and notification of serious adverse reactions [131], [132].

On the national level - in Germany - the EU regulations and directives are implemented mainly by four laws: the Transplantationsgesetz (TPG), the Transfusionsgesetz (TFG), the Arzneimittelgesetz (AMG), and the Gewebegesetz (GewebeG). In the TPG, mainly organ donation is regulated [26]. The TFG aims at providing the population with blood and blood products, but also states the regulations concerning the acquisition and processing of blood and blood products [25]. The AMG is responsible for the provision of the human population and animals with pharmaceuticals and drugs, and to ensure the quality, efficacy, and harmlessness of the pharmaceuticals [23]. The GewebeG is a law which amends and alters the other three laws insofar, as these laws are also valid for tissues and cells [24].

Following the mentioned regulations, appropriate premises, equipment, laboratories, personnel, and administration is needed to be able to use ATMP for the treatment of patients. This is only possible in appropriately equipped and

certified clinics/centres. To establish such structures, vast monetary resources are needed. This might be especially difficult for clinics, since they are not able to operate as profit-oriented as companies.

Another aspect is, that these regulations are also valid for the use of autologous cells of a patient, when his/her cells are not used in the same operation again, but have to be stored and/or amplified. Even the simple act of saving healthy tissue/cells for later use when debriding a burn patient, cannot be conducted without having to follow the regulations. This limits the possible ways of treatment considerably, especially in small hospitals, which cannot meet the technical and administrational requirements. Therefore, simplified regulations would be desirable. Regardless, the safety of the patients needs to be ensured.

In every case, the principles and guidelines of good manufacturing practice (GMP) need to be followed, which is explicitly stated in the EU regulations. EU wide GMP principles are laid down in Commission Directive 2003/94/EC, but also in other countries similar regulations are present. The guidelines include an adequate quality management and quality control (including self-inspection), appropriately trained personnel, suitable premises and equipment, and an extensive documentation of all steps of the manufacture, storage and distribution of the products [39], [121]. Therefore, concerning our printing setup, vast technical adaptations need to be implemented to reach GMP standard. This includes e.g. the encapsulation of the printing area into a laminar flow hood to ensure sterility. Also, as many of the components used in the printing process and the cell culture as possible should be disposable to minimise contamination [30].

A further issue concerns the components of our skin constructs. In our project, Matriderm® was used as a carrier matrix. A carrier was needed to stabilise the printed skin constructs as they only comprised 40 cell layers in height and therefore were very fragile. Without a carrier matrix underneath, the skin constructs could not have been moved from the printing setup to the culture plates, nor could they have been placed into the skin wounds of the mice. In this context, the use of Matriderm® was due to two important facts. First, it is already used in clinical applications as a dermal substitute in connection with autologous split-thickness skin grafts. As such, no new trials and applications concerning the biosafety and biocompatibility are needed. This, in turn, may lead to a quick introduction of tissue engineered skin substitutes by LIFT in the clinic. Second, Matriderm® acts as a dermal substitute, consisting of freeze dried collagen and elastin. The cells are able to migrate into this scaffold easily and vascular networks can be formed [103], [104] (see also the previous section 4.3.2). Additionally, Matriderm® can easily be stored, handled, and sutured. Therefore, it represents a feasible and very suitable stabilisation matrix for our tissue engineered skin constructs. Also, others have already used Matriderm® to create skin substitutes [57].

4.4 Further applications of LIFT

Apart from tissue engineering as such, bioprinting can also be used for other biological or biomedical applications. Here, laser based as well as inkjet printing prove useful. In research often assays with very small amounts of volumes are needed (e.g. in case of DNA or protein assays) to achieve a high throughput and save samples. Bioprinting allows for the deposition of small volumes of

biomolecules with a high spatial resolution and as such is the optimal choice to produce such assays. Two different complementary DNAs (cDNAs) were printed by laser based bioprinting onto a coated glass slide to create a microarray [33]. The cDNAs transferred with bioprinting were equivalent to those created by pin microspotting, microspotting being the common way to produce microarrays. Signal intensity and gene discrimination capacity were similar and the laser pulse did not cause damage to the transferred DNA. Due to the fact that bioprinting is easily automatised, it might represent a feasible and promising alternative to hitherto used methods of producing microarrays. The costs of each method, however, need to be assessed and compared.

In a similar way proteins were transferred with laser based as well as inkjet bioprinting to form microarrays. With laser based bioprinting the volume of each transferred drop is dependent on the used energy and can range from nanolitres to femtolitres [14]. A great uniformity and symmetry of the printed protein droplets could be reached while printing biotinylated bovine serum albumin (BSA) onto a coated glass slide [141]. After incubation with Cy5-labelled streptavidin the transferred BSA could be detected by fluorescence. Similar results could be obtained by inkjet based printing of proteins. Here, also biotinylated BSA was transferred into a specific pattern and detected by a fluorescent dye coupled to streptavidin [170]. This proves that the protein - at least its active site - is not destroyed by the printing process. By laser printing of proteins the spot size can be decreased dramatically compared to standard arraying procedures. This results in an increase of array density and therefore also in an enhanced assay efficiency [141]. Using inkjet printing, hydrated protein solutions can be used, in contrast to other spotting techniques. This enables the use of liposomes in the cartridges to print membrane-bound proteins. Those are difficult to immobilize in patterns with other spotting techniques [170]. Bearing the above mentioned examples in mind, bioprinting may be used to detect diseases early and inexpensively, by creating DNA, ribonucleic acid (RNA) or protein biochips containing disease markers.

Similar to printing protein or nucleic acids in a controlled way, also different types of cells were co-printed to form specific 2D patterns [141], [170], [14], [82]. An interesting application is to use bioprinting as a migration assay in 2D as well as in 3D. To examine their interactions with respect to vessel formation, ASC were printed together with ECFCs in a 3D migration assay using fibrinogen/hyaluronic acid and thrombin as a printing matrix [60]. The matrix served to fix the transferred cells in their final position but also provided the height for the 3D constructs. At first, the ASC migrated towards the ECFCs. After contact, the ECFCs began to form vascular-like networks, growing towards the ASC spots and remaining stable for two weeks in *in vitro* culture. As was shown before, cells can exactly be deposited in a grid pattern with a defined spot spacing. Any cell-cell ratio, cell quantity and cell-type combination is possible. Therefore, laser based bioprinting can be used to study complex relationships between cells and their local environment.

A rather different assay in which a specific printed pattern could be useful is an antimicrobial assay. Here, inkjet based bioprinting was used to deposit living *Escherichia coli* bacteria onto agar-coated substrates with a high density. Subsequently, gradient concentrations of antibiotics were placed onto them to

determine their minimum inhibitory concentration (MIC) [178]. Also, other drugs may be printed in different combinations with cells or proteins to prove their effectiveness. The automation of bioprinting allows for a high throughput of those applications.

Apart from using bioprinting to produce assays, it can also be used for gene or protein transfer to (mammalian) cells. This is especially useful if other transfection techniques result in very low transfection rates or if rather large molecules need to be inserted into the cells. This often proves difficult to achieve. Also, it is much faster than microinjection. In this context, inkjet printing was used to temporarily disrupt the cell membranes of NIH3T3 fibroblasts without affecting cell viability [127]. During the printing process they incorporated the fluorescently labelled g-actin monomers present in their surroundings in the bioink. Transformation by bioprinting seems to be a potent technique for the generation of genetically modified cells.

Returning to the field of tissue engineering, bioprinting can also be used to deposit different cell types into a 3D scaffold. By laser based bioprinting, ovine endothelial cells and smooth muscle cells were printed into a 3D scaffold made by two-photon polymerization (2PP) technique and remained viable after transfer. The cells did not leak out of the scaffold and remained at their deposition location [126]. The combination of 2PP and laser based bioprinting may result in the realisation of 3D multicellular tissue constructs as the location and density of printed cells can easily be controlled.

But also plane surfaces can be printed with a specific pattern of different cell types. In this context, MSC were co-printed with HUVEC cells in a specific pattern onto cardiac patches. MSC are thought to inhibit apoptosis of endothelial cells in hypoxic conditions, increase their survival, and enhance vessel formation and angiogenesis. Therefore, HUVEC were printed onto the patches in a network forming the edges of squares and MSC were deposited into the squares. Control patches were randomly seeded with the same cells. The printed patches exhibited increased vessel formation and significant functional improvement of the heart in comparison to the controls after being used in an infarction model in rats. The transferred cells were shown to be incorporated into the murine vascular system [53].

In summary, laser or inkjet based bioprinting may be used for many different applications, including different assays (DNA, protein, migration, and antimicrobial drugs), transfection of cells and the specific deposition of different cells types in various surroundings and settings. For all these utilisations, the easy automation of this technique is a major asset.

5 Outlook

In our co-operation, the fundamentals of a successful transfer of different cell types and the creation of a simple skin equivalent via LIFT were established. Nevertheless, this is only the beginning of an exciting and most important field of tissue engineering as the creation of functional skin is only possible by the addition of further different cell types. These comprise cells like hair follicle cells and perspiratory glands, which are necessary for the ability to sweat. This in turn is especially important in case of a large burned area, where the patient's ability to maintain a normal thermo homeostasis may be impaired.

Another critical problem and therefore really important challenge is the limited perfusion of skin substitutes. To ensure graft take, sufficient vascularisation needs to be achieved, but its development is often protracted. This problem may be solved by the incorporation of endothelial cells into the dermis via LIFT, forming a preset network. The cells are expected to quickly form new vessels, which are then connected to the host vessel system by inosculation. As possible alternative and autologous cell sources, different cell types have been proposed, including EPCs and MSC, the MSC originating from adipose tissue, bone marrow, or sweat glands. However, the safe use of stem cells is not ensured, as e.g. tumour cells recruit stem cells into their surroundings, causing their transformation into malignant cells (see also section 4.3.2.3).

Furthermore, in order to increase the aesthetic outcome, melanocytes should be included into the skin substitutes. Other cells types, which might be of advantage to be included as well, are nerve cells or Schwann cells. Moreover, the addition of growth factors like keratinocyte growth factor (KGF) or VEGF and their impact on the differentiation of keratinocytes and vascularisation, respectively, may be tested.

Skin substitutes produced by LIFT are not only suitable for the treatment of burn injuries, but may also be used for other clinical applications, e.g. the therapy of pigmentary abnormality. In this case, skin containing the right amount of melanocytes could be produced. Also, the treatment of chronic wounds and ulcer might benefit from the production of skin substitutes via LIFT. All in all, we aim to develop a skin substitute which is as functional, physiological and true-to-life as possible.

To approach clinical applicability of the here established LIFT and its application for the creation of skin equivalents, the setup has to be enlarged and adapted to sterile conditions. Up to now, the largest possible area of printing with our setup is 2.5 x 2.5 cm^2. However, for the treatment of burn injuries a much larger sheet of skin is often needed. Therefore, a scale-up of the whole equipment needs to be carried out, including the hardware as well as the controlling software. In this context, a key issue is the reduction of the processing time via the use of a higher repetitive laser. Additionally, several laser beams with a donor slide each could be used to print the cells onto the same Matriderm® sheet in parallel, to shorten the production time. Furthermore, the inclusion of the whole equipment

into a laminar flow chamber for a sterile printing environment needs to be realised. The complete automation of the LIFT process including the transfer as such as well as all preparative steps would be very helpful to prevent human errors and possible infection and furthermore would be very time-saving. If possible, an automation of the cell culture would also be preferable for the same reasons. The automation would clearly contibute to the realisation of the GMP guidelines, as they enhance the quality of the production process immensely. Moreover, technical and administrational requirements stated by the EU and German law concerning advanced therapies need to be considered and realised appropriately (see also section 4.3.3).

Concerning the biological aspects, new methods for the cultivation of the resulting large skin constructs need to be developed. Finally, they need to be tested in a large animal model (e.g. pig). For this, the isolation and culture of porcine skin cells is necessary as no immunosuppressed pigs can be used.

Apart from the application of LIFT for tissue engineering, also other purposes may be followed. As bioprinting allows for the deposition of very small volumes of biomolecules with a high spatial resolution, cDNA or protein arrays could successfully be produced. Furthermore, LIFT was used to print a 2D as well as 3D migration assay or an antimicrobial assay. Even the transfection of cells with rather large molecules was shown. Therefore, LIFT can be applied for many different purposes, either for clinical use or for research.

6 Conclusions

In conclusion, it can be said that bioprinting offers a great potential in tissue engineering and other fields of research and clinical use. Cells are not harmed by the transfer and behave like non-transferred cells, including stem cells, which maintain their stem cell character. Because of its very high resolution, LIFT is uniquely suited to create complex tissues, including many different cell types. Also - in contrast to inkjet printing - LIFT enables the transfer of cells in a very high density. This is especially important for tissues like skin.

As I could show in this thesis, LIFT was successfully used to create skin substitutes. They showed functional tissue formation and proliferation *in vitro* and *in vivo* as well as beginning keratinocyte differentiation and vascularisation *in vivo*.

The used printing matrix needs to be adapted to the desired purpose and the employed cell types. As demonstrated by the printing of skin cells, this might not be trivial at all.

Bibliography

[1] Berufsgenossenschaftliches Universitätsklinikum Bergmannsheil, www.bergmannsheil.de.

[2] http://www.cryosites.com/shared/img/s/skin_k3rrr.jpeg.

[3] B. Akgül, R. García-Escudero, L. Ghali, H.J. Pfister, P.G. Fuchs, H. Navsaria, and A. Storey. The E7 protein of cutaneous human papillomavirus type 8 causes invasion of human keratinocytes into the dermis in organotypic cultures of skin. *Cancer Res*, 65:2216 – 2223, 2005.

[4] B. Alberts, A. Johnson, J. Lewis, M. Raff, K. Roberts, and P. Walter. *Molecular biology of the cell*. Garland Science, 2008. Fifth Edition.

[5] B. R. Alexander, K. E. Murphy, J. Gallagher, G. F. Farrell, and G. Taggart. Gelation time, homogeneity, and rupture testing of alginate-calcium carbonate-hydrogen peroxide gels for use as wound dressings. *J Biomed Mater Res B Appl Biomater*, page doi: 10.1002/jbm.b.31965, 2011.

[6] P. K. Ambrose, A. S. Juszczyk, R. K. Clark, and D. R. Radford. Effect of two different disinfectants on dimensional stability of newer alginate impression materials over five days. *Eur J Prosthodont Restor Dent*, 19:142 – 145, 2011.

[7] K. Arai, S. Iwanaga, T. Toda, C. Genci, Y. Nishiyama, and M. Nakamura. Three-dimensional inkjet biofabrication based on designed images. *Biofabrication*, 3:034113, 2011.

[8] J. Asai, H. Takenaka, M. Ii, M. Asahi, S. Kishimoto, N. Katoh, and D.W. Losordo. Topical application of ex vivo expanded endothelial progenitor cells promotes vascularisation and wound healing in diabetic mice. *Int Wound J*, pages doi: 10.1111/j.1742–481X.2012.01010.x., 2012.

[9] A. Atala, W. Kim, K. T. Paige, C. A. Vacanti, and A. B. Retik. Endoscopic treatment of vesicoureteral reflux with a chondrocyte-alginate suspension. *J Urol*, 152:641 – 643, 1994.

[10] A. Atala, D. Mooney, J. P. Vacanti, and Langer R., editors. *Tissue Engineering - Synthetic biodegradable polymer scaffolds*. Birkhäuser. ISBN 0-8176-3919-5.

[11] A. Athanassopoulos, G. Tsaknakis, S.E. Newey, A.L. Harris, J. Kean, M.P. Tyler, and S.M. Watt. Microvessel networks in pre-formed artificial clinical grade dermal substitutes *in vitro* using cells from haematopoietic tissues. *Burns*, 38:691 – 701, 2012.

[12] C. Auxenfans, C. Lequeux, E. Perrusel, A. Mojallal, B. Kinikoglu, and O. Damour. Adipose-derived stem cells (ASCs) as a source of endothelial cells in the reconstruction of endothelialized skin equivalents. *J Tissue Eng Regen Med*, 6:512 – 518, 2012.

[13] J. A. Barron, D. B. Krizman, and B. R. Ringeisen. Laser printing of single cells: statistical analysis, cell viability, and stress. *Ann Biomed Eng*, 33:121 – 130, 2005.

[14] J.A. Barron, P. Wu, H.D. Ladouceur, and B.R. Ringeisen. Biological laser printing: a novel technique for creating heterogeneous 3-dimensional cell patterns. *Biomed Microdevices*, 6:139 – 147, 2004.

[15] F. Bernerd, D. Asselineau, C. Vioux, O. Chevallier-Lagente, B. Bouadjar, A. Sarasin, and T. Magnaldo. Clues to epidermal cancer proneness revealed by reconstruction of DNA repair-deficient xeroderma pigmentosum skin *in vitro*. *Proc Natl Acad Sci U S A*, 98:7817 – 7822, 2001.

[16] S. Bessou, J.E. Surlève-Bazeille, E. Sorbier, and A. Taïeb. Ex vivo reconstruction of the epidermis with melanocytes and the influence of UVB. *Pigment Cell Res*, 8:241 – 249, 1995.

[17] A.F. Black, F. Berthod, N. L'heureux, L. Germain, and F.A. Auger. *In vitro* reconstruction of a human capillary-like network in a tissue-engineered skin equivalent. *FASEB J*, 12:1331 – 1340, 1998.

[18] T. Boland, V. Mironov, A. Gutowska, E.A. Roth, and R. R. Markwald. Cell and organ printing 2: fusion of cell aggregates in three-dimensional gels. *Anat Rec A Discov Mol Cell Evol Biol*, 272:497 – 502, 2003.

[19] U. Bommas-Ebert, P. Teubner, and R. Voß. *Kurzlehrbuch Anatomie und Embryologie, Kapitel 1.* Georg Thieme Verlag. 3. Auflage.

[20] P. Boorboor, P.M. Vogt, F.G. Bechara, Q. Alkandari, M. Aust, A. Gohritz, and M. Spies. Toxic epidermal necrolysis: Use of Biobrane® for skin coverage reduces pain, improves mobilisation and decreases infection in elderly patients. *Burns*, 34:487 – 492, 2008.

[21] C. Born, Z. Zhang, M. Al-Rubeai, and C.R. Thomas. Estimation of disruption of animal cells by laminar shear stress. *Biotechnol Bioeng*, 40:1004 – 1010, 1992.

[22] L. K. Branski, R. Mittermayr, D. N. Herndon, M. G. Jeschke, M. Hofmann, O. E. Masters, W. B. Norbury, D. L. Traber, S. Tangl, and H. Redl. Fibrin sealant improves graft adherence in a porcine full-thickness burn wound model. *Burns*, 37:1360 – 1366, 2011.

[23] Bundestag and Bundesrat. Arzneimittelgesetz (AMG), Gesetz über den Verkehr mit Arzneimitteln. http://www.gesetze-im-internet.de/bundesrecht/amg_1976/gesamt.pdf.

[24] Bundestag and Bundesrat. Gewebegesetz (GewebeG), Gesetz über Qualität und Sicherheit von menschlichen Geweben und Zellen. http://www.rechtliches.de/info_Gewebegesetz.html.

[25] Bundestag and Bundesrat. Transfusionsgesetz (TFG), Gesetz zur Regelung des Transfusionswesens. http://www.gesetze-im-internet.de/bundesrecht/tfg/gesamt.pdf.

[26] Bundestag and Bundesrat. Transplantationsgesetz (TPG), Gesetz über die Spende, Entnahme und Übertragung von Organen und Geweben. http://www.gesetze-im-internet.de/bundesrecht/tpg/gesamt.pdf.

[27] J.F. Burke, I.V. Yannas, W.C. Quinby, C.C. Bondoc, and W.K. Jung. Successful use of a physiologically acceptable artificial skin in the treatment of extensive burn injury. *Ann Surg*, 194:413 – 428, 1981.

[28] S. Catros, J.C. Fricain, B. Guillotin, B. Pippenger, R. Bareille, M. Remy, E. Lebraud, B. Desbat, J. Amédée, and Guillemot F. Laser-assisted bioprinting for creating on-demand patterns of human osteoprogenitor cells and nano-hydroxyapatite. *Biofabrication*, 3:Epub 2011 Apr 28, 2011.

[29] B.K. Chan, C.C. Wippich, C.J. Wu, P.M. Sivasankar, and G. Schmidt. Robust and semi-interpenetrating hydrogels from poly(ethylene glycol) and collagen for elastomeric tissue scaffolds. *Macromol Biosci*, 12:1490 – 1501, 2012.

[30] C.C. Chang, E.D. Boland, S.K. Williams, and J.B. Hoying. Direct-write bioprinting three-dimensional biohybrid systems for future regenerative therapies. *J Biomed Mater Res B Appl Biomater*, 98:160 – 170, 2011.

[31] R. Chang, J. Nam, and W. Sun. Effects of dispensing pressure and nozzle diameter on cell survival from solid freeform fabrication-based direct cell writing. *Tissue Eng Part A*, 14:41 – 48, 2008.

[32] C.A. Charles, C.A. Ricotti, S.C. Davis, P.M. Mertz, and R.S. Kirsner. Use of tissue-engineered skin to study *in vitro* biofilm development. *Dermatol Surg*, 35:1334 – 1341, 2009.

[33] M. Colina, P. Serra, J.M. Fernández-Pradas, L. Sevilla, and J.L. Morenza. DNA deposition through laser induced forward transfer. *Biosens Bioelectron*, 20:1638 – 1642, 2005.

[34] X. Cui, K. Breitenkamp, M.G. Finn, M. Lotz, and D.D. D'Lima. Direct human cartilage repair using three-dimensional bioprinting technology. *Tissue Eng Part A*, 18:1304 – 1312, 2012.

[35] B.G. Cuiffo and A.E. Karnoub. Mesenchymal stem cells in tumor development: emerging roles and concepts. *Cell Adh Migr*, 6:220 – 230, 2012.

[36] O. Damour, C. Augustin, and A.F. Black. Applications of reconstructed skin models in pharmaco-toxicological trials. *Med Biol Eng Comput*, 36:825 – 832, 1998.

[37] S. Danner, M. Kremer, A.E. Petschnik, S. Nagel, Z. Zhang, U. Hopfner, A.K. Reckhenrich, C. Weber, T.L. Schenck, T. Becker, C. Kruse, H.G. Machens, and J.T. Egaña. The use of human sweat gland-derived stem cells for enhancing vascularization during dermal regeneration. *J Invest Dermatol*, 132:1707 – 1716, 2012.

[38] S.K. Dekker, R. van Doorn, J. Kempenaar, N.A. Gruis, B.J. Vermeer, and M. Ponec. Skin equivalent: an attractive model to evaluate early melanoma metastasis. *Melanoma Res*, 10:127 – 140, 2000.

[39] Leitfaden der Guten Herstellungspraxis Teil 1. Anlage 2 zur Bekanntmachung des Bundesministeriums für Gesundheit zu § 2 Nr. 3 der Arzneimittel- und Wirkstoffherstellungsverordnung vom 27. Oktober 2006 (Banz. S. 6887). Bundesministerium für Gesundheit, http://www.bmg.bund.de.

[40] F. Djouad, P. Plence, C. Bony, P. Tropel, F. Apparailly, J. Sany, D. Noël, and C. Jorgensen. Immunosuppressive effect of mesenchymal stem cells favors tumor growth in allogeneic animals. *Blood*, 102:3837 – 3844, 2003.

[41] A. Doğan, M. E. Yalvaç, F. Şahin, A. V. Kabanov, A. Palotás, and A. A. Rizvanov. Differentiation of human stem cells is promoted by amphiphilic pluronic block copolymers. *Int J Nanomedicine*, 7:4849 – 4860, 2012.

[42] J. Drukała, L. Bandura, K. Cieślik, and W. Korohoda. Locomotion of human skin keratinocytes on polystyrene, fibrin, and collagen substrata and its modification by cell-to-cell contacts. *Cell Transplant*, 10:765 – 771, 2001.

[43] J. C. Dumville, S. O'Meara, S. Deshpande, and K. Speak. Alginate dressings for healing diabetic foot ulcers. *Cochrane Database Syst Rev*, page 2:CD009110, 2012.

[44] R. L. Eckert, M. T. Sturniolo, A.-M. Broome, M. Ruse, and E. A. Rorke. Transglutaminase function in epidermis. *J Invest Dermatol*, 124:481 – 492, 2005.

[45] A. El Ghalbzouri, P. Hensbergen, S. Gibbs, J. Kempenaar, R. van der Schors, and M. Ponec. Fibroblasts facilitate re-epithelialization in wounded human skin equivalents. *Lab Invest*, 84:102 – 112, 2004.

[46] Committee for Advanced Therapies European Medicines Agency. Reflection paper on stem cell-based medicinal products. http://www.ema.europa.eu/docs/en_GB/document_library/Scientific_guideline/2011/02/WC500101692.pdf.

[47] V. Falanga. Stem cells in tissue repair and regeneration. *J Invest Dermatol*, 132:1538 – 1541, 2012.

[48] N. E. Fedorovich, J. Alblas, J. R. de Wijn, W. E. Hennink, A. J. Verbout, and W. J. Dhert. Hydrogels as extracellular matrices for skeletal tissue engineering: state-of-the-art and novel application in organ printing. *Tissue Eng*, 13:1905 – 1925, 2007.

[49] A. Ferretti, E. Boschi, S. Stefani, A. Spiga, M. Romanelli, M. Lemmi, A. Giovannetti, B. Longoni, and F. Mosca. Angiogenesis and nerve regeneration in a model of human skin equivalent transplant. *Life Sci*, 73:1985 – 1994, 2003.

[50] Organisation for Economic Co-operation and Development (OECD). OECD guideline for the testing of chemicals, Skin sensitization: Local lymph node assay. http://iccvam.niehs.nih.gov/SuppDocs/FedDocs/OECD/OECD-TG429-2010.pdf.

[51] J. Fransson. Tumour necrosis factor-alpha does not influence proliferation and differentiation of healthy and psoriatic keratinocytes in a skin-equivalent model. *Acta Derm Venereol*, 80:416 – 420, 2000.

[52] S. Fu, P. Ni, B. Wang, B. Chu, J. Peng, L. Zheng, X. Zhao, F. Luo, Y. Wei, and Z. Qian. In vivo biocompatibility and osteogenesis of electrospun poly(ε-caprolactone)-poly(ethylene glycol)-poly(ε-caprolactone)/nano-hydroxyapatite composite scaffold. *Biomaterials*, 33:8363 – 8371, 2012.

[53] R. Gaebel, N. Ma, J. Liu, J. Guan, L. Koch, C. Klopsch, M. Gruene, A. Toelk, W. Wang, P. Mark, F. Wang, B. Chichkov, W. Li, and G. Steinhoff. Patterning human stem cells and endothelial cells with laser printing for cardiac regeneration. *Biomaterials*, 32:9218 – 9230, 2011.

[54] T. C. Gamboa-Martínez, D. M. García Cruz, C. Carda, J. L. Ribelles, and G. G. Ferrer. Fibrin-chitosan composite substrate for in vitro culture of chondrocytes. *J Biomed Mater Res A*, page [Epub ahead of print] doi: 10.1002/jbm.a.34330, 2012.

[55] D.J. Geer and S.T. Andreadis. A novel role of fibrin in epidermal healing: plasminogen-mediated migration and selective detachment of differentiated keratinocytes. *J Invest Dermatol*, 121:1210 – 1216, 2003.

[56] S. Gibbs. *In vitro* irritation models and immune reactions. *Skin Pharmacol Physiol*, 22:103 – 113, 2000.

[57] P.A. Golinski, N. Zöller, S. Kippenberger, H. Menke, J. Bereiter-Hahn, and A. Bernd. Development of an engraftable skin equivalent based on Matriderm® with human keratinocytes and fibroblasts. *Handchir Mikrochir Plast Chir*, 41:327 – 332, 2009.

[58] M. Gruene, A. Deiwick, L. Koch, S. Schlie, C. Unger, N. Hofmann, I. Bernemann, B. Glasmacher, and B. Chichkov. Laser printing of stem cells for biofabrication of scaffold-free autologous grafts. *Tissue Eng Part C Methods*, 17:79 – 87, 2011.

[59] M. Gruene, M. Pflaum, A. Deiwick, L. Koch, S. Schlie, C. Unger, M. Wilhelmi, A. Haverich, and B.N. Chichkov. Adipogenic differentiation of laser-printed 3D tissue grafts consisting of human adipose-derived stem cells. *Biofabrication*, 3:015005, 2011.

[60] M. Gruene, M. Pflaum, C. Hess, S. Diamantouros, S. Schlie, A. Deiwick, L. Koch, M. Wilhelmi, S. Jockenhoevel, A. Haverich, and B. Chichkov. Laser printing of three-dimensional multicellular arrays for studies of cell-cell and cell-environment interactions. *Tissue Eng Part C Methods*, 17:973 – 982, 2011.

[61] M. Gruene, C. Unger, L. Koch, A. Deiwick, and B. Chichkov. Dispensing pico to nanolitre of a natural hydrogel by laser-assisted bioprinting. *Biomed Eng Online*, 10:19, 2011.

[62] B. Guillotin, A. Souquet, S. Catros, M. Duocastella, B. Pippenger, S. Bellance, R. Bareille, M. Rémy, L. Bordenave, J. Amédée, and F. Guillemot. Laser assisted bioprinting of engineered tissue with high cell density and microscale organization. *Biomaterials*, 31:7250 – 7256, 2010.

[63] S. Hamada and T. Shimosegawa. *Pancreatic cancer and tumor microenvironment, Chapter 6: Pancreatic cancer stem cell and mesenchymal stem cell*. Transworld Research Network, 2012.

[64] B. Hartmann, A. Ekkernkamp, C. Johnen, J. C. Gerlach, C. Belfekroun, and M. V. Kuntscher. Sprayed cultured epithelial autografts for deep dermal burns of the face and neck. *Ann Plast Surg*, 58:70 – 73, 2007.

[65] W. Haslik, L.P. Kamolz, F. Manna, M. Hladik, T. Rath, and M. Frey. Manangement of full-thickness skin defects in the hand and wrist region: first long-term experiences with the dermal matrix Matriderm®. *J Plast Reconstr Aesthet Surg*, 63:360 – 364, 2010.

[66] S.J. Hedley, C. Layton, M. Heaton, K.H. Chakrabarty, R.A. Dawson, D.J. Gawkrodger, and S. MacNeil. Fibroblasts play a regulatory role in the control of pigmentation in reconstructed human skin from skin types I and II. *Pigment Cell Res*, 15:49 – 56, 2002.

[67] D.M. Heimbach, G.D. Warden, A. Luterman, M.H. Jordan, N. Ozobia, C.M. Ryan, D.W. Voigt, W.L. Hickerson, J.R. Saffle, F.A. DeClement, R.L. Sheridan, and A.R. Dimick. Multicenter postapproval clinical trial of Integra® dermal regeneration template for burn treatment. *J Burn Care Rehabil*, 24:42 – 48, 2003.

[68] S.W. Hendrix, J.V. Rogers, and B.E. Hull. Differential response of basal keratinocytes in a human skin equivalent to ultraviolet irradiation. *Arch Dermatol Res*, 290:420 – 424, 1998.

[69] D. Herndon, editor. *Total Burn Care*. W.B. Saunders, 2002. Second Edition.

[70] L. Highton, C. Wallace, and M. Shah. Use of suprathel® for partial thickness burns in children. *Burns*, 39:136 – 141, 2013.

[71] B. Hopp, T. Smausz, N. Kresz, N. Barna, Z. Bor, L. Kolozsvári, D.B. Chrisey, A. Szabó, and A. Nógrádi. Survival and proliferative ability of various living cell types after laser-induced forward transfer. *Tissue Eng*, 11:1817 – 1823, 2005.

[72] E. Houben, K. De Paepe, and V. Rogiers. A keratinocyte's course of life. *Skin Pharmacol Physiol*, 20:122 – 132, 2007.

[73] J. W. Huang, W. J. Chen, S. K. Lioa, C. Y. Yang, S. S. Lin, and C. C. Wu. Osteoblastic differentiation of rabbit mesenchymal stem cells loaded in a carrier system of Pluronic F127 and Interpore. *Chang Gung Med J*, 29:363 – 372, 2006.

[74] S. Iyama, T. Sato, K. Murase, S. Kikuchi, Y. Kamihara, K. Ono, K. Takada, K. Miyanishi, Y. Sato, R. Takimoto, M. Kobune, T. Obama, M. Miyajima, A. Watanabe, T. Higami, Y. Hirayama, and J. Kato. Successful treatment by fibrin glue sealant for pneumothorax with chronic GVHD resistant to autologous blood patch pleurodesis. *Intern Med*, 51:2011 – 2014, 2012.

[75] K. Jakab, C. Norotte, F. Marga, K. Murphy, G. Vunjak-Novakovic, and G. Forgacs. Tissue engineering by self-assembly and bio-printing of living cells. *Biofabrication*, 2:022001, 2010.

[76] A. Joly, J. F. Desjardins, B. Fremond, M. Desille, J. P. Campion, Y. Malledant, Y. Lebreton, G. Semana, F. Edwards-Levy, M. C. Levy, and B. Clement. Survival, proliferation, and functions of porcine hepatocytes encapsulated in coated alginate beads: a step toward a reliable bioartificial liver. *Transplantation*, 63:795 – 803, 1997.

[77] S. H. Kamil, R. D. Eavey, M. P. Vacanti, C. A. Vacanti, and C. J. Hartnick. Tissue-engineered cartilage as a graft source for laryngotracheal reconstruction. *Arch Otolaryngol Head Neck Surg*, 130:1048 – 1051, 2004.

[78] T. Kataoka, M. Umeda, T. Shigeta, H. Takahashi, and T. Komori. A new in vitro model of cancer invasion using AlloDerm®, a human cadaveric dermal equivalent: a preliminary report. *Kobe J Med Sci*, 55:E106 – 115, 2010.

[79] K. Kehe, M. Abend, K. Kehe, R. Ridi, R. U. Peter, and D. van Beuningen. Tissue engineering with HaCaT cells and a fibroblast cell line. *Arch Dermatol Res*, 291:600 – 605, 1999.

[80] S.W. Kim, H.Z. Zhang, L. Guo, J.M. Kim, and M.H. Kim. Amniotic mesenchymal stem cells enhance wound healing in diabetic NOD/SCID mice through high angiogenic and engraftment capabilities. *PLoS One*, 7:e41105, 2012.

[81] L. Koch, A. Deiwick, S. Schlie, S. Michael, M. Gruene, V. Coger, D. Zychlinski, A. Schambach, K. Reimers, P.M. Vogt, and B. Chichkov. Skin tissue generation by laser cell printing. *Biotechnol Bioeng*, 109:1855 – 1863, 2012.

[82] L. Koch, S. Kuhn, H. Sorg, M. Gruene, S. Schlie, R. Gaebel, B. Polchow, K. Reimers, S. Stoelting, N. Ma, P.M. Vogt, G. Steinhoff, and B. Chichkov. Laser printing of skin cells and human stem cells. *Tissue Eng Part C Methods*, 16:847 – 854, 2010.

[83] N.V. Konstantinova, N.A. Lemak, and M. Duvic. Nerve growth factor in normal and psoriatic skin equivalent models. *Arch Dermatol Res*, 290:610 – 614, 1998.

[84] M.I. Koster. Making an epidermis. *Ann N Y Acad Sci*, 1170:7-10, 2009.

[85] S. Kuhn, C. Radtke, C. Allmeling, P.M. Vogt, and K. Reimers. *Skin Biopsy - Perspectives, Chapter 13: Keratinocyte Culture Techniques in Medical and Scientific Applications*. InTech, November 2011. ISBN 978-953-307-290-6.

[86] S. Lal, R.E. Barrow, S.E. Wolf, D.L. Chinkes, D.W. Hart, J.P. Heggers, and D.N. Herndon. Biobrane® improves wound healing in burned children without increased risk of infection. *Shock*, 14:314 – 319, 2000.

[87] K.Y. Lee and D.J. Mooney. Hydrogels for Tissue Engineering. *Chem Rev*, 101:1869 – 1879, 2001.

[88] S.H. Lee, S.Y. Jin, J.S. Song, K.K. Seo, and K.H. Cho. Paracrine effects of adipose-derived stem cells on keratinocytes and dermal fibroblasts. *Ann Dermatol*, 24:136 – 143, 2012.

[89] S.S. Lee, B.J. Huang, S.R. Kaltz, S. Sur, C.J. Newcomb, S.R. Stock, R.N. Shah, and S.I. Stupp. Bone regeneration with low dose BMP-2 amplified by biomemetic supramolecular nanofibers within collagne scaffolds. *Biomaterials*, 34:452 – 459, 2013.

[90] H. Li, Y. Chu, Z. Zhang, G. Zhang, L. Jiang, H. Wu, S. Liu, C. Yu, and Y. Jin. Construction of bilayered tissue-engineered skin with human amniotic mesenchymal cells and human amniotic epithelial cells. *Artif Organs*, doi: 10.1111/j.1525-1594.2012.01461.x. [Epub ahead of print], 2012.

[91] F. Liu, X.S. Luo, H.Y. Shen, J.S. Dong, and J. Yang. Using human hair follicle-derived keratinocytes and melanocytes for constructing pigmented tissue-engineered skin. *Skin Res Technol*, doi: 10.1111/j.1600-0846.2011.00510.x., 2011.

[92] J. Liu, H. H. Xu, H. Zhou, M. D. Weir, Q. Chen, and C. A. Trotman. Human umbilical cord stem cell encapsulation in novel macroporous and injectable fibrin for muscle tissue engineering. *Acta Biomater*, page [Epub ahead of print], 2012.

[93] J. Liu, Y. Zhang, L. Bai, X. Cui, and J. Zhu. Rat bone marrow mesenchymal stem cells undergo malignant transformation via indirect co-cultured with tumour cells. *Cell Biochem Funct*, page doi: 10.1002/cbf.2844., 2012.

[94] J. Liu, H. Zhou, M. D. Weir, H. H. Xu, Q. Chen, and C. A. Trotman. Fast-degradable microbeads encapusulating human umbilical cord stem cells in alginate for muscle tissue engineering. *Tissue Eng Part A*, page Epub ahead of print], 2012.

[95] P. Liu, Z. Deng, S. Han, T. Liu, N. Wen, W. Lu, X. Geng, S. Huang, and Y. Jin. Tissue-engineered skin containing mesenchymal stem cells improves burn wounds. *Artif Organs*, 32:925 – 931, 2008.

[96] X. Liu, M.N. Rahaman, and Q. Fu. Bone regeneration in strong porous bioactive glass (13-93) scaffolds with an oriented microstructure implanted in rat calvarial defects. *Acta Biomater*, 9:4889 – 4898, 2013.

[97] M. Macfarlane, P. Jones, C. Goebel, E. Dufour, J. Rowland, D. Araki, M. Costabel-Farkas, N.J. Hewitt, J. Hibatallah, A. Kirst, P. McNamee, F. Schellauf, and J. Scheel. A tiered approach to the use of alternatives to animal testing for the safety assessment of cosmetics: skin irritation. *Regul Toxicol Pharmacol*, 54:188 – 196, 2009.

[98] A. Margariti, B. Winkler, E. Karamariti, A. Zampetaki, T.N. Tsai, D. Baban, J. Ragoussis, Y. Huang, J.D. Han, L. Zeng, Y. Hu, and Q. Xu. Direct reprogramming of fibroblasts into endothelial cells capable of angiogenesis and reendothelialization in tissue-engineered vessels. *Proc Natl Acad Sci U S A*, 109:13793 – 13798, 2012.

[99] European Medicines Agency. Advanced Therapies. http://ec.europa.eu/health/human-use/advanced-therapies/index_en.htm.

[100] M. Mehdizadeh, H. Weng, D. Gyawali, L. Tang, and J. Yang. Injectable citrate-based mussel-inspired tissue bioadhesives with high wet strength for sutureless wound closure. *Biomaterials*, 33:7972 – 7983, 2012.

[101] H. Mertsching, M. Weimer, S. Kersen, and H. Brunner. Human skin equivalent as an alternative to animal testing. *GMS Krankenhhyg Interdiszip*, 3, 2008. ISSN 1863-5245.

[102] A.D. Metcalfe and M.W. Ferguson. Skin stem and progenitor cells: using regeneration as a tissue-engineering strategy. *Cell Mol Life Sci*, 65:24 – 32, 2008.

[103] S. Michael, H. Sorg, C. T. Peck, L. Koch, A. Deiwick, B. Chichkov, P. M. Vogt, and K. Rimers. Tissue engineered skin substitutes created by laser-assisted bioprinting form skin-like structures in the dorsal skin fold chamber in mice. *PLOS ONE*, 8:e57741, 2013.

[104] S. Michael, H. Sorg, C.T. Peck, K. Reimers, and P.M. Vogt. The mouse dorsal skin fold chamber as a means for the analysis of tissue engineered skin. *Burns*, 39:82 – 88, 2013.

[105] P. J. Mishra, P. J. Mishra, R. Humeniuk, D. J. Medina, G. Alexe, J. P. Mesirov, S. Ganesan, J. W. Glod, and D. Banerjee. Carcinoma-associated fibroblast-like differentiation of human mesenchymal stem cells. *Cancer Res*, 68:4331 – 4339, 2008.

[106] R. Mądry, J. Strużyna, A. Stachura-Kułach, Ł Drozdz, and M. Bugaj. Effectiveness of suprathel® application in partial-thickness burns, frostbites and lyell syndrome treatment. *Pol Przegl Chir*, 83:541 – 548, 2011.

[107] I. Moll, editor. *Duale Reihe Dermatologie, Kapitel 1.* Georg Thieme Verlag, 2010. 7. Auflage.

[108] W. E. G. Mueller. Molecular phylogeny of metazoa (animals): monophyletic origin. *Naturwissenschaften*, 82:321 – 329, 1995.

[109] W. E. G. Mueller. Therapeutic potential of bone marrow-derived mesenchymal stem cells for cutaneous wound healing. *Front Immunol*, 3:192, 2012.

[110] T. Nagakura, H. Hirata, M. Tsujii, T. Sugimoto, K. Miyamoto, T. Horiuchi, M. Nagao, T. Nakashima, and A. Uchida. Effect of viscous injectable pure alginate sol on cultured fibroblasts. *Plast Reconstr Surg*, 116:831 – 838, 2005.

[111] Y. Nahmias, R. E. Schwartz, C. M. Verfaillie, and D. J. Odde. Laser-guided direct writing for three-dimensional tissue engineering. *Biotechnol Bioeng*, 92:129 – 136, 2005.

[112] M. Nakamura, S. Iwanaga, C. Henmi, K. Arai, and Y. Nishiyama. Biomatrices and biomaterials for future developments of bioprinting and biofabrication. *Biofabrication*, 2:014110, 2010.

[113] M. Nakamura, A. Kobayashi, F. Takagi, A. Watanabe, Y. Hiruma, K. Ohuchi, Y. Iwasaki, M. Horie, I. Morita, and S. Takatani. Biocompatible inkjet printing technique for designed seeding of individual living cells. *Tissue Eng*, 11:1658 – 1666, 2005.

[114] N. A. Nallamuthu, M. Braden, and M. P. Patel. Some aspects of the formulation of alginate dental impression materials - setting characteristics and mechanical properties. *Dent Mater*, 28:756 – 762, 2012.

[115] S. Natesan, D. O. Zamora, L. J. Suggs, and R. J. Christy. Engineering a bilayered hydrogel to control ASC differentiation. *J Vis Exp*, 63:e3953:doi: 10.3791/3953, 2012.

[116] D. Nelson and R.J. Gay. Effects of UV irradiation on a living skin equivalent. *Photochem Photobiol*, 57:830 –837, 1993.

[117] R. M. Nhari, A. Ismail, and Y. B. Che Man. Sutureless fixation with fibrin glue of lightweight mesh in open inguinal hernia repair: Effect on postoperative pain: A double-blind, randomized trial versus standard heavyweight mesh. *Surgery*, page [Epub ahead of print], 2012.

[118] G. D. Nicodemus and S. J. Bryant. Cell encapsulation in biodegradable hydrogels for tissue engineering applications. *Tissue Eng Part B*, 14:149 – 165, 2008.

[119] Y. Nishiyama, M. Nakamura, C. Henmi, K. Yamaguchi, S. Mochizuki, H. Nakagawa, and K. Takiura. Development of a three-dimensional bioprinter: construction of cell supporting structures using hydrogel and state-of-the-art inkjet technology. *J Biomech Eng*, 131:035001, 2009.

[120] C. Norotte, F.S. Marga, L.E. Niklason, and G. Forgacs. Scaffold-free vascular tissue engineering using bioprinting. *Biomaterials*, 30:5910 – 5917, 2009.

[121] The Commission of the European Communities. Commision Directive 2003/94/EC. http://eur-lex.europa.eu/.

[122] M. Okazaki, Y. Suzuki, K. Yoshimura, and K. Harii. Construction of pigmented skin equivalent and its application to the study of congenital disorders of pigmentation. *Scand J Plast Reconstr Surg Hand Surg*, 39:339 – 343, 2005.

[123] C. N. Okeke, R. Tsuboi, and H. Ogawa. Quantification of Candida albicans actin mRNA by the LightCycler system as a means of assessing viability in a model of cutaneous candidiasis. *J Clin Microbiol*, 39:3491 – 3494, 2001.

[124] R. Osborne and M.A. Perkins. An approach for development of alternative test methods based on mechanisms of skin irritation. *Food Chem Toxicol*, 32:133 – 142, 1994.

[125] C.M. Othon, X. Wu, J.J. Anders, and B.R. Ringeisen. Single-cell printing to form three-dimensional lines of olfactory ensheathing cells. *Biomed Mater*, 3:034101, 2008.

[126] A. Ovsianikov, M. Gruene, M. Pflaum, L. Koch, F. Maiorana, M. Wilhelmi, A. Haverich, and B. Chichkov. Laser printing of cells into 3D scaffolds. *Biofabrication*, 2:014104, 2010.

[127] A.B. Owczarczak, S.O. Shuford, S.T. Wood, S. Deitch, and D. Dean. Creating transient cell membrane pores using a standard inkjet printer. *J Vis Exp*, 16:pii 3681, 2012.

[128] N. Pallua and S. von Bülow. Methods of burn treatment. Part II: Technical aspects - Behandlungskonzepte bei Verbrennungen. *Chirurg*, 77:179 – 186, 2006.

[129] D. Pankajakshan, V. Kansal, and D.K. Agrawal. *In vitro* differentiation of bone marrow derived porcine mesenchymal stem cells to endothelial cells. *J Tissue Eng Regen Med*, doi: 10.1002/term.1483. [Epub ahead of print], 2012.

[130] The European Parliament and the Council. Regulation 2004/23/EC. http://eur-lex.europa.eu/.

[131] The European Parliament and the Council. Regulation 2006/17/EC. http://eur-lex.europa.eu/.

[132] The European Parliament and the Council. Regulation 2006/86/EC. http://eur-lex.europa.eu/.

[133] The European Parliament and the Council. Regulation (EC) No 1394/2007. http://eur-lex.europa.eu/.

[134] The European Parliament and the Council. Regulation (EC) No 726/2004. http://eur-lex.europa.eu/.

[135] M.E. Pepper, V. Seshadri, T. Burg, B.W. Booth, K.J. Burg, and R.E. Groff. Cell settling effects on a thermal inkjet bioprinter. *Conf Proc IEEE Eng Med Biol Soc*, pages 3609 – 3612, 2011.

[136] J. Pérez-Guisado, K. L. Gaston, J. R. Benítez-Goma, E. Cabrera-Sánchez, F. T. Fidalgo-Rodríguez, L. F. Rioja, and S. J. Thomas. Smoking and diabetes mellitus type 2 reduce skin graft take; the use of fibrin glue might restore graft take to optimal levels. *Eur J Dermato*, 21:895 – 898, 2011.

[137] M. Ponec, E. Boelsma, S. Gibbs, and M. Mommaas. Characterization of reconstructed skin models. *Skin Pharmacol Appl Skin Physiol*, 15 Suppl 1:4 – 17, 2002.

[138] E. Proksch, J.M. Brandner, and J.M. Jensen. The skin: an indispensable barrier. *Exp Dermatol*, 17:1063 – 1072, 2008.

[139] C. Rasmussen, K. Gratz, F. Liebel, M. Southall, M. Garay, S. Bhattacharyya, N. Simon, M. Vander Zanden, K. Van Winkle, J. Pirnstill, S. Pirnstill, A. Comer, and B.L. Allen-Hoffmann. The StrataTest® human skin model, a consistent in vitro alternative for toxicological testing. *Toxicology In Vitro*, 24:2020 – 2029, 2010.

[140] B.R. Ringeisen, H. Kim, J.A. Barron, D.B. Krizman, D.B. Chrisey, S. Jackman, R.Y. Auyeung, and B.J. Spargo. Laser printing of pluripotent embryonal carcinoma cells. *Tissue Eng*, 10:483 – 491, 2004.

[141] B.R. Ringeisen, H. Kim, H.D. Young, B.J. Spargo, R.C.Y. Auyeung, and P.K. Wu. Cell-by-cell construction of living tissue. *MRS Proceedings*, 698:doi:10.1557/PROC–698–Q5.1.1, 2001.

[142] N.C. Rivron, C.C. Raiss, J. Liu, A. Nandakumar, C. Sticht, N. Gretz, R. Truckenmüller, and C.A. Rouwkema, J.and van Blitterswijk. Sonic hedgehog-activated engineered blood vessels enhance bone tissue formation. *Proc Natl Acd Sci USA*, 109:4413 – 4418, 2012.

[143] J.A. Rowley, G. Madlambayan, and D.J. Mooney. Alginate hydrogels as synthetic extracellular matrix materials. *Biomaterials*, 20:45 – 53, 1999.

[144] H. Ryssel, E. Gazyakan, G. Germann, and M. Ohlbauer. The use of Matriderm® in early excision and simultaneous autologous skin grafting in burns - A pilot study. *Burns*, 34:93 – 97, 2008.

[145] M. Schaller, R. Mailhammer, and H.C. Korting. Cytokine expression induced by Candida albicans in a model of cutaneous candidosis based on reconstituted human epidermis. *J Med Microbiol*, 51:672 – 676, 2002.

[146] J.S. Schechner, S.K. Crane, F. Wang, A.M. Szeglin, G. Tellides, M.I. Lorber, A.L. Bothwell, and J.S. Pober. Engraftment of a vascularised human skin equivalent. *FASEB J*, 17:2250 – 2256, 2003.

[147] J. Schneider, T. Biedermann, D. Widmer, I. Montano, M. Meuli, E. Reichmann, and C. Schiestl. Matriderm® versus Integra®: A comparative experimental study. *Burns*, 35:51 – 57, 2009.

[148] V.M. Schoop, N. Mirancea, and N.E. Fusenig. Epidermal organization and differentiation of HaCaT keratinocytes in organotypic coculture with human dermal fibroblasts. *J Invest Dermatol*, 112:343 – 353, 1999.

[149] H. Schwarze, M. Küntscher, C. Uhlig, H. Hierlemann, L. Prantl, C. Ottomann, and B. Hartmann. Suprathel®, a new skin substitute, in the management of partial-thickness burn wounds: results of a clinical study. *Ann Plast Surg*, 60:181 – 185, 2008.

[150] L. Sheng, M. Yang, H. Li, Z. Du, Y. Yang, and Q. Li. Transplantation of adipose stromal cells promotes neovascularization of random skin flaps. *Tohoku J Exp Med*, 224:229 – 234, 2011.

[151] H. Shin, S. Jo, and A. G. Mikos. Biomimetic materials for tissue engineering. *Biomaterials*, 24:4353 – 4364, 2003.

[152] M.A. Shokrgozar, M. Fattahi, S. Bonakdar, I. Ragerdi Kashani, M. Majidi, N. Haghighipour, V. Bayati, H. Sanati, and S.N. Saeedi. Healing potential of mesenchymal stem cells cultured on a collagen-based scaffold for skin regeneration. *Iran Biomed J*, 16:68 – 76, 2012.

[153] T.G. Smijs and J.A. Bouwstra. Focus on skin as a possible port of entry for solid nanoparticles and the toxicological impact. *J Biomed Nanotechnol*, 6:469 – 484, 2010.

[154] W.D. Spotnitz. Efficacy and safety of fibrin sealant for tissue adherence in facial rhytidectomy. *Clin Cosmet Investig Dermatol*, 5:43 – 51, 2012.

[155] W. Sterry. *Kurzlehrbuch Dermatologie, Kapitel 1.* Georg Thieme Verlag.

[156] W. Sterry, W. Burgdorf, and R. Paus. *Checklisten der aktuellen Medizin - Checkliste Dermatologie, Venerologie, Allergologie, Phlebologie, Andrologie, Kapitel 1.* Georg Thieme Verlag, 2010. 6. Auflage.

[157] K. J. Sultzbaugh and T. J. Speaker. A method to attach lectins to the surface of spermine alginate microcapsules based on the avidin biotin interaction. *J Microencapsul*, 13:363 – 376, 1996.

[158] H. E. Thu, M. H. Zulfakar, and S. F. Ng. Alginate based bilayer hydrocolloid films as potential slow-release modern wound dressing. *Int J Pharm*, 434:375 – 383, 2012.

[159] C. Todd, S.D. Hewitt, J. Kempenaar, K. Noz, A.J. Thody, and M. Ponec. Co-culture of human melanocytes and keratinocytes in a skin equivalent model: effect of ultraviolet radiation. *Arch Dermatol Res*, 285:455 – 459, 1993.

[160] N. Trivedi, M. Keegan, G. M. Steil, J. Hollister-Lock, W. M. Hasenkamp, C. K. Colton, S. Bonner-Weir, and G. C. Weir. Islets in alginate macrobeads reverse diabetes despite minimal acute insulin secretory responses. *Transplantation*, 71:203 – 211, 2001.

[161] O. Tsur-Gang, E. Ruvinov, N. Landa, R. Holbova, M. S. Feinberg, J. Leor, and S. Cohen. The effects of peptide-based modification of alginate on left ventricular remodelling and function after myocardial infarction. *Biomaterials*, 30:189 – 195, 2009.

[162] H. Uludag, P. De Vos, and P. A. Tresco. Technology of mammalian cell encapsulation. *Adv Drug Deliv Rev*, 42:29 – 64, 2000.

[163] C. Unger, M. Gruene, L. Koch, J. Koch, and B.N. Chichkov. Time-resolved imaging of hydrogel printing via laser-induced forward transfer. *Appl Phys A*, 103:271 – 277, 2011.

[164] P.M. Vogt, A. Jokuszies, A. Niederbichler, Busch. K., C.Y. Choi, and S. Kall. Early surgical management of severe burns - Primäre chirurgische Therapie bei Verbrennungen. *Unfallchirurg*, 109:270 – 277, 2006.

[165] P.M. Vogt, P. Kolokythas, A. Niederbichler, K. Knobloch, K. Reimers, and C.Y. Choi. Innovative wound therapy and skin substitutes for burns - Innovative Wundtherapie und Hautersatz bei Verbrennungen. *Chirurg*, 78:335 – 342, 2007.

[166] Z. Y. J. Wang and I. J. Stern. Disposition in rats of a polyoxypropylene-polyoxyethylene copolymer used in plasma fractions. *Drug Metab Dispos*, 3:536 – 542, 1975.

[167] C. Weinand, I. Pomerantseva, C.M. Neville, R. Gupta, E. Weinberg, I. Madisch, F. Shapiro, H. Abukawa, M.J. Troulis, and J.P. Vacanti. Hydrogel-beta-TCP scaffolds and stem cells for tissue engineering bone. *Bone*, 38:555 – 563, 2006.

[168] H. Wendt, A. Hillmer, K. Reimers, J. W. Kuhbier, F. Schäfer-Nolte, C. Allmeling, C. Kasper, and P. M. Vogt. Artificial skin-culturing of different skin cell lines for generating an artificial skin substitute on cross-weaved spider silk fibres. *PLoS One*, 6:e21833, 2011.

[169] I.S. Whitaker, S. Worthington, S. Jivan, and A. Phipps. The use of Biobrane® by burn units in the United Kingdom: A national study. *Burns*, 33:1015 – 1020, 2007.

[170] W.C. Jr. Wilson and T. Boland. Cell and organ printing 1: protein and cell printers. *Anat Rec A Discov Mol Cell Evol Biol*, 272:491 – 496, 2003.

[171] T. Y. Wong, L. A. Preston, and N. L. Schiller. Alginate lyase: review of major sources and enzyme characteristics, structure-function analysis, biological roles, and applications. *Annu Rev Microbiol*, 54:289 – 340, 2000.

[172] Y. Xie, S.C. Rizzi, R. Dawson, E. Lynam, S. Richards, D.I. Leavesley, and Z. Upton. Development of a three-dimensional human skin equivalent wound model for investigating novel wound healing therapies. *Tissue Eng Part C Methods*, 16:1111 – 1123, 2010.

[173] T. Xu, J. Jin, C. Gregory, J. J. Hickman, and T. Boland. Inkjet printing of viable mammalian cells. *Biomaterials*, 26:93 – 99, 2005.

[174] H. Zhang, S. Dai, J. Bi, and K.K. Liu. Biomimetic three-dimensional microenvironment for controlling stem cell fate. *Interface Focus*, 1:792 – 803, 2011.

[175] S.M. Zhang and E.S. Loker. Representation of an immune responsive gene family encoding fibrinogen-related proteins in the freshwater mollusc Biomphalaria glabrata, an intermediate host for Schistosoma mansoni. *Gene*, 341:255 – 266, 2004.

[176] W. Zhang, J. Chen, J. Tao, Y. Jiang, C. Hu, L. Huang, J. Ji, and H. W. Ouyang. The use of type 1 collagen scaffold containing stromal cell-derived factor-1 to create a matrix environment conducive to partial-thickness cartilage defects repair. *Biomaterials*, 34:713 – 723, 2013.

[177] J.F. Zhao, Y.J. Zhang, J. Kubilus, X.H. Jin, R.M. Santella, M. Athar, Z.Y. Wang, and D.R. Bickers. Reconstituted 3-dimensional human skin as a novel in vitro model for studies of carcinogenesis. *Biochem Biophys Res Commun*, 254:49 – 53, 1999.

[178] Q. Zheng, J. Lu, H. Chen, L. Huang, J. Cai, and Z. Xu. Application of inkjet printing technique for biological material delivery and antimicrobial assays. *Anal Biochem*, 410:171 – 176, 2011.

[179] P. A. Zuk, M. Zhu, H. Mizuno, J. Huang, J. W. Futrell, A. J. Katz, P. Benhaim, H. P. Lorenz, and M. H. Hedrick. Multilineage cells from human adipose tissue: implications for cell-based therapies. *Tissue Eng*, 7:211 – 228, 2001.

Appendix A Supplementary pictures

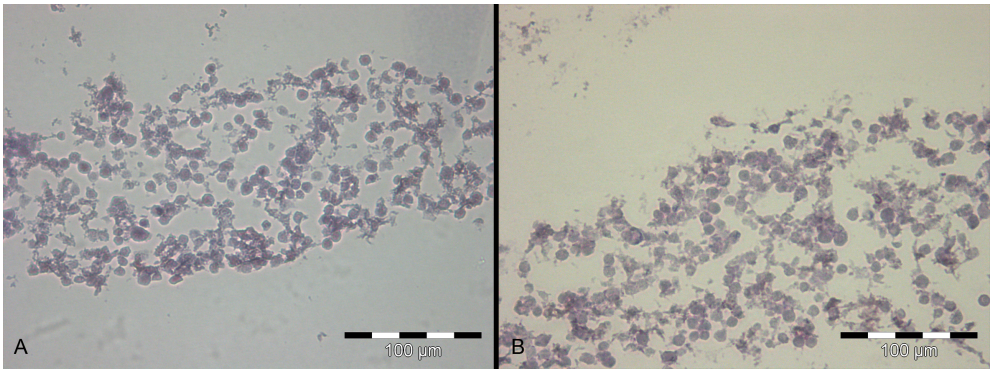

Figure A.1: HE staining of 3D printed skin cells in alginate after two weeks The figure shows a 3D printed skin construct cultured at the air-liquid-interface for two weeks. Keratinocytes were printed on top of fibroblasts, all of them embedded in alginate as a printing matrix. As can be seen, the cells neither stretched out nor formed a tissue. Nonetheless, nuclei and cell membranes indicated that the cells were alive.

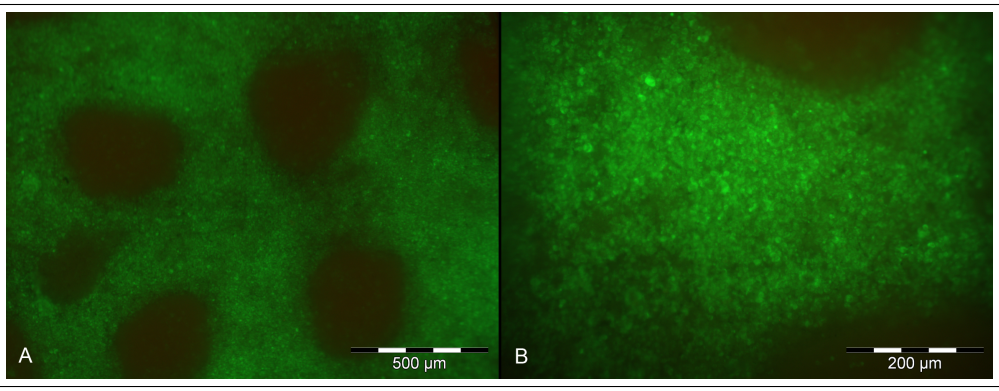

Figure A.2: LiveDead staining of 3D printed NIH3T3 The figure depicts 3D printed NIH3T3 (murine fibroblasts) using alginate as a matrix. (A) gives an overview, whereas (B) shows the details. The cells were incubated with calcein-AM and ethidium-homodimer-1, which mark living cells in green and dead cells in red. As can be seen, the majority of the cells lived after two weeks of submerged culturing. Note that the cells still exhibited a rounded shape and did not stretch out.

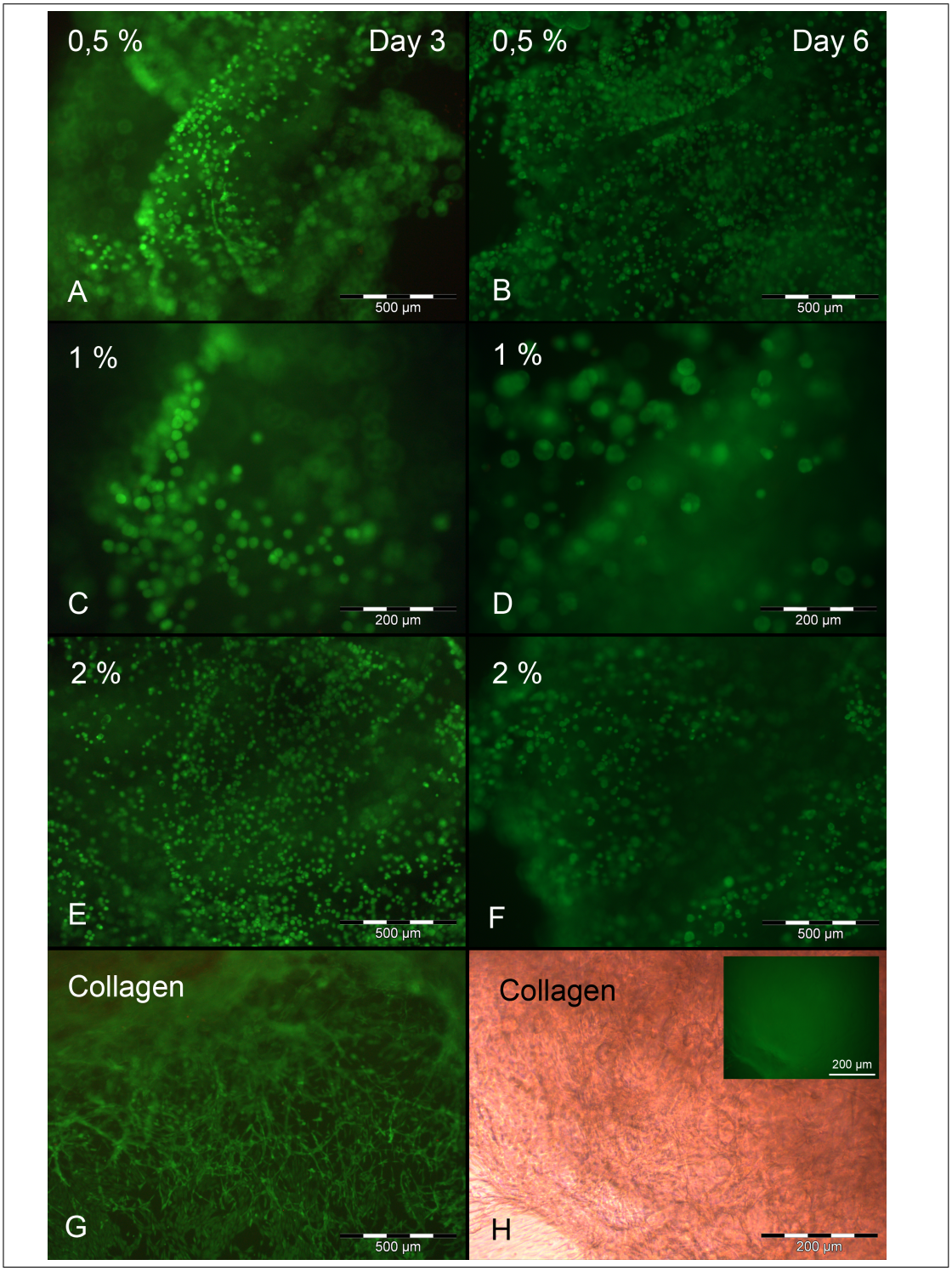

Figure A.3: Growth of fibroblasts in different concentrations of alginate gel To test the effect of alginate on the growth behaviour of fibroblasts, these were seeded into different concentrations of alginate gels and cultured under submerged conditions *in vitro*. In all concentrations of alginate gels the fibroblasts (NIH3T3) did not stretch out but stayed rounded, even up to 6 days (A - F). In corresponding controls, consisting of collagen gels, the fibroblasts already stretched out after 3 days, resulting in a thick clot of cells and gel after 6 days (G - H). The cells were stained with calcein-AM and ethidium-homodimer-1, indicating that most of the cells stayed alive (green = live, red = dead).

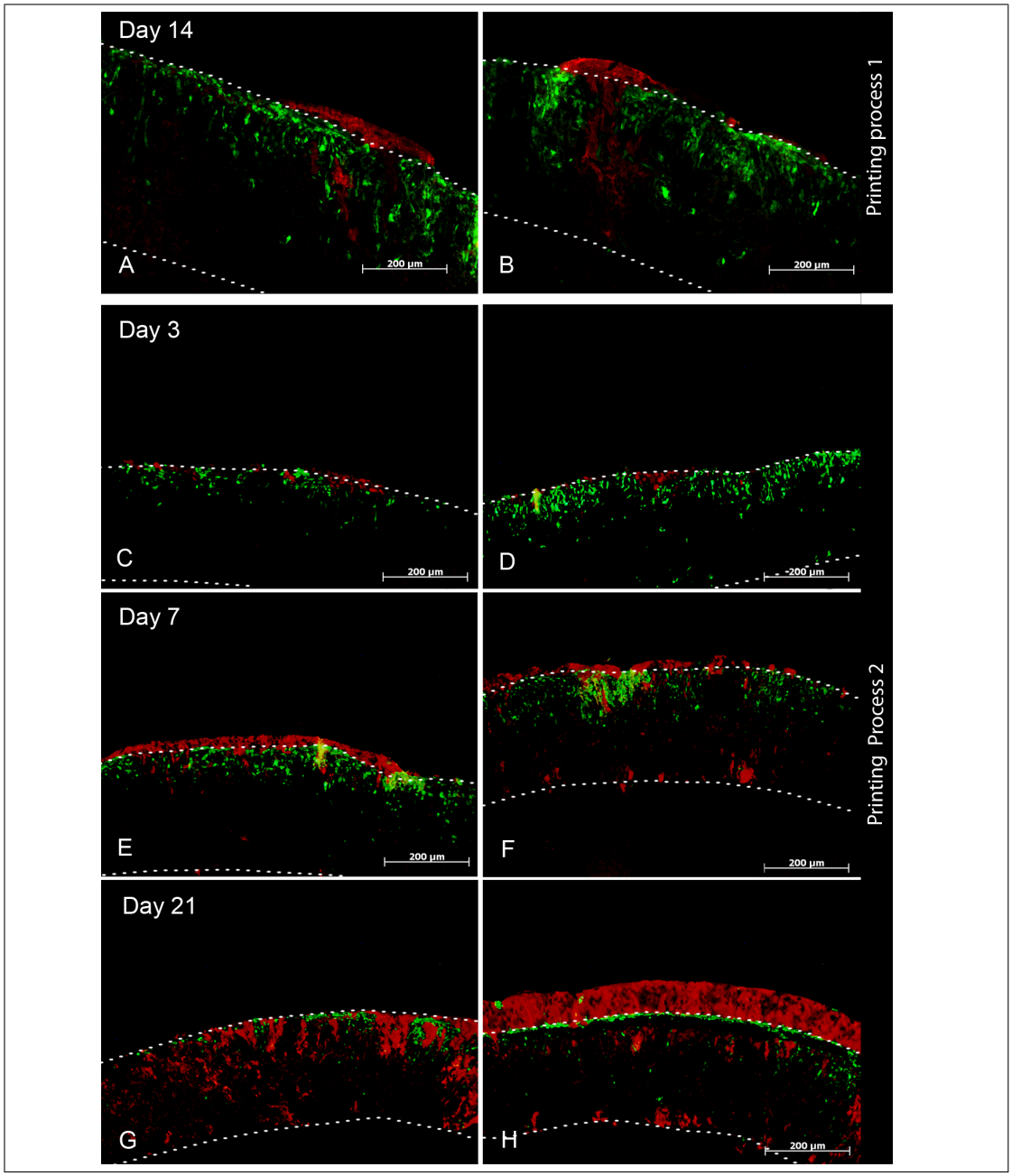

Figure A.4: Sections of printed skin cells with fibrin as a matrix Skin cells were printed in 3D with fibrin as a printing matrix and subsequently cultured *in vitro* at the air-liquid-interface for different periods of time. 20 layers of keratinocytes (HaCaT, red) were printed on top of 20 layers of fibroblasts (NIH3T3, green). Matriderm® serves as a stabilizing matrix underneath. Two different printing processes were carried out with three replicates for each investigated timepoint. Two typical pictures of each time point are shown. The white dotted lines depict the borders of the Matriderm®. (A) and (B) comprise the first printing process, which was ended after 14 days. The fibroblasts migrated into the Matriderm®. Also the keratinocytes migrated into the Matriderm®, forming mushroom-like structures. The second printing process (C - H) was carried out with the same parameters for reproducibility. After 3 days the keratinocytes could still be found on top of the fibroblasts, they started to migrate into the Matriderm® after 7 days. In some skin constructs they completely invaded the Matriderm® after 21 days (G) while in other replicates they formed a dense and thick tissue above the fibroblasts with only some keratinocytes migrating into the deeper layers (H). In this case, the fibroblasts formed a layer directly underneath the keratinocytes on top of the Matriderm® with only some of them migrating into deeper layers.

Appendix B Acknowledgement

In Hannover, at the canal bend,
I lived together with my boyfriend.

I started my PhD with much elation,
but got to feel a lot of frustration.

Why don't the cells grow as expected?
Why can't the LIFT work with our matrix?

But finally, my results were there,
and I didn't feel as much despair.

Publications were written, data were shown,
the dissertation shall be the crown.

So what was the issue?
To create tissue!

Also, new talents and skills I could gain,
liking to lecture and to explain.

Then, my boyfriend and I became married,
and our party was very merry.

For all your help and understanding,
I want to thank everybody by saying:

Thanks for support, encouragement and glee,
talking and listening and counselling me.

Giving advice for work or for life,
went without saying, helped me to thrive.

All my questions about techniques were replied,
as well as on help regarding computers I relied.

Now it is finished, this episode of life.
What will now follow? Can you guess right?

Whatever will happen, I know you are there,
I thank you profoundly for help and for care.

My family and friends

My husband Morris Michael
My sister Alexandra Gens
My parents Eva-Maria and Jürgen Kuhn

All my friends in the drumming course and the choir, especially

Katrin Oestern
Inken and Karsten Friese
Gudrun Schneidewind
Kerstin and Daniel Matern
Ilona Seibt
Marion Tiede and Irv Housinger
Horst Fritz
Angelika Habenicht

All my friends from other occasions, especially

Dietmar Riese
Stefan Meyerthole
Sabine Nies
Kathrin Lepke
Annika Kohlmann
Iris Stein

My supervisors and referees

Peter M. Vogt
Kerstin Reimers
Anaclet Ngezahayo
Ulrike Köhl

My labteam

Andrea Lazaridis
Sarah Strauß
Ulli Fuhrmann
Reinhild Schnabel
Angela Fülbier
Claas-Tido Peck
Birgit Weyand
Hanna Wendt
Heiko Sorg
Jörn Kuhbier
Sabine Braun
Nina Wistuba
Hossein Naghilou Hidaji
David Beverungen
Georgios Papaikonomou
Vincent Coger
Franziska Schäfer-Nolte
Yang An
Christina Allmeling
Mehmet Altintas
Judith Müller
Vesna Bucan
Eileen Gülke
Corinna Kerzel
Simone Hübner
Renata Sonnenfeld
Jieli Liu
Christine Radtke
Insa Janssen
Stella Matthes
Milad Neyazi
Sabrina Jahn
Inas Nasser
Felix Adams
Khaled Dastagir
Annett Bischoff
Jasper Killat
Gülshan Ahmadli
Anastasia Chaika
Nina Hirsch
Anja Hillmer
Nikolas Bautsch
Tobias Husemann
Vincent Pritzel
Annika Köhler
Viktor Maurer
Kevin Hake

My co-operation partners

Lothar Koch
Martin Grüne
Sabrina Schlie
Andrea Deiwick
Boris Chichkov

Ralf Gäbel
Gustav Steinhoff

Daniela Zychlinski
Axel Schambach

Renata Stripecke
Gustavo Andres Salguero Lopez

Jutta Fuhlrott
Anneke Loos

Alexander Heisterkamp
Alexander Krüger

Appendix C Curriculum Vitae

Stefanie Michael, neé Kuhn, Biologist (Diploma)

Professional Experience

since 01/2008
: Research assistant (Wissenschaftliche Mitarbeiterin) in the laboratory of the Plastic, Hand and Reconstructive Surgery of the Hannover Medical School
PhD student within the framework of the interdisciplinary special research field Transregio 37 (SFB TR37)
Topic: "Laser induced forward transfer of biomaterials to create a skin substitute for burn patients"

10/2006 - 08/2007
: PhD scholarship at the Hannover Medical School within the framework of the International Research Training Group IRTG 1273 "Strategies of human pathogens to establish acute and chronic infections"
Topic: "Genetic adaptation of *H. pylori* to the host individual"

Education

10/1999 - 07/2006
: Studies of Biology, University of Bielefeld
Topic of my diploma thesis: "Molecular genetic analysis of accessory plasmids of endogenous *Sinorhizobium meliloti* strains"
Diploma in Biology

09/2003 - 01/2004
: Semester abroad at the University of Uppsala, Sweden

1999
: Abitur in Bielefeld

Further Experiences

11/2002 - 02/2003
: Student research assistant (Studentische Hilfskraft)
University of Bielefeld, Faculty of Biology

03/2003
: Internship
Herz- und Diabeteszentrum Bad Oeynhausen

Appendix D List of Publications

D.1 Publications in Journals

M. Stiens, S. Schneiker, M. Keller, S. Kuhn, A. Pühler, A. Schlüter
Sequence analysis of the 144-kilobase accessory plasmid pSmeSM11a, isolated from a dominant *Sinorhizobium meliloti* strain identified during a long-term field release experiment.
Appl Environ Microbiol 2006 May; 72(5):3662-72.

S. Kuhn, M. Stiens, A. Pühler, A. Schlüter
Prevalence of pSmeSM11a-like plasmids in indigenous *Sinorhizobium meliloti* strains isolated in the course of a field release experiment with genetically modified *S. meliloti* strains.
FEMS Microbiol Ecol 2008 Jan; 63(1):118-31. Epub 2007 Nov 20.

L. Koch*, S. Kuhn*, H. Sorg*, M. Gruene*, S. Schlie, R. Gaebel, B. Polchow, K. Reimers, S. Stoelting, N. Ma, P.M. Vogt, G. Steinhoff, B. Chichkov
* equally contributed
Laser printing of skin cells and human stem cells.
Tissue Eng Part C Methods 2010 Oct; 16(5):847-54.

L. Kennemann, X. Didelot, T. Aebischer, S. Kuhn, B. Drescher, M. Droege, R. Reinhardt, P. Correa, T.F. Meyer, C. Josenhans, D. Falush, S. Suerbaum
Helicobacter pylori genome evolution during human infection.
Proc Natl Acad Sci U S A 2011 Mar 22; 108(12):5033-8. Epub 2011 Mar 7.

L. Koch, A. Deiwick, S. Schlie, S. Michael, M. Gruene, V. Coger, D. Zychlinski, A. Schambach, K. Reimers, P.M. Vogt, B. Chichkov
Skin tissue generation by laser cell printing.
Biotechnol Bioeng 2012 Jul; 109(7):1855-63. doi: 10.1002/bit.24455. Epub 2012 Feb 13.

S. Michael, H. Sorg, C.T. Peck, K. Reimers, P.M. Vogt
The mouse dorsal skin fold chamber as a means for the analysis of tissue engineered skin.
Burns 2013 Feb; 39(1):82-8. doi: 10.1016/j.burns.2012.05.010. Epub 2012 Jun 18.

S. Michael, H. Sorg, C.T. Peck, L. Koch, A. Deiwick, B. Chichkov, P.M. Vogt, K. Reimers
Tissue engineered skin substitutes created by laser-assisted bioprinting form skin-like structures in the dorsal skin fold chamber in mice
PLOS ONE 2013 Mar; 8(3):e57741. doi: 10.1371/journal.pone.0057741

D.2 Book chapter

S. Kuhn, C. Radtke, C. Allmeling, P. M. Vogt and K. Reimers
Skin Biopsy - Perspectives
Chapter 13: Keratinocyte Culture Techniques in Medical and Scientific Applications
Edited By: Uday Khopkar
ISBN 978-953-307-290-6, Hard cover, 336 pages
Publisher: InTech
Publication date: November 2011

D.3 Congresses

S. Kuhn, L. Koch, M. Grüne, K. Reimers, B. Chichkov, P. M. Vogt
Successful Laser-Induced-Forward-Transfer (LIFT) of cultured skin cells
Chirurgische Forschungstage, 25.-27.09.2008, Freiburg (Poster)

M. Grüne, L. Koch, S. Schlie, B. Chichkov, S. Kuhn, K. Reimers, P. M. Vogt, H. Sorg, R. Gäbel, G. Steinhoff
Laser-induced forward transfer of skin cells and human mesenchymal stem cells: detailed quantitative viability studies
Bioprinting and Biofabrication, 06.-08.07.2009, Bordeaux, France (Lecture)

H. Sorg , R. Gäbel, S. Kuhn, K. Reimers , L. Koch, M. Grüne, S. Schlie, N. Ma, B. Chichkov, G. Steinhoff, P.M.Vogt
Laser-induced forward transfer (LIFT) of skin cell lines and human mesenchymal stem cells: investigations of vitality, proliferation and cellular behaviour after LIFT
European Plastic Surgery Research Council (EPSRC), 20.-23.08.2009, Hamburg (Lecture)

L. Koch, M. Grüne, S. Schlie, S. Kuhn, K. Reimers, H. Sorg, R. Gäbel, G. Steinhoff, P. M. Vogt, B. Chichkov
Generation of 3D cellular matrix constructs by laser printing
Congress of the European Society of Artificial Organs (ESAO), 02.-05.09.2009, Compiègne, France (Lecture)

S. Kuhn, M. Grüne, L. Koch, S. Schlie, K. Reimers, H. Sorg, R. Gäbel, B. Chichkov, G. Steinhoff, P. M. Vogt
Erfolgreicher Laserinduzierter Vorwärtstransfer (LIFT) von kultivierten Hautzellen
40. Jahrestagung der Deutschen Gesellschaft für Plastische, Rekonstruktive und Ästhetische Chirurgie (DGPRAEC), 10.-12.09.2009, Hannover, Plastische Chirurgie, Supplement 1, 9. Jahrgang, September 2009, Abstracts (Poster)

H. Sorg, R. Gäbel, S. Kuhn, K. Reimers, L. Koch, M. Grüne, S. Schlie, N. Ma, B. Chichkov, P.M. Vogt, G. Steinhoff
Laser-induzierter Vorwärtstransfer (LIFT) von Biomaterialien: Untersuchungen zur Vitalität und zum Zellverhalten nach LIFT von humanen mesenchymalen Stammzellen

40. Jahrestagung der Deutschen Gesellschaft für Plastische, Rekonstruktive und Ästhetische Chirurgie (DGPRAEC), 10.-12.09.2009, Hannover, Plastische Chirurgie, Supplement 1, 9. Jahrgang, September 2009, Abstracts (Lecture)

S. Kuhn, H. Sorg, M. Grüne, L. Koch, R. Gäbel, S. Schlie, K. Reimers, B. Chichkov, G. Steinhoff, P. M. Vogt
Successful laser induced forward transfer (LIFT) of skin and stem cells in 2D and 3D patterns
World conference on regenerative medicine (WCRM), 29.-31.10.2009, Leipzig (Poster)

L. Koch, M. Grüne, C. Unger, A. Deiwick, S. Schlie, B. Chichkov, R. Gäbel, H. Sorg, N. Ma, G. Steinhoff, S. Kuhn, K. Reimers, P.M. Vogt
Tissue Engineering mittels Laser Printing
Fortbildungskolloquium der Klinik und Poliklinik für Dermatologie und Allergologie, Klinikum der Universität München, 16.06.2010, Munich (Invited talk)

Innovatives Tissue Engineering von Haut - Transregio 37
P. M. Vogt, S. Kuhn, H. Sorg, S. Strauß, K. Reimers
128. Kongress der Deutschen Gesellschaft für Chirurgie (DGCH), 03.-06.05.2011, Munich (Invited talk)

S. Michael, H. Sorg, L. Koch, S. Schlie, M. Grüne, B. Chichkov, K. Reimers, P. M. Vogt
Erfolgreicher Transfer von Hautzellen mittels Laserinduziertem Vorwärtstransfer (LIFT)
Jahreskongress der Deutschen Gesellschaft für Wundheilung und Wundbehandlung e.V. (DGfW), 14.-16.06.2012 (Lecture)

L.Koch
Skin tissue generation by laser cell printing
3rd Lübeck Regenerative Medicine Symposium "3D and skin organ culture models", 21.-22.06.2012, Lübeck (Invited talk)

Anhang E Eidesstattliche Erklärung

Erklärung zur Dissertation

Hierdurch erkläre ich, dass die Dissertation „Laser induced forward transfer of biomaterials to create a skin substitute for burn patients“ selbständig verfasst und alle benutzten Hilfsmittel sowie evtl. zur Hilfeleistung herangezogene Institutionen vollständig angegeben wurden.

Die Dissertation wurde nicht schon als Diplom- oder ähnliche Prüfungsarbeit verwendet.

21.03.2013, Hannover